AD-A107 712 NEW MEXICO ENGINEERING RESEARCH INST ALBUQUERQUE F/G 1/5
RAPID DAMAGE ASSESSMENT. VOLUME II. DEVELOPMENT AND TESTING OF --ETC(U)
FEB 81 C W WILSON F29601-76-C-0015
UNCLASSIFIED NMERI-5.08-AP-39 AFESC/ESL-TR-80-47-VOL-2 NL

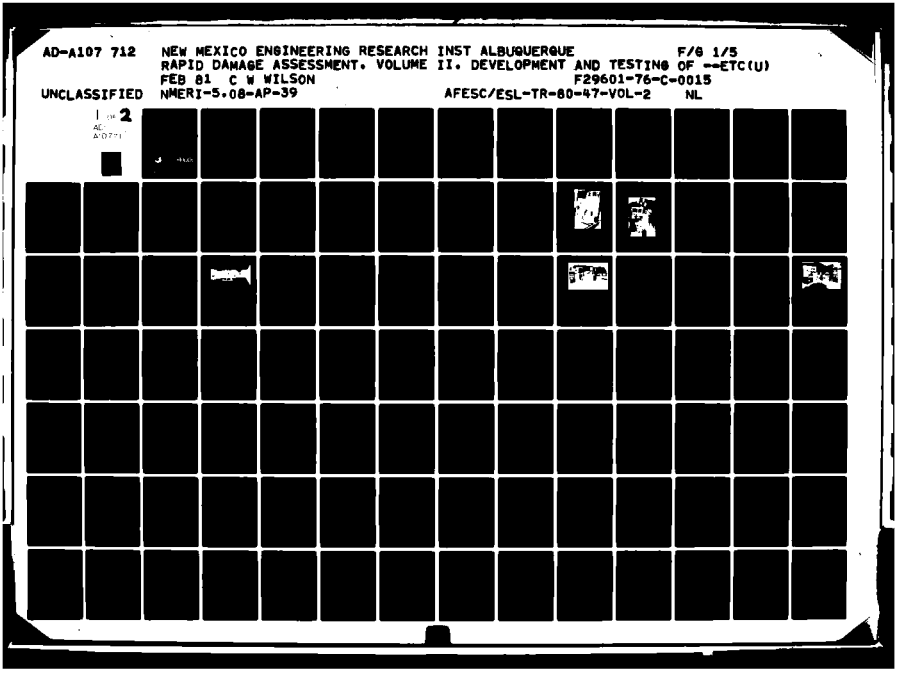

LEVEL

ESL-TR-80-47

RAPID DAMAGE ASSESSMENT

VOLUME II: DEVELOPMENT AND TESTING OF RAPID DAMAGE ASSESSMENT SYSTEM

NEW MEXICO ENGINEERING RESEARCH INSTITUTE
ALBUQUERQUE, NEW MEXICO 87131

FEBRUARY 1981

FINAL REPORT
JUNE 1979 - NOVEMBER 1980

AFESC

ENGINEERING AND SERVICES LABORATORY
AIR FORCE ENGINEERING AND SERVICES CENTER
TYNDALL AIR FORCE BASE, FLORIDA 32403

NOTICE

Please do not request copies of this report from HQ AFESC/RD (Engineering and Services Laboratory). Additional copies may be purchased from:

National Technical Information Service
5285 Port Royal Road
Springfield, Virginia 22161

Federal Government agencies and their contractors registered with Defense Technical Information Center should direct requests for copies of this report to:

Defense Technical Information Center
Cameron Station
Alexandria, Virginia 22314

UNCLASSIFIED
SECURITY CLASSIFICATION OF THIS PAGE (When Data Entered)

REPORT DOCUMENTATION PAGE

READ INSTRUCTIONS BEFORE COMPLETING FORM

1. REPORT NUMBER: ESL-TR-80-47, Volume II	2. GOVT ACCESSION NO.: AD-A107712
3. RECIPIENT'S CATALOG NUMBER:	
4. TITLE (and Subtitle): RAPID DAMAGE ASSESSMENT. Volume II. Development and Testing of Rapid Damage Assessment System.	5. TYPE OF REPORT & PERIOD COVERED: Final Report. June 1979 — November 1980
	6. PERFORMING ORG. REPORT NUMBER: NMERI-5.08-AP-39
7. AUTHOR(s): Christopher W. Wilson	8. CONTRACT OR GRANT NUMBER(s): F29601-76-C-0015
9. PERFORMING ORGANIZATION NAME AND ADDRESS: New Mexico Engineering Research Institute, University of New Mexico, Box 25, University Station, Albuquerque, New Mexico 87131	10. PROGRAM ELEMENT, PROJECT, TASK AREA & WORK UNIT NUMBERS: PE: 63723F; JON: 2104-2B-24
11. CONTROLLING OFFICE NAME AND ADDRESS: Air Force Engineering and Services Center, Tyndall Air Force Base, Florida 32403	12. REPORT DATE: February 1981
	13. NUMBER OF PAGES: 148
14. MONITORING AGENCY NAME & ADDRESS (if different from Controlling Office)	15. SECURITY CLASS. (of this report): Unclassified
	15a. DECLASSIFICATION/DOWNGRADING SCHEDULE

16. DISTRIBUTION STATEMENT (of this Report)

Approved for public release; distribution unlimited.

17. DISTRIBUTION STATEMENT (of the abstract entered in Block 20, if different from Report)

18. SUPPLEMENTARY NOTES

Availability of this report is specified on verso of front cover

19. KEY WORDS (Continue on reverse side if necessary and identify by block number)

Crater Repair Quality	Crater	Unexploded Ordnance	Spalls
Damage Assessment System	Camouflet	Minimum Operating Strip	
Flight Sensor Package	Bomb Damage	Airbase	
Image Analysis System	Runway	Rapid Runway Repair	

20. ABSTRACT (Continue on reverse side if necessary and identify by block number)

This report describes the damage assessment system for rapid runway repair developed for concept verification. In the damage assessment system, an airborne linear CCD array sensor and an interactive image processing system are used to locate, size, and classify damages. The repair area is selected by minicomputer. Results of the testing, the tradeoff analyses, and the field demonstration are presented. Recommendations are made for the development of a prototype system.

DD FORM 1 JAN 73 1473 EDITION OF 1 NOV 65 IS OBSOLETE

UNCLASSIFIED
SECURITY CLASSIFICATION OF THIS PAGE (When Data Entered)

PREFACE

This report was prepared by the New Mexico Engineering Research Institute, University of New Mexico, Box 25, University Station, Albuquerque, New Mexico 87131, under contract F29601-76-C-0015 with the Air Force Engineering and Services Center, Tyndall Air Force Base, Florida 32403. The work described here was performed at the Eric H. Wang Civil Engineering Research Facility, Kirtland Air Force Base, New Mexico.

This report consists of two volumes. This is Volume II, which summarizes work done between 14 June 1979 and 30 November 1980.

This report has been reviewed by the Public Affairs Office (PA) and it is releasable to the National Technical Information Service (NTIS). At NTIS, it will be available to the general public, including foreign nationals.

The findings and recommendations in this document are not to be construed as an official Department of the Air Force position. The use of trade names in this report does not constitute an official endorsement or approval of commercial products. This report may not be cited for purposes of advertisement.

This technical report has been reviewed and is approved for publication.

GARY A. CLEMENTS, Capt. USAF
Project Officer

JAMES R. VAN ORMAN
Chief, Rapid Runway Repair Branch

FRANCIS B. CROWLEY, III, Col, USAF
Dir, Engineering & Services Lab

(The reverse of this page is blank)

TABLE OF CONTENTS

Section	Title	Page
I	INTRODUCTION	1
	Objective	1
	System Overview	1
	Report Outline	2
II	BACKGROUND INFORMATION	3
	General Background	3
	Damage Definitions	4
	Repair Equations	7
III	DAMAGE ASSESSMENT SYSTEM	13
	General Description	13
	Flight Sensor Package	13
	Image Analysis System	22
IV	SYSTEM DEVELOPMENT AND TESTING	39
	Development History	39
	Effects of Adverse Weather on FSP Sensor	42
	Effects of Nonideal Camera Motion	50
	Lighting Requirements	57
	Conceptual Lighting System and Platform Designs for FSP	64
	Data Link Tradeoff Analysis	70
	Stabilized Platform Versus Image Correction	75
	Sensor Tradeoff Analysis	82
	Testing of FSP Sensor	90
	Testing of IAS	94

TABLE OF CONTENTS (CONCLUDED)

Section	Title	Page
V	FIELD DEMONSTRATION.	96
	Gathering Imagery Data Using Flight Sensor Package.	96
	Data Quantity and Rates	98
	Determination of Resolution Element Size.	99
	Data Entry to Image Analysis System	99
	Image Analysis Using Image Analysis System.	100
	Repair Area Selection	101
	Demonstration of Total System Function.	102
VI	CONCLUSIONS AND RECOMMENDATIONS.	104
	REFERENCES	109
Appendix		
A	SAMPLE MOS SELECTION SOFTWARE INPUT AND OUTPUT	111

LIST OF FIGURES

Figure	Title	Page
1	Required Crater Repair Quality (Single-Direction Takeoff)	10
2	Spacing Template	11
3	Flight Sensor Package Mounted in Test Aircraft	14
4	Image Analysis System	15
5	Block Diagram of Damage Assessment System	16
6	AVD-1 Output Data Format	20
7	Cessna 180	22
8	Sample PDP-11/34 Configuration	26
9	Block Diagram of Image Controller System	27
10	Image Controller System Hardware	28
11	Block Diagram of Image Processor System	30
12	Image Processor System	32
13	Scattering Area Ratio for Transmissivity Calculation	48
14	Axes of Rotation	52
15	Design for Stabilized Platform	68
16	Stabilized Platform Mounted on H-1 Helicopter	69
17	Resolution Test Targets for DAS Field Demonstration	93
18	Resolution Target Arrangement	97
19	Multiple Video Processing Station DAS	106
20	Hardcopy DAS	107
21	Real Time DAS	108

LIST OF TABLES

Table	Title	Page
1	Distribution of Discrete Damages	5
2	Damage Types Recognized by Damage Assessment System	6
3	Units for Variables in Repair Equations	8
4	Minimum Crater Repair Time Estimates	12
5	General Specifications for Model CCD 1400 Line-Scan Camera Subsystem	17
6	AVD-1 Timing Summary	21
7	Component List for Image Controller System	24
8	ADI-2 Timing Summary	27
9	Component List for Image Processor System	30
10	Programmable Function Key Operations	31
11	Meaning of Integers in IPS Data Record	35
12	Transmittance Due to Absorption by Water Vapor	46
13	Transmittance of a 6000-Foot Path Through Rain	49
14	Spectral Reflectance of Common Materials	60
15	Data Quantities and Rates from Imagery Data of Kirtland AFB Runway	98
16	Measured Resolution Element Dimensions	99
17	DAS Functions and Time Requirements	103

SECTION I
INTRODUCTION

OBJECTIVE

The objective of the effort documented in this report was to develop a system that would locate and identify runway damage resulting from an attack with conventional weaponry and select the 5000-foot by 50-foot section of runway that could be repaired most rapidly. The system had to be capable of operating in a hostile postattack environment in which unexploded ordnance and chemical and biological hazards may be present. The goal was a system that could complete the reconnaissance, data analysis, and repair area selection within 30 minutes.

SYSTEM OVERVIEW

The Damage Assessment System (DAS) developed consists of two major subsystems: an airborne Flight Sensor Package (FSP) and a ground-based, computerized Image Analysis System (IAS). The FSP consists of an electronic line-scan camera, a magnetic tape recorder, and conditioning electronics. The FSP is carried by an aerial reconnaissance vehicle. The IAS consists of a minicomputer system host, bulk data storage disks, an interactive digital image processing system, an input data interface, multiple terminals, a printer-plotter, and a hardcopy recorder.

The system functions in the following manner. After an attack, the FSP is carried aloft by the aerial reconnaissance vehicle. The aircraft makes a low-level pass over the damaged pavements while the signal from the electronic camera is recorded. The aircraft lands, and the recorded data are transferred to the IAS storage disks. The minicomputer processes the imagery data and presents the operator with a low-resolution image on the digital image-processing system. The operator interactively identifies and classifies damages on the video display while the minicomputer accumulates the type, size, and location of the damages. The operator calls up high-resolution images as required to complete the damage-classification process. A program

is then run on the minicomputer to select a ranked set of damaged areas requiring the shortest repair times. The commander, considering the available manpower, equipment, materials, and access routes, then selects the area to be repaired.

The hardcopy recorder provides an alternate method of locating and classifying damages. The data recorded by the FSP are transferred, by means of an alternate path in the input data interface, to the fiber optic hardcopy recorder. The recorder produces a continuous hardcopy image of the pavement surfaces. The damages are manually located, sized, and classified from this image, and the information is manually entered from a keyboard terminal to the minicomputer. The data are then processed by the same repair area selection software described above.

REPORT OUTLINE

General background information, including types of damage to be expected and the methods used to calculate repair times, is presented in Section II. In Section III the DAS developed under this subtask is described in detail. Development of the various components in the DAS (including conceptual designs and tradeoff analyses) and testing of the system are discussed in Section IV. Section V describes the field demonstration of the system held at Kirtland Air Force Base, New Mexico, as well as the results of this demonstration. In Section VI conclusions and recommendations for modifications to the system during prototype development are presented.

SECTION II
BACKGROUND INFORMATION

GENERAL BACKGROUND

The dependence of modern jet aircraft on high-quality airfield surfaces makes the airfield runway a high-priority target. The probability of attack on vulnerable airfield runways is further increased by the United States Air Force (USAF) policy of using hardened aircraft shelters. At present, the USAF has no system for rapidly locating and evaluating the magnitude of the damage that would result from an enemy attack, with conventional weaponry, on runway surfaces. The purpose of the effort documented in this report was to develop a system for concept verification that could rapidly assess the damage to runway surfaces after an attack and select from the damaged pavements the minimum operating strip (MOS) that could be made operational in the shortest time.

The parameters that affect the damage assessment process, the limitations placed on the DAS, the types of damages anticipated, the development of equations for estimating damage repair time, the evaluation of damage assessment methodologies, and the conceptual design of the DAS selected for development by the USAF are discussed in detail in Volume I of this report. For the reader's convenience, several of these topics are summarized in this section. Additional background material is also presented.

Several parameters have a bearing on any assessment and repair effort:

1. The large pavement areas that must be examined for damage.
2. The quantity of data that must be reduced.
3. The difficulty of accurately determining the type and magnitude of damage.
4. The time required to repair various types of damage.
5. The time required to clear the area of unexploded ordnance.
6. The possibility of encountering unexploded ordnance that cannot be removed.
7. The distance and access time from the aircraft shelters to the selected repair area.
8. The proximity of construction materials to the selected repair area.

The DAS must deal with these parameters in order to determine accurately the best area for repair.

When the New Mexico Engineering Research Institute (NMERI) began this effort, the following limitations were placed on the system:

1. Must function independently, without relying on other base facilities.
2. Must not exceed 30-minute maximum.
3. Must use limited manpower and simple equipment.
4. Must not employ electronic cameras.
5. Must not require sensing devices.
6. Must not require elevation or optical monitoring equipment.
7. Must not employ computers.
8. Must function in adverse environments.

Research was conducted for approximately three months as NMERI personnel attempted unsuccessfully to devise a system that met all of the constraints. NMERI then presented to the USAF a briefing that demonstrated seven systems that had been investigated in detail, none of which conformed to all of the limitations listed. Consequently, the criteria were changed so that only two constraints were placed on the proposed system. First, the system should be capable of locating and assessing the magnitude of the damage and selecting the repair area in the least possible time. Second, the system should be as simple as possible consistent with the time constraint imposed for selecting repair areas. Under these new guidelines, the time requirement was considered to be the single most important variable in the selection of the most effective system. NMERI recommended a system based on an airborne linear CCD-array electronic camera and a ground-based, computerized, interactive image-processing system. The conceptual design of this system was accepted by the Air Force Engineering and Services Center (AFESC), and development of a concept verification system was authorized.

DAMAGE DEFINITIONS

The research conducted under this effort was based on an assumed enemy attack in which conventional weapons would be used. Table 1 lists the number

TABLE 1. DISTRIBUTION OF DISCRETE DAMAGES

Number	Type of Damage	Percentage of Total
62	Spalls (large enough to require repair)	50
4	Unexploded Ordnance (not including anti-personnel mines)	3
15	Large Craters (36-foot-diameter or greater)	12
31	Small or Intermediate Craters	25
9	Camouflets (with pavement upheaval)	7
4	Camouflets	3
125		100

and types of damage resulting from a hypothetical enemy attack that were assumed by NMERI in the evaluation and development of the damage assessment system.

The quantity and types of damage that might be sustained by an airfield pavement may vary considerably from those used in the design of the system, but NMERI determined that the system should be capable of handling at least this quantity of data. The quantity of damage represents approximately 1/40th of the damage sustained, for example, at the airport in Cyprus during the Greek and Turkish conflict of 1975.

The types of damage listed in Table 1 are grouped in four basic categories and are defined in detail in Volume I of this report. The four categories are reviewed briefly in the following paragraphs.

Type I damage is the standard crater. The diameter of a standard crater may range from 3 to 4 feet for a small explosive head to 50 feet for a 750-pound bomb. Generally the only dimensions that are readily distinguishable to an observer are the apparent radius and the apparent depth.

Type II damage is the camouflet. A weapon that forms a camouflet penetrates the pavement--sometimes cleanly--and detonates at some distance below the surface of the pavement in the subgrade. The result of the explosion is a crater formed beneath the pavement. The pavement immediately surrounding the port of entry of the explosive device may be undisturbed or moderately to radically upheaved. The only parameter that is readily distinguishable by an observer is the apparent radius of the camouflet.

Type III damage is caused by unexploded ordnance (UXO) that penetrate the pavement and come to rest in the subgrade without detonating. The diameter of the port of entry is a direct indication of the size of the explosive head of the weapon. In order to distinguish a UXO from a camouflet, the cavity created by the weapon may have to be closely examined.

Type IV damage is the surface spall. A surface spall is defined as a rupture in the pavement surface that does not penetrate to the subgrade.

During the development of the DAS, the number of damage categories was expanded to six so that unexploded ordnance that did not penetrate the pavement could be considered in determining the best MOS. The six damage types recognized by the DAS are listed in Table 2.

TABLE 2. DAMAGE TYPES RECOGNIZED BY DAMAGE ASSESSMENT SYSTEM

Type 1	Crater
Type 2	Camouflet
Type 3	Spall Field
Type 4	Bomblet Field
Type 5	Surface Unexploded Ordnance
Type 6	Buried Unexploded Ordnance

The type 1 crater, type 2 camouflet, and type 6 buried UXO listed in Table 2 correspond, respectively, to the type I, type II, and type III damages described in Volume I. The type 3 spall field corresponds to the type IV spall described in Volume I, but the DAS identifies groups of spalls as a single spall field with a field radius and number of spalls.

The type 4 bomblet field is a group of small unexploded ordnance lying on the pavement surface. Each bomblet is generally less than 2 feet long and less than 6 inches wide. The field diameter and the number of bomblets are observed quantities associated with the bomblet field.

The type 5 surface UXO is a single large piece of unexploded ordnance that remains above the surface of the pavement. The maximum dimension of the surface UXO is the only observable feature considered by the DAS. Distinguishing specific types of bomblets, surface UXOs, and fuzing mechanisms and determining clearance times were beyond the scope of this effort.

REPAIR EQUATIONS

During Phase 3 of the effort documented in Volume I of this report, NMERI used dimensional analysis to determine a relationship between the area of the moderately upheaved pavement (A), the weight of the explosive head (W), the ultimate compressive strength of the concrete (f'_c), and the apparent radius of the crater (R). Because there is a significant difference between the area of moderately upheaved pavement that must be removed for expedient repair (A_E) and that which must be removed for semipermanent repair (A_{SP}), separate relationships exist for each of the conditions. It is also necessary to distinguish standard craters from camouflets and to derive separate equations for each of the various types of damage. The data used to determine the equations were extracted from References 1, 2, and 3 and from tests on large craters conducted by the U.S. Army Waterways Experiment Station (WES) and by the USAF at Eglin and Tyndall Air Force Bases. The data, the derivation of equations, and the development of nomographs are documented in Section IV (Repair Equations) of Volume I of this report. The repair equations and nomographs are also given here for convenience.

The areas of moderately upheaved pavement that must be removed for expedient and semipermanent repair of craters are given in Equations (1) and (2), respectively.

$$A_E = R^2 \left[\left\{ \frac{f'_c R^2}{W(12.5 \times 10^6)} \right\}^C - 1 \right] \qquad C = -0.98 \tag{1}$$

$$A_{SP} = CR^2 \ln \left\{ \frac{f'_c R^2}{W(12.5 \times 10^6)} \right\} \qquad C = -13.12 \tag{2}$$

The areas of moderately upheaved pavement that must be removed for expedient and semipermanent repair of camouflets are given in Equations (3) and (4), respectively.

$$A_E = R^2 \left[\frac{f'_c R^2}{W(7.395 \times 10^6)} \right]^{-1.124} \tag{3}$$

$$A_{SP} = R^2 \left[\frac{f'_c R^2}{W(4.133 \times 10^7)} \right]^{-1.002} \tag{4}$$

The repair time for a given area of upheaved pavement that must be removed is given by Equation (5).

$$t = (59.9) \left(\frac{A}{144} \right)^{0.16} \tag{5}$$

The units for the variables used in Equations (1) through (5) are given in Table 3.

TABLE 3. UNITS FOR VARIABLES IN REPAIR EQUATIONS

Variable	Unit
A	in^2
f'_c	lb/in^2
R	in
t	sec
W	lb

Late in the development of the DAS, AFESC provided crater repair time estimates based on apparent radius of craters and on repair quality. Five repair qualities were defined; these range from A (best quality, requiring most repair time) to E (worst quality, requiring least repair time). Repair qualities required for damaged areas located at various distances from the start of the takeoff roll are shown in Figure 1. When multiple damages occur along the MOS, the spacing of the damaged areas must be considered in determining the quality of the repairs to be made. A minimum spacing between damaged areas is determined from the air density ratio and the distance from start of roll. If damaged areas are closer together than the minimum spacing required, one of them must be repaired to A quality. Figure 2 is a typical spacing template for a density ratio of 1.0, developed by AFESC for use in the manual MOS selection procedure. The location of the first damaged area is plotted along the equidistance line. The location of the second damaged area is then plotted along a horizontal line through the first damaged area. If the second area falls within the shaded portion of the template, an A quality repair is required. The spacing criterion provided by AFESC is for an F-4E aircraft. Repair time estimates used by NMERI for various apparent crater diameters and repair qualities are given in Table 4. The original roughness criteria development work is documented in Reference 4.

NMERI developed software implementing Equations (1), (3), and (5) to determine crater and camouflet repair times. When AFESC provided crater repair time estimates based on spacing criteria and repair quality, the software was modified to use these estimates. Equations (3) and (5) were retained for determining camouflet repair times.

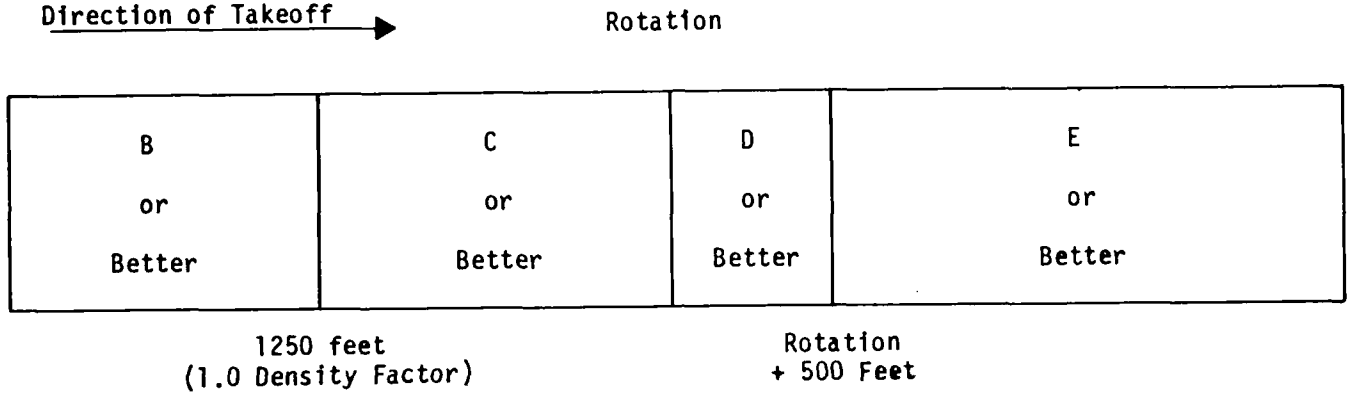

Category of Repair

A - Best Quality (Longest Repair Time)

E - Lowest Quality (Shortest Repair Time)
(Requires Barrier for Landing Aircraft)

Figure 1. Required Crater Repair Quality (Single-Direction Takeoff)

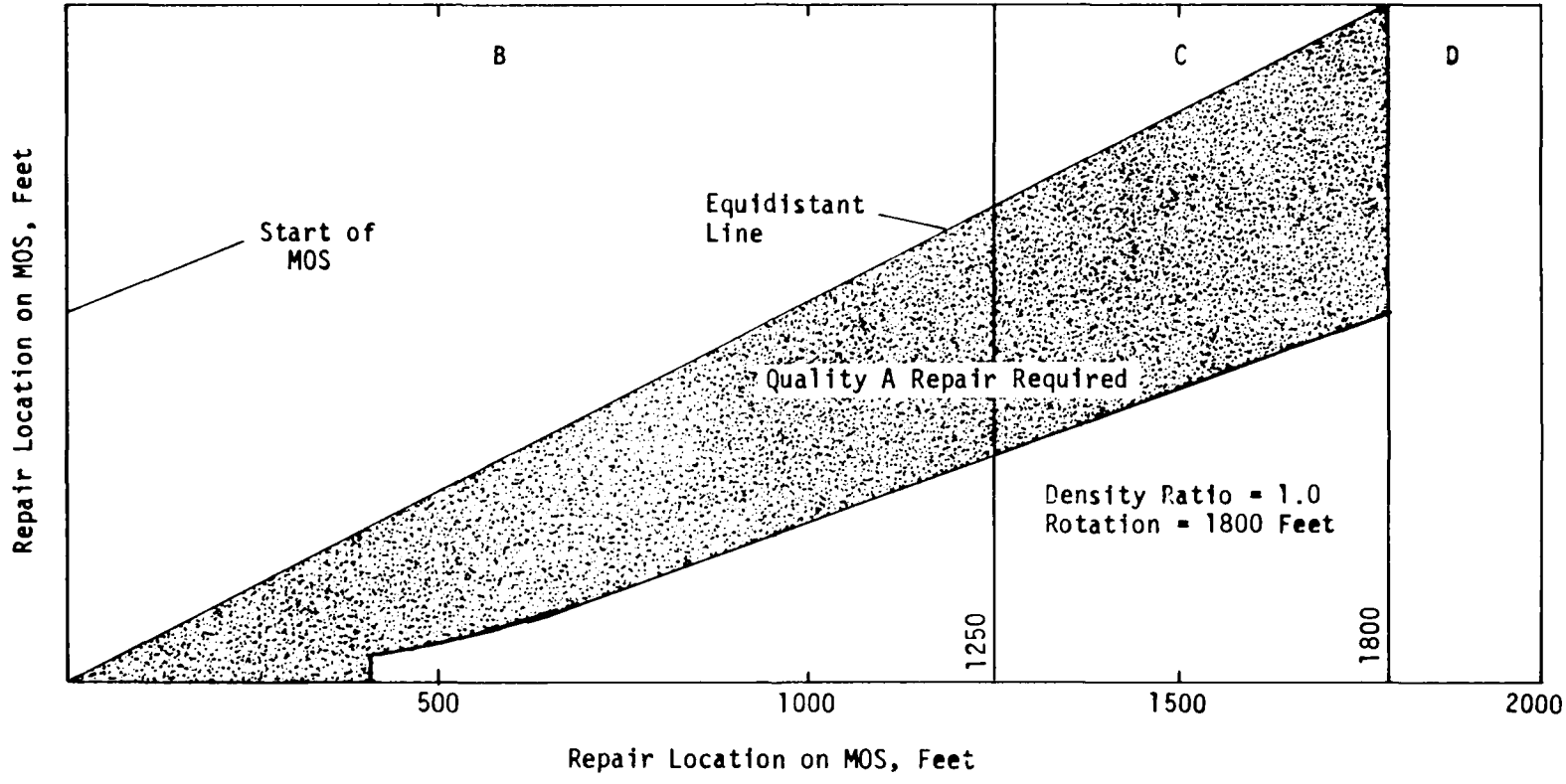

Figure 2. Spacing Template

TABLE 4. MINIMUM CRATER REPAIR TIME ESTIMATES

Apparent Crater Diameter, ft	Time, min				
	A Quality	B Quality	C Quality	D Quality	E Quality
10	180	150	115	105	80
20	200	170	135	125	100
30	215	205	175	175	150
40	250	245	225	220	200
50	290	275	255	255	205
60	350	330	300	300	215
70	410	385	355	355	230

SECTION III
DAMAGE ASSESSMENT SYSTEM

GENERAL DESCRIPTION

The DAS is divided into two main subsystems: the FSP and the IAS. The FSP consists of an electronic line-scan camera, an airborne tape recorder, and conditioning electronics. The sensor is a Fairchild CCD 1400-line scan camera with a Vivitar f2.0 24-mm lens. The data link is a 14-track Ampex AR 1700 high-bit-rate (HBR) airborne digital tape recorder. The conditioning electronics consist of an A/D converter, an interface to the tape recorder, and controls that start, stop, and control the data recording. The electronics were custom-built to NMERI specifications by the Washington Analytical Services Center (WASC) Division of EG&G, Inc. The FSP mounted in the test aircraft is shown in Figure 3.

The IAS consists of a minicomputer image controller, an interactive image analyzer system, bulk data storage disks, input data interface, a printer-plotter, and a hardcopy recorder. The minicomputer image controller is a Digital Equipment Corporation PDP 11/34A with dual RK05 disks, an LA-36 terminal, and two VT-100 terminals. The interactive image analyzer system is an Interpretation Systems Incorporated Views I system. The bulk data storage disks are two 80-megabyte (Mbyte) AMPEX DM 980 disks. The input data interface was built to NMERI specifications by EG&G. The printer-plotter is a Versatec 1110 A. The hardcopy recorder is a Tektronix 4633A continuous hardcopy recorder. The IAS is shown in Figure 4.

A block diagram of the DAS, indicating data flow paths, is shown in Figure 5.

FLIGHT SENSOR PACKAGE

Sensor

The sensor selected for the concept verification system was the Fairchild CCD 1400 line-scan camera. The camera consists of a camera head and a control unit. Both units are compact and lightweight. Specifications for the Fairchild camera are listed in Table 5. This camera is commercially available.

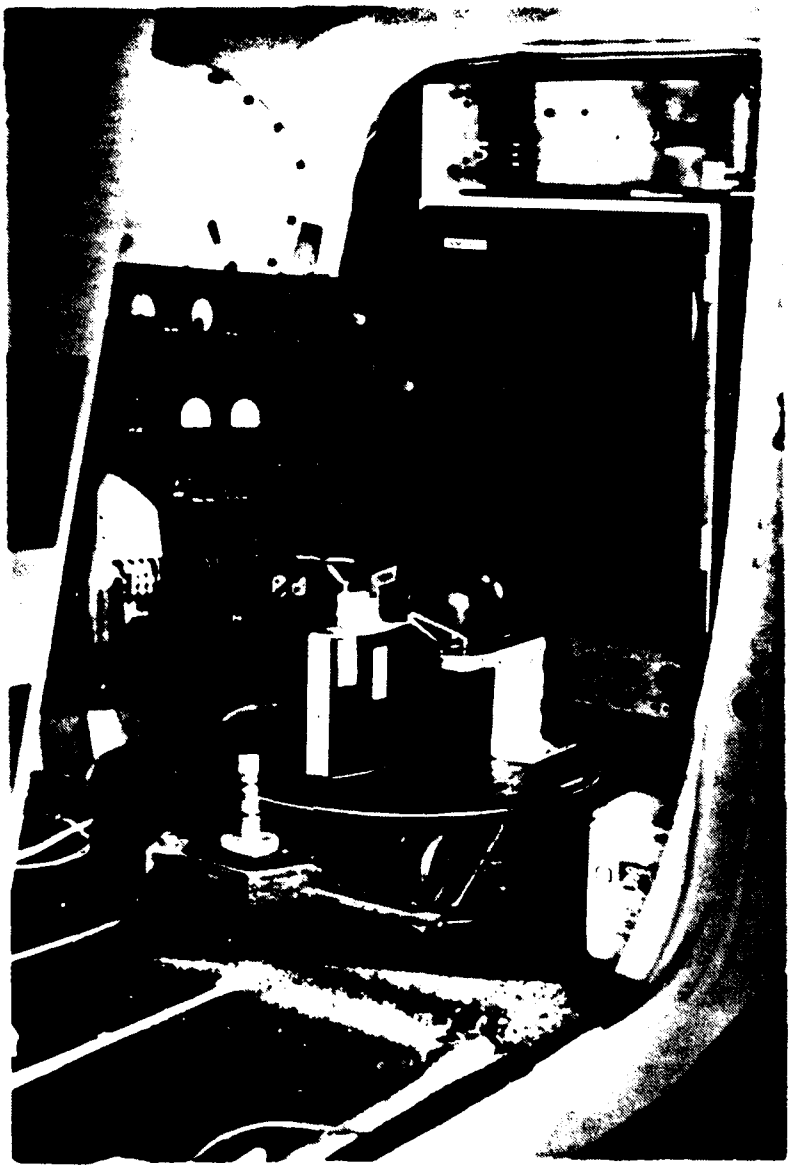

Figure 3. Flight Sensor Package Mounted in Test Aircraft

Figure 4. Image Analysis System

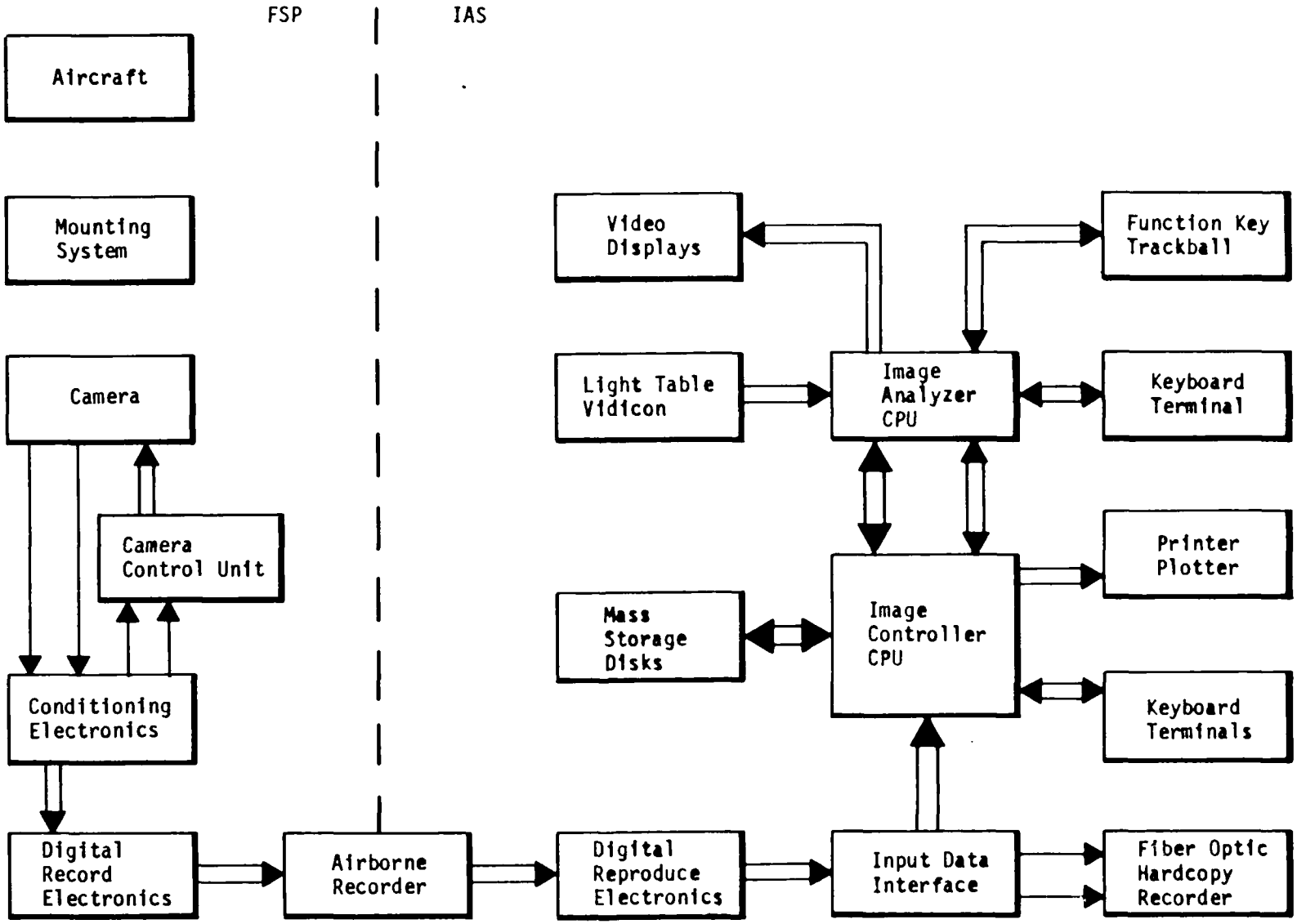

Figure 5. Block Diagram of Damage Assessment System

TABLE 5. GENERAL SPECIFICATIONS FOR MODEL CCD 1400 LINE-SCAN CAMERA SUBSYSTEM

Performance		
Sensor	CCD 121	
Maximum Resolution	1728 elements, 0.51 millinch (13 μm) center-to-center spacing	
Dynamic Range	>200:1	
Responsivity	16 V/ft cd s using a 2854°K tungsten source	
Photoresponse Nonuniformity	±50 mV measured at 500 mV output level using fixed gain setting	
Saturation Exposure	0.06 ft cd s	
Video Output		
Analog	$1V_{pp}$ video (75 Ω)	
Binary	"1" = white; "0" = black (75 Ω)	
AGC Range	10:1	
Data Rate	100 kHz to 10 MHz	
Line-Scan Rate	80 Hz to 10 kHz	
Exposure Time	12 ms to 100 μs	
Spectral Response	Approximately visible response (CIE) (IR is blocked by a built-in filter that can be removed at the factory by special orders)	
Input Power	105-125 V_{ac} 50-440 Hz 0.1 A 210-240 V_{ac} 50-440 Hz 0.05 A	
Power Requirements	Camera	Control Unit
	+15 V 150 mA -15 V 100 mA +5 V 350 mA +6 V 50 mA -6 V 60 mA	+15 V 50 mA -15 V 60 mA +5 V 100 mA
Temperature (ambient)	0°C to 40°C (operating)	
Physical Data	Camera	Control Unit
Size (without lens)		
Width	2.6 in (6.6 cm)	12.0 in (30.5 cm)
Height	5.5 in (14.0 cm)	4.1 in (10.4 cm)
Length	6.0 in (15.2 cm)	8.0 in (20.3 cm)
Weight	1.7 lb (0.77 kg)	5.4 lb (2.45 kg)
Connector	CINCH DB-255 F179 BNCs	CINCH DBC-255 BNCs
Mount	Tripod 1/4 x 20 Dovetail Front faceplate, two 8-32 tapped holes	

Although it is not designed for airborne operation, it proved adequate for testing and concept verification. A Vivitar f2.0 24-mm lens was attached to the camera using a Universal to C-mount adapter. The sensor-lens combination provides a ground resolution element size of 1.9 by 1.9 inches when operating at an altitude of 300 feet, a ground speed of 70 knots, and a line-scan rate of 730 lines per second.

The sensor element of the Fairchild camera is a 1728-element linear CCD array. A CCD array was chosen because of its high resolution, good sensitivity, zero waste data output, simplicity, ruggedness, and low cost. Early in the development effort it was determined that the lighting requirement of the CCD sensor, at the data rates dictated by resolution requirements and aircraft speed, was extremely high. Development of the concept verification system using the CCD array continued with the understanding that the lighting requirements of the sensor would have to be drastically reduced in the prototype system. The reduction would be accomplished by using an image intensifier with a CCD array or by using a different sensor.

For concept verification the camera was rigidly mounted over a vertically oriented port in the floor of the test aircraft. The axis of the array was fixed perpendicular to the roll axis of the aircraft and parallel to the pitch axis. While the aircraft is in flight, the line-scan rate and data rates are controlled by the EG&G conditioning electronics. Sensor exposure is controlled by manually adjusting the lens aperture setting. An automatic gain control (AGC) is available in the Fairchild camera, but it was not used extensively during testing. The AGC sets the highest signal in each line scan equal to the maximum signal output level and scales the rest of the signal proportionately. This improves contrast for the purpose of visual inspection, but it also produces a banding effect in the image that is detrimental to automated image analysis.

Data Recorder

An Ampex AR 1700 HBR digital airborne tape recorder was selected as the data link for the concept verification of the DAS. An airborne recorder was chosen for reasons of reliability, simplicity of implementation, and relative

low cost and because the 1.5-MHz data rate of the sensor had to be reduced to under 500 kHz for input to the IAS. The digital data format was required to preserve the 200:1 dynamic range of the video data produced by the sensor.

The Ampex AR 1700 HBR system consists of an AR 1700 tape transport with 14-track record and reproduce heads and direct record and reproduce electronics, 10 channels of HBR digital record electronics mounted in a separate airborne chassis, and 10 channels of HBR digital record and reproduce electronics mounted in a separate ground chassis. The ground chassis also includes test electronics.

In operation, eight bits per picture element (pixel) of digitized video data are recorded in parallel, one bit per channel, on the AR 1700. The video valid signal from the Fairchild camera is recorded on the ninth channel, and the HBR electronics uses the tenth digital channel for synchronization. All digital data are recorded using the Miller^2 (Miller squared) code. In the aircraft, tape speed is controlled by an external clock signal from the conditioning electronics, which also controls the camera data rate and the analog-to-digital converter. In the playback mode, the tape speed is controlled by a clock signal from the data input interface, which reduces the data rate by a factor of 4:1 to 375 kHz. For the DAS concept verification, only one tape transport was acquired. Therefore, the airborne tape transport must be removed from the aircraft and connected to the ground electronics for playback. If two tape transports were used in the DAS, only the tape would have to be transported.

Conditioning Electronics

Conditioning electronics were developed for NMERI by EG&G to provide an interface between the Fairchild camera and the Ampex AR 1700 HBR. The airborne electronics package was designated the AVD-1. The AVD-1 produces signals that control both the data rate and the line scan rate of the Fairchild camera and the tape speed of the AR 1700. The video data are digitized to 8 bits per pixel by the AVD-1, and line and run numbers are inserted at the end of each video line. The run number is set on the front panel of the AVD-1. Data recording starts and stops are also controlled by the AVD-1. Figure 6 shows the data format produced by the AVD-1. Table 6 lists the various timing signals associated with the AVD-1.

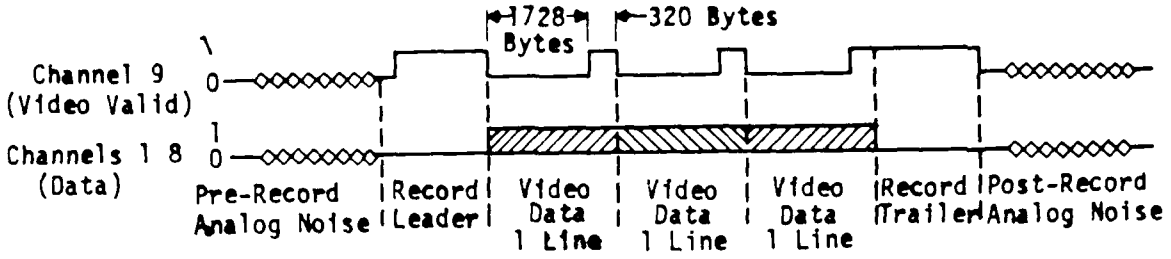

(a) Video Data Tape Format

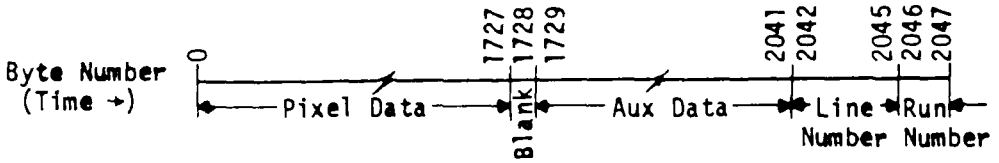

(b) Scan Line Format

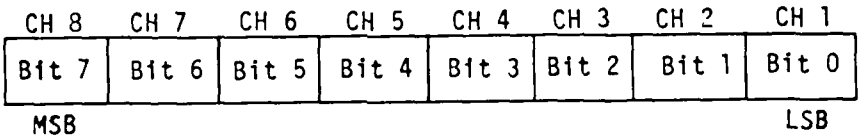

(c) Byte Format

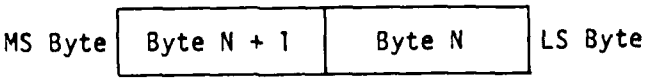

(d) Word Format

Figure 6. AVD-1 Output Data Format

TABLE 6. AVD-1 TIMING SUMMARY

Camera Data Rate	1.5 M pixels/s
Camera Line Rate	732.4 lines/s
Pixels per Line	1728 video 314 blank 4 line number (binary) 2 run number (BCD) --- 2048 total
Pixel Resolution	8 bits
Tape Record Speed	56 IPS
Record Clock	1.5 MHz
Digitizer Master Clock	6 MHz
ADC Conversion Rate Clock	1.5 MHz
ADC Conversion Time	75 ns

Carrier Aircraft and FSP Mounting System

A Cessna 180 modified for aerial photography was used as the carrier aircraft for concept verification of the DAS. The flying characteristics of the Cessna 180 are similar to those of the T-41, one of the aircraft originally considered as a carrier for the FSP. Attempts to obtain a USAF H-1 helicopter for testing and demonstration were unfruitful. The Cessna 180 is shown in Figure 7. Modifications to the aircraft for testing purposes included the addition of a 16-inch vertical camera port in the floor behind the front seats, reinforcement of the rear floor, removal of rear seats, and addition of batteries and electrical outlets in the rear compartment.

The FSP was mounted in the Cessna in three pieces (Figure 3). The Fairchild camera was mounted rigidly over the vertical camera port. The AR 1700, digital electronics, AVD-1, and camera control unit were mounted in a rack at the rear of the cabin. (The AR 1700 can be removed independently of the other FSP components.) An inverter to provide 115-volt AC power for the camera and the AVD-1 was mounted under the passenger seat.

Figure 7. Cessna 180

IMAGE ANALYSIS SYSTEM

Overview

The IAS developed by NMERI is essentially a computerized data-processing system. Imagery data from the FSP are first processed to locate, size, and classify damage to a runway surface. The damage data are then processed to determine which MOS could be repaired in the least amount of time. The IAS can be separated into two major subsystems: the Image Controller System (ICS) and the Image Processor System (IPS). The ICS stores and controls the flow of imagery and damage data through the IAS, performs large-scale manipulations of the imagery data, and processes the damage data to select an MOS. The IPS displays the imagery data and interacts with an operator to identify, locate, size, and classify damages. Both the ICS and the IPS can operate as independent, stand-alone systems. Each has its own central processing unit (CPU),

memory, input/output (I/O) terminals, and software operating system. In the integrated IAS, the ICS acts as the CPU for the IAS, and the IPS acts as a terminal to the ICS.

The hardcopy recorder, which produces a continuous hardcopy image from the recorded imagery data, is discussed separately in this section. The recorder is not directly linked to either the ICS or the IPS and was originally intended only for sensor testing and evaluation. However, the recorder does provide an alternate method for processing the recorded imagery data that has been considered for use in a future DAS.

Specialized software was developed to perform the damage assessment and MOS selection tasks required of the IAS. This software allows the IAS to accept data from the data link; convert the imagery data to a more useful format; transfer data and commands between the ICS and the IPS; and, on the basis of the damage data, select the MOS requiring the least repair time. Most of this software operates on the ICS.

System Operation

The recorded imagery data are transferred from the data link to the mass storage disks in the ICS. The transfer process is controlled by the ICS minicomputer. The full-resolution imagery data are then compressed by a factor of 64:1 on the ICS minicomputer. In the compressed image, 16 by 16 pixel areas of full-resolution imagery data are represented by a single pixel. The low-resolution imagery data are transferred to the IPS in segments representing approximately 3000 feet of the scanned runway. An operator quickly examines each runway segment on the IPS video displays. The operator interactively marks reference features, runway edges, and areas to be examined at full resolution and locates, sizes, and classifies damages on the low-resolution image. This information is transferred back to the ICS. When the operator has completed his examination of the low-resolution image, the areas marked for full-resolution study are transferred automatically from the ICS to the IPS. The interactive damage-identification procedure is then repeated on each high-resolution image. When the damage identification has been completed, the operator starts the MOS selection program on the ICS. The MOS

selection program establishes a repair time for each possible MOS on the runway surface and determines the three best MOS in each take-off direction and the three best bidirectional MOS. The program then prints a summary of repair times, number and types of damage, and damage locations for each of the nine MOS. From this summary, and after considering additional factors such as access routes; explosive ordnance disposal (EOD) clearance times; and the availability of repair crew personnel, equipment, and materials, the commander selects the MOS to be repaired.

Image Controller System

The ICS consists of a minicomputer image controller with small disk storage devices and multiple keyboard terminals, two large mass storage disks, a printer-plotter, an input data interface, and interfaces for the IPS. Table 7 is a detailed list of the components, make, and model numbers used in the ICS.

TABLE 7. COMPONENT LIST FOR IMAGE CONTROLLER SYSTEM

IMAGE CONTROLLER
DEC PDP 11-34A
128 k Bytes MOS Memory
KY 11 LB Prog Panel
DL 11-C Serial Line Unit (2 required)
RK 11-J 2.5 MB Disk and Controller
RK 05-J Disk Drive
DR 11-B Interface (DMA) (to Views)
DR 11-C Interface (PGM I/O) (to Views)
VT-100 Video Display Terminal (2)
H-967 or H-960-CA Cabinet
RSX 11-M Operating System (Class E License)
Fortran IV
DL 11W Line Frequency Clock
LA36 Decwriter
System Software
System Integration
AMPEX DM 980 DP 80 Mbyte Disk Drive (2) and Controller
Model 1110A Printer/Plotter
Model 121 Controller
Versaplot Software for RSX-11

The PDP-11/34 is a widely used, midrange, 16-bit minicomputer. It was selected for use in the concept verification DAS for several reasons. It provided adequate performance at a reasonable cost. Software and many peripherals would be upwardly compatible with more powerful minicomputers in the PDP-11 family. Parts, service, and programming expertise were readily available. In addition, because the IPS equipment had previously been interfaced to a PDP-11/34, development time could be shortened. A basic block diagram of the PDP-11/34 is shown in Figure 8.

The PDP-11/34, as configured for the ICS, includes 64 k words MOS memory, interfaces for one LA-36 Decwriter terminal, two VT-100 terminals, driver and interface for two RK05 disks, driver and interface for the Versatec 1110-A printer-plotter, driver and interface for two Ampex DM980 disks, a Direct Memory Access (DMA) interface for the input data interface, and DMA and parallel I/O interfaces for the IPS. The RSX-11M version 3.1 operating system was used to make possible a multiuser, multitask operation of the system. The LA-36 is a printing terminal that is used as the system terminal. The VT-100s are video terminals that were used for software development and data input. The RK05 disks are small 1.2-M-word removable disks. The operating system is stored on one of the RK05 disks.

Two 80-Mbyte Ampex DM 980 mass storage disk drives were selected for the IAS. These units were selected for their high (1.2 Mbyte/s) data-transfer rates. The drives are dual ported.

The ADI-2 input data interface was developed by EG&G to transfer data from the Ampex HBR digital-reproduce electronics to the PDP-11/34 memory. The ADI-2 receives nine channels of parallel data from the Ampex electronics, formats a 16-bit data word, and writes this data word to the PDP-11/34 memory by means of a DMA interface. The ADI-2 is also capable of converting the 8-bit parallel digital video data to an analog video signal. A ramp signal, synchronized with the start of each video line, is also produced. These two signals are used by the hardcopy recorder to produce a hardcopy image. The ADI-2 provides a clock for the recorder at either 1.5 MHz or 375 kHz. The data transfer to PDP-11/34 memory operates only at the 375-kHz setting. A timing summary for the ADI-2 is shown in Table 8.

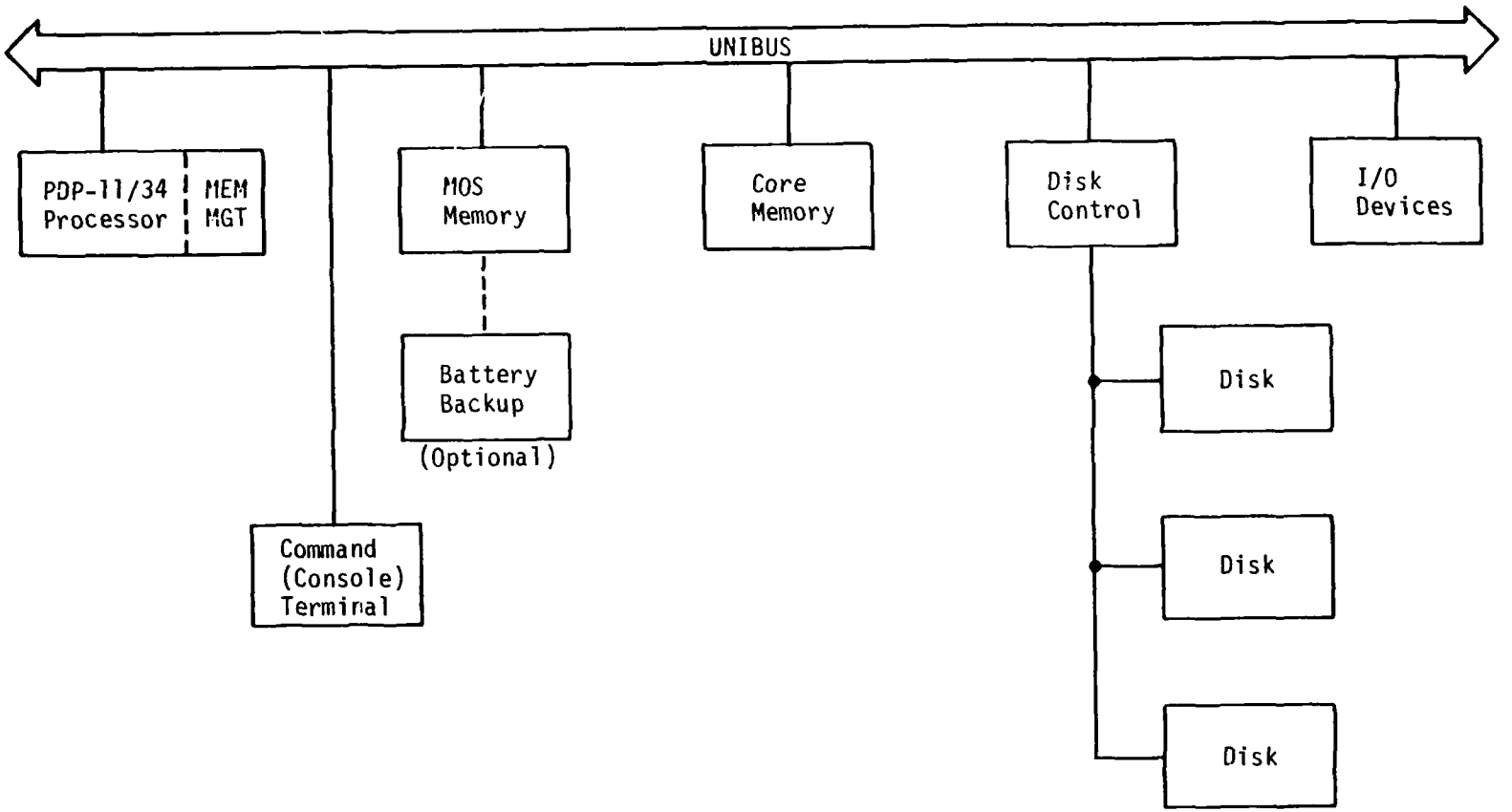

Figure 8. Sample PDP-11/34 Configuration

TABLE 8. ADI-2 TIMING SUMMARY

Tape Reproduce Speed	14 IPS
Reproduce Clock	375 kHz
CPU Interface Master Clock	6 KHz
DAC Conversion Rate Clock	1.5 MHz
DAC Conversion Time	35 ns
Transfer Rate, Data to CPU	187.5 K words/s
Recorder Drive Sweep Time	1.15 ms

A block diagram of the ICS is shown in Figure 9. The ICS hardware is shown in Figure 10.

Image Processor System

The original DAS conceptual design indicated that computerized automatic feature recognition would be the key to extremely fast damage assessment and would be required if the 30-minute goal for repair area selection was to be met.

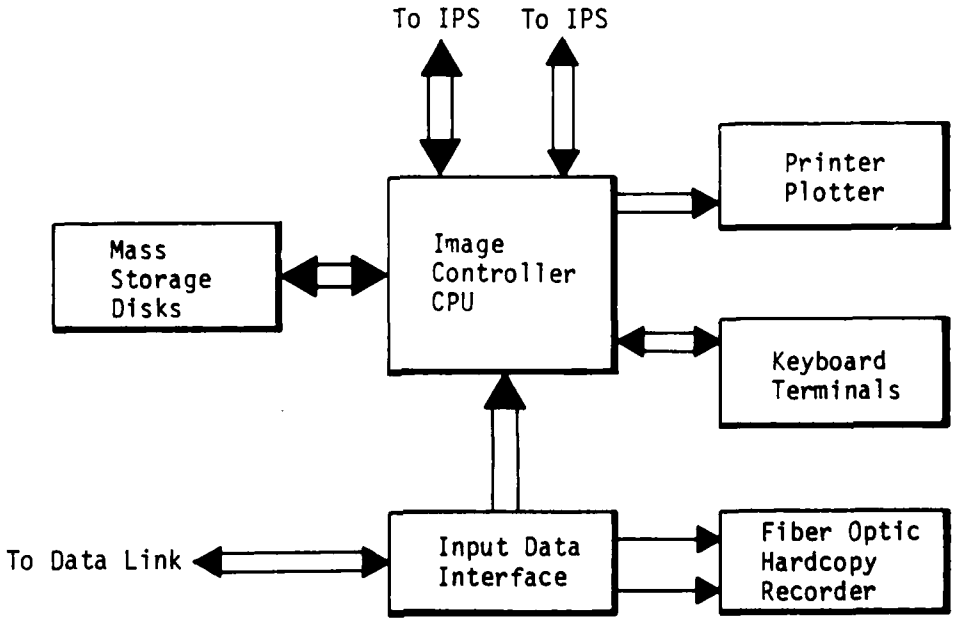

Figure 9. Block Diagram of Image Controller System

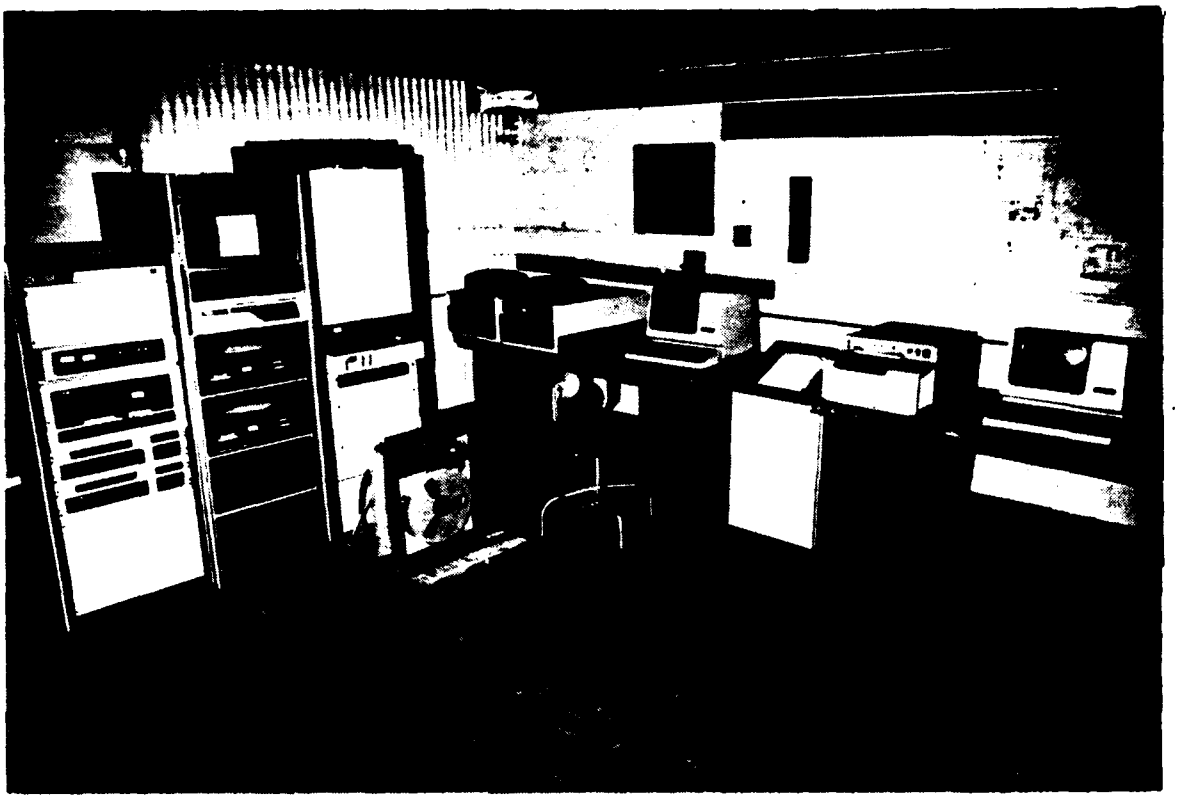

Figure 10. Image Controller System Hardware

The conceptual design called for the operator to interactively mark typical damage of each type on the IPS. In this way the feature-recognition software would be trained and could then locate, size, and classify the remaining damaged areas. Unfortunately, no feature-recognition software could be found or developed that would quickly and reliably process the large quantities of data produced by the FSP. Therefore, in the DAS developed by NMERI an operator must interactively identify each damaged area using the IPS. This procedure requires more time than the 30 minutes originally planned for the entire damage assessment process.

The IPS is manufactured by Interpretation Systems Inc. (ISI). It consists of an LSI-11 microprocessor, a VDI-200 video display processor, an FD-2 dual floppy diskette subsystem, an FT-1 function key-trackball module, a CG-1 cursor generator, a DM-1 system CRT terminal, 512 kbytes of refresh memory, a CR-20 color monitor, an XY-1 isometric projection generator with x-y display

monitor, a video digitizer light table subsystem, IF-3 DMA and IF-2 parallel interfaces, and VIEWS basic software. A list of the IPS equipment is presented in Table 9. The capabilities and operational details of the ISI VIEWS system are discussed fully in Section VI of Volume I of this report. A functional block diagram of the IPS as configured for the concept verification DAS is shown in Figure 11.

The IPS essentially acts as a terminal to the ICS during damage assessment operations. The IPS receives commands that prepare it to accept imagery data and to assign the desired functions to the programmable function keys by means of the IF-2 parallel interface. Imagery data are transferred to refresh memory by means of the IF-3 DMA interface. The function key/trackball unit is used to interactively enhance the image gray scale, magnify the image, scroll and translate within the image, move the cursor and window, and adjust the size of the window. These standard image capabilities are discussed in detail in Volume I of this report. The programmable function keys are programmed to move the image up and down (low-resolution mode); move the window to the cursor; read cursor location and window corner locations from the video display; mark and assign type values to features; transfer location, size, and type information back to the ICS by means of the IF-2 interface; call for other image sections from the ICS through the IF-2 interface; and terminate IPS operation. Most of the programmable function keys perform several operations at once. The programmable function keys are U1 through U8 and Y1 through Y8. The other function keys are preprogrammed by the VIEWS system. Table 10 lists the programmable function key operations for the low-resolution and high-resolution modes. The IPS is shown in Figure 12.

Software

Four specialized software programs were developed for the IAS. These programs transfer imagery data form the data link to mass storage, compress the full-resolution image to a lower resolution enhanced image, allow communication and data transfer between the ICS and the IPS, and process damage data in order to select the MOSs requiring the least amount of repair time.

TABLE 9. COMPONENT LIST FOR IMAGE PROCESSOR SYSTEM

IMAGE PROCESSOR SYSTEM

- VIEWS I
  - VDI-200 Display Processor
    Racks, Table
    FD-2 Dual Floppy Diskette Subsystem
    FT-1 Function Key-Trackball Module
    DM-1 System CRT Terminal
    CG-1 Cursor Generator
    Software (Views Basic)
    Integration with Total System
- RM-256 k Bytes Refresh Memory
- XM-256 k Bytes Refresh Memory
- CR-20 Color Monitor
- IF-3 DMA Interface
- IF-2 Interface
- Video Digitizer Subsystem
  - CVC-1 TV Camera
    LT 130 Light Table
    Video Digitizer
- XY-1 Isometric Projection Generator
  - XY Display Monitor

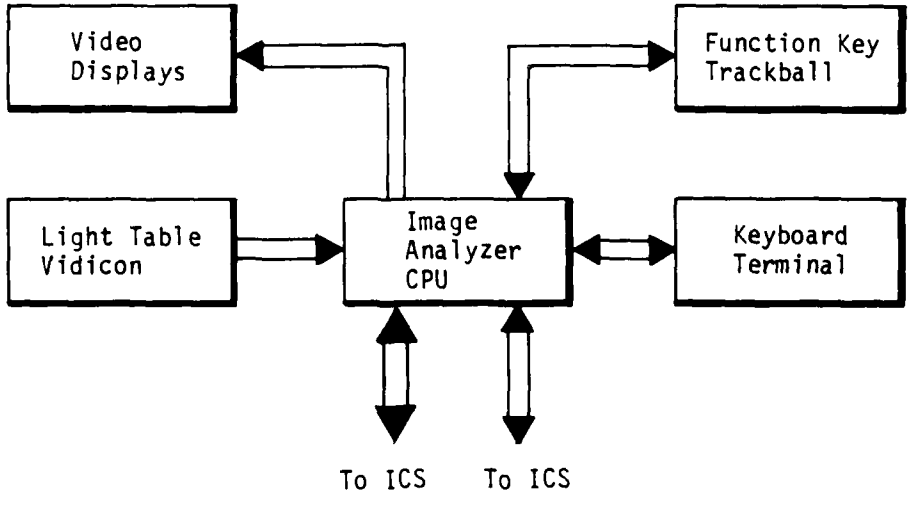

Figure 11. Block Diagram of Image Processor System

TABLE 10. PROGRAMMABLE FUNCTION KEY OPERATIONS

Key	Resolution	Title	Function
Y1	Low	IMAGE UP	Move image 3/4 frame up; move cursor to center left edge; connect cursor to trackball; disable trackball vertical.
	High	...	No function.
Y2	Low	IMAGE DOWN	Move image 3/4 frame down; move cursor to center left edge; connect cursor to trackball; disable trackball vertical.
	High	...	No function.
Y3	Low	LOCATION POINT (TYPE POINT NO.)	Read point number from terminal; read cursor location; write reference point record to 11/34; connect trackball to cursor.
	High	...	No function.
Y4	Both	WINDOW TO CURSOR	Read cursor location; calculate window corner locations; move window; connect window size to trackball; turn on window outline.
Y5	Both	NEXT IMAGE	Write end segment record to 11/34.
Y6	Both	RESET DISPLAY	Run initialization procedure; display text.
Y7	Both	RESTORE TEXT	Display text.
Y8	Both	EXIT	Write exit record to 11/34.
U1	Both	MARK CRATER	Read cursor location; read window corners; calculate window width; write damage record to 11/34; mark damage on display; connect cursor to trackball.
U2	Both	MARK CAMO-HEAVE[a]	
U3	Both	MARK SPALL FIELD	
U4	Both	MARK BOMBLET FIELD	
U5	Both	MARK SURFACE UXO	
U6	Both	MARK BURIED UXO	
U7	Low	MARK CLOSEUP WINDOW	Read cursor location; calculate window corners; write window record; mark display; connect cursor to trackball.
	High	DELETE DAMAGE	Read cursor value; read window corners; calculate window width; write damage-delete record to 11/34; mark removed damage; connect cursor to trackball.
U8	Low	MARK EDGE	Read cursor location; write edge record to 11/34; enable trackball vertical; connect cursor to trackball.
	High	...	No function.

a. The term camo-heave indicates a camouflet with upheaved pavement. This type of camouflet may be the only type that the IPS can distinguish.

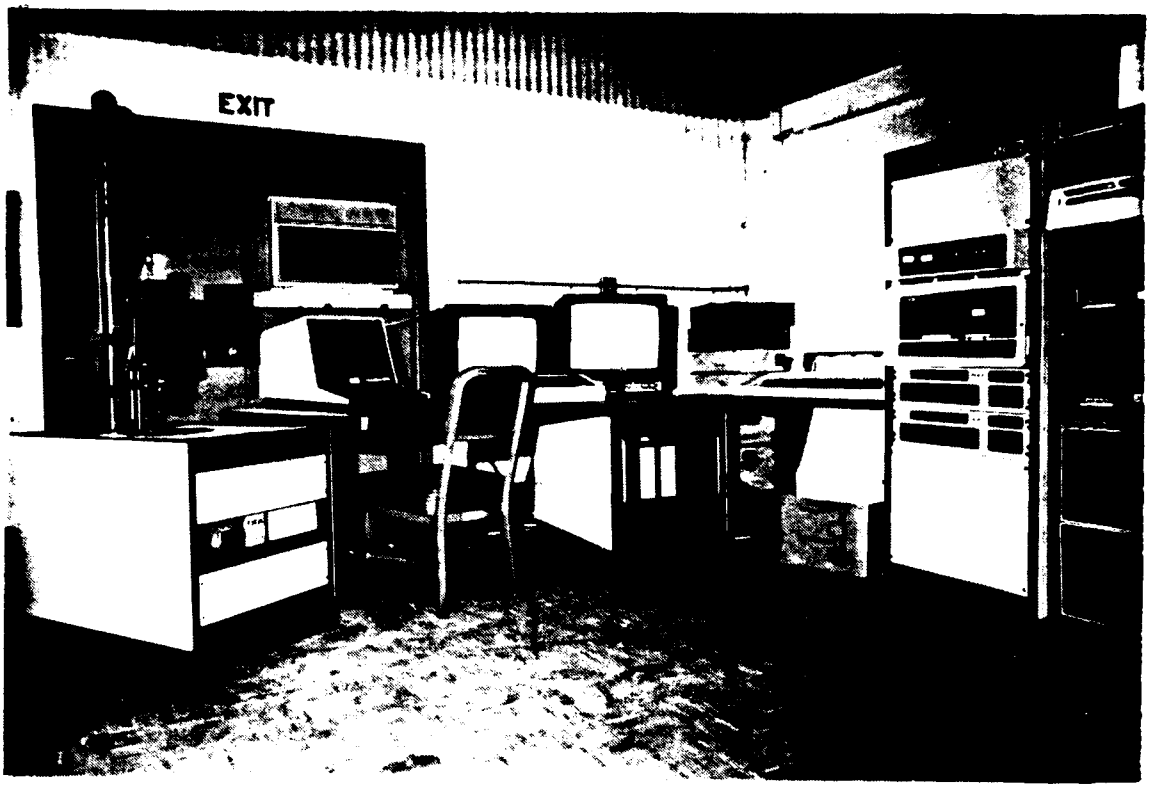

Figure 12. Image Processor System

XFR.TSK is the program that transfers imagery data from the data link to the mass storage disks. This program was developed by EG&G to operate in conjunction with the ADI-2. It is coded in assembly language for speed of operation. The program disables the operating system while it is running, which dedicates the entire ICS to the transfer process. The tape drive runs at one-fourth the record speed, which produces a data rate of 187k 16-bit words per second. This is close to the maximum data transfer rate of which the CPU (PDP-11/34) is capable. The sign bit of each data byte is inverted in the ADI-2 to speed the processing of the data in the image compression program. The XFR.TSK program alternately reads 2048 byte lines into two 8-line buffers and writes the data in the buffers to successive absolute mass storage disk addresses. After the data transfer is complete, the program writes a log file containing the line count and any error information. The XFR.TSK program is

capable of transferring up to 134 Mbytes of imagery data. The imagery data stored on disk have the same resolution and dynamic range as the image data recorded from the camera.

BUILDC.TSK is the program that compresses the full-resolution imagery data. This program creates a 64:1 reduced size file for rapid examination by an operator on the IPS. The compressed image is required because of the large number (512) of video screen size images (512 by 512 pixels) in the full-resolution data base. It requires 10 seconds to transfer each 512 by 512 pixel image from the ICS to the IPS and an average of 10 seconds to examine each image. Thus it would require more than 2 hours and 50 minutes just to look at all the full-resolution imagery data. The compressed image requires only four 20-second, 256 by 2048 pixel transfers and the examination of 32 frames, for an examination time of 10 minutes.

The compression program is coded in assembly language and, like XFR.TSK, it disables the operating system. BUILDC.TSK reads imagery data alternately into two 8-line buffers (1728 bytes per line). Each buffer is divided into 216 8-byte by 8-byte blocks. Each 64-byte block is processed by the program to produce one byte in the output file. The algorithm used to compress each 64-byte block into one pixel performs the compression in two steps. First ten sample points within the 64-byte block are examined, and the lowest value, the highest value, and the mean value of the sample points are determined. If the highest value minus the lowest value is less than a predetermined limit, the mean of the sample points is used as the output value for the compressed block. This routine is very fast, and the program can be forced to run in this mode exclusively when the limit on the difference between the high value and low value is set to 255. If the limit is not set at 255 and the difference between the high and low values is greater than the limit, a second routine is performed. In this routine, the horizontal and vertical change in value across each of the 36 internal pixels in the 64-byte block is determined. If the highest change value is less than the previously mentioned limit, then the high or low pixel value closest to the mean is used as the output value for the compressed block. If the highest change is greater than

this limit, the pixel value that corresponds to the highest change in value is used. This routine saves some of the high-resolution information that is lost when only the mean pixel value is used.

BUILDC.TSK was developed by NMERI in FORTRAN. Once the program had been debugged, EG&G converted the program to assembly language in order to increase its speed. This program also disables the operating system and monopolizes the ICS. Six minutes 3 seconds are required to produce a compressed version of the entire high-resolution data base on the mass storage disks.

DRIVER.TSK is the program that communicates between the ICS and the IPS. This program uses both a DR-11B interface to transfer imagery data and a DR-11C interface to transfer commands and damage data. Option A of DRIVER.TSK transfers a segment of the compressed image created by BUILDC.TSK to refresh memory on the IPS, establishes the proper memory organization, and programs the VIEWS system function keys for low-resolution damage assessment. After the transfer has been completed and the VIEWS system has been initialized, DRIVER.TSK waits for data from the IPS. All data returned from the IPS are formatted in eight integer records. The meaning of each integer is explained in Table 11. DRIVER.TSK writes these data to three disk files, one for low-resolution data, one for high-resolution data, and one that stores information for restart. Each file is duplicated to prevent the loss of data. Option B of DRIVER.TSK transfers full-resolution images from the ICS to the IPS, establishes the proper memory organization, and programs the VIEWS system function keys for high-resolution damage assessment. High-resolution data are indicated by a number 5 in data record integer 6. Programmable function key operations for the high-resolution mode are given in Table 10.

DRIVER.TSK was originally developed by ISI as part of the IAS integration and was later streamlined by NMERI. It was programmed in FORTRAN and operates under the RSX-11M operating system. It requires 10 seconds to transfer one 512-by-512 pixel image between the ICS and the IPS. Twenty seconds are required to transfer a 256-by-2048 pixel image.

TABLE 11. MEANING OF INTEGERS IN IPS DATA RECORD

Integer 1:	Action Code 1 = Store data 2 = Send next segment or image 3 = End option
Integer 2:	Data Type 1 = Crater 2 = Camouflet 3 = Spall Field 4 = Bomblet Field 5 = Surface UXO 6 = Buried UXO 7 = Area for Full-Resolution Inspection 8 = Edge Mark 9 = Scale and Location Mark
Integer 3:	Image Line Number
Integer 4:	Image Pixel Number
Integer 5:	Diameter for Types 1-6; Mark Number for 7-8
Integer 6:	Segment Number
Integer 7:	Unused
Integer 8:	Unused

The MOS selection program is divided into four parts. PART00.TSK reformats the data in the low-resolution and high-resolution data files produced by DRIVER.TSK for use in PART02.TSK. PART01.TSK accepts manually input damage data from the keyboard terminals. PART02.TSK processes the damage data to select a ranked set of MOS requiring the least amount of repair time. PART03.TSK prints out the results of PART02.TSK.

PART00.TSK converts the image coordinates and pixel dimensions of the damage data stored by DRIVER.TSK into station coordinates and dimensions in feet. The program requires the station coordinates of the location reference points marked during the damage assessment process. PART00.TSK, using the edge marks stored during damage assessment, also corrects for image distortion due to aircraft roll motion and lateral drift. The output of PART00.TSK is a fixed-length file of 150 5-integer field records. Field 1 is damage type.

Field 2 is distance from start of runway in feet. Field 3 is distance from centerline in feet (+ = right; - = left). Field 4 is damage diameter in feet. Field 5 is the count of damages in spall or bomblet fields.

PART01.TSK accepts damage data input from a terminal and creates a runway damage file of the same format as that produced by PART00.TSK. PART01.TSK also creates damage data files for ramp and taxiway damage and can correct the damage data files produced by PART00.TSK and PART01.TSK.

PART02.TSK uses the damage files stored by PART00.TSK and PART01.TSK to select the three best MOSs in the down-runway direction, the three best MOSs in the up-runway direction, and the three best bidirectional MOSs. The MOS selection program essentially moves an MOS template over the entire runway surface in fixed lateral, longitudinal, and angular increments, calculating repair times for each MOS location.

PART02.TSK considers six types of damage: craters, camouflets, spall fields, bomblet fields, surface UXOs, and buried UXOs. To determine the repair time for a given MOS, each damaged area in the runway damage file is tested to determine whether its radius of effect lies within the MOS. The radius of effect of a crater was assumed to be approximately the same as the repair radius and was calculated using the following equation:

$$R_E = 5\ (D)^{0.5} \tag{6}$$

where R_E is the radius of effect and D is the apparent crater diameter, both in feet. The radius of effect for camouflets, surface UXOs, and buried UXOs was set at 25 feet. The radius of effect for spalls and bomblet fields was assumed to be one-half of the field diameter.

If the radius of effect of a damaged area falls within the MOS, a repair time is determined. Repair times for craters and camouflets are determined by the methods discussed under Repair Equations in Section II of this report. Location within the MOS and multiple damage spacing criteria are used to determine the repair quality for craters; the apparent radius and the repair quality are used to determine a crater repair time from a lookup table

(Table 3). Repair times for camouflets are determined by using Equations (3) and (5). It is assumed that it will take 60 seconds to repair each spall. No repair times are assigned to bomblet fields or surface UXOs, but their number, size, and location are stored with the MOS they affect. Buried UXOs are considered in one of two ways. The operator determines which method will be used at the beginning of PART02.TSK. All buried UXOs are assumed either to be duds, in which case a repair time of 10 minutes is assigned for each, or to have exploded, leaving craters that must be repaired. The size of the crater formed by a buried UXO is estimated from the diameter of the port of entry. All buried UXO crater repairs are assumed to be A quality. Repair times for up-runway, down-runway, and bidirectional orientations are calculated. Access repair times determined from the ramp and taxiway damage files produced in PART01.TSK are added to the MOS repair time, and the total MOS repair time is tested against the three best repair times in each MOS category. Only the three best repair times, along with MOS locations and damage information, are saved. After all possible MOS locations have been examined, data for the three best MOSs in each category are written to an output file.

In PART02.TSK, the operator can set the MOS size and the lateral, longitudinal, and angle increments. The operator can also specify whether buried UXOs are to be considered as having exploded and formed detonation craters or as being duds whose damage can be repaired without danger from explosions. The operator provides the air-density ratio required by PART02.TSK for the determination of the crater repair spacing criterion.

PART03.TSK prints the results of PART02.TSK. Full damage details, repair times, and MOS locations are listed for the three best MOSs in each category.

The MOS selection programs were developed by NMERI in FORTRAN. All parts run under the RSX-11M operating system.

Hardcopy Recorder

The hardcopy recorder included in the IAS is a Tektronics 4633A continuous hardcopy recorder. This unit requires an analog video signal and a ramp signal to produce a two-dimensional black-on-white image. As dry silver paper

is continuously passed in front of a fiber optic face plate attached to a CRT, the intensity of the CRT beam is modulated by the video signal, and the deflection of the beam is controlled by the ramp signal. The exposed paper is thermally developed as it leaves the CRT. The paper used in the hardcopy recorder is 8-inch-wide 3M Type 7772 dry silver paper. The paper speed is adjustable to 10, 20, 25, 50, and 100 mm/s. The 100-mm/s speed was used to produce a hardcopy of the recorded imagery data at the 1.5-MHz data rate. The spot size of the CRT beam is 6 mils. The image produced has approximately 16 distinguishable gray levels.

In the IAS the hardcopy recorder is connected only to the input data interface. Output of the hardcopy recorder can be visually inspected for damage. The damage location and size can be measured from the image. Information on the location, size, and type of damage can then be fed to the ICS manually, by means of a keyboard terminal. This method provides an alternative to processing the imagery data on the IPS. There are two problems with this procedure. First, the resolution of the hardcopy image is about one-half that of the full-resolution video data. Second, the time required to obtain the location and size of the damaged area and to feed the data through a terminal is longer than that required for the IPS.

SECTION IV
SYSTEM DEVELOPMENT AND TESTING

DEVELOPMENT HISTORY

During February 1978, NMERI presented a briefing to AFESC on the results of the investigation of various damage assessment methodologies. AFESC then selected for further development a DAS based on an airborne Vidicon camera and a computerized image processing system. In August 1978 NMERI received guidance and approval for a limited development effort on the selected DAS. NMERI initiated the development of a conceptual stabilized platform design, hardware and software specifications, and a conceptual lighting system design, as well as verification of the system's compatibility with Quick Strike Reconnaissance (QSR). A contract for the development and testing of a linear CCD array camera was awarded in September 1978.

The hardware and software specifications, the conceptual lighting system and stabilized platform designs, the QSR verification, the weather effects study, and the carrier aircraft evaluation had been completed by November 1978. The lighting requirements of the linear CCD array were determined to be extremely high. The lighting system had to be carefully stabilized and aligned with the CCD camera. It also required large amounts of electrical power and was extremely bulky. Guidance from AFESC received in June 1979 indicated that the development of the concept verification system using the CCD sensor should continue, but that only a partial lighting system would be required. The requirement to construct the lighting system was later deleted. At the same time, methods for improving the sensitivity of the sensor were to be investigated for use in a future system. The possibility of using image-correction software in conjunction with, or instead of, a stabilized platform was also to be investigated.

During January 1979, deficiencies were discovered in the CCD camera that was being developed under subcontract. Between January and May 1979, efforts were made to solve noise, timing, adjustment, and testing problems. However, the subcontract was terminated in May 1979, and a replacement sensor was ordered. The replacement sensor selected was a Fairchild CCD 1400 line-scan

camera. Fairchild agreed to conduct sensitivity testing of the sensor, and NMERI was to conduct vibration testing. The sensor was delivered and testing was completed by October 1979.

In June 1979, NMERI received the necessary guidance and approval to continue development of the DAS. NMERI provided the list of required image-processing equipment, which was approved by AFESC. A subcontract for the computerized image-processing equipment and system integration was awarded to Interpretation Systems, Inc. (ISI). Components of the system were delivered in August and November 1979. Integration of the system was not completed until June 1980 because of equipment and software problems.

Investigation of automated image-processing techniques and available image-processing software began in January 1979 and continued through the end of the project. It had become apparent by April 1979 that more sophisticated algorithms than had been originally envisioned would be required for automatic damage assessment. The reliability and accuracy of the available techniques were somewhat questionable, and the time required to process the extremely large full-resolution data base appeared to be much greater than that required to manually identify the damages from the imagery. NMERI was unable to test any automatic feature-recognition software on the IAS because of the lack of realistic imagery data and limited development time.

A data link tradeoff analysis was conducted during the summer of 1979. The analysis was completed in September 1979, and AFESC approved the procurement of an Ampex AR1700 HBR airborne digital tape recorder. The recorder was delivered in May 1980.

The design of interfaces for linking the airborne camera and the recorder, and the recorder and the IAS, began in November 1979. Final design specifications had to await completion of the IAS integration software supplied by ISI. The integration software format was completed in late January 1980, and a contract for development of the interfaces was awarded to EG&G in April 1980. The airborne interface was completed in August 1980, and the IAS interface was completed in October 1980.

A tradeoff analysis of methods for reducing the lighting requirements of the CCD sensor was conducted between October 1979 and June 1980. Alternate sensors as well as image intensifiers were investigated. NMERI recommended the use of a laser line-scan sensor, which would require no additional lighting system, in a future DAS. Further investigation of a relief-measuring sensor was also recommended.

In March 1980 AFESC requested that NMERI present a limited demonstration of the DAS during the Interim Crater Repair Test to be held at North Field, South Carolina, in August 1980. NMERI demonstrated the FSP using the hardcopy recorder to display output. Damage assessment procedures developed for the IPS were demonstrated on a similar system provided by ISI. The ISI equipment was also used in the demonstration of the MOS selection software program. In addition, two formal presentations explaining the DAS were made during the test. Valuable imagery data were acquired during the demonstration; these were used in completing the system development and evaluation.

Portions of the IAS software were developed independently by ISI, EG&G, and NMERI between July 1979 and November 1980. ISI developed the software that allowed communication between the ICS and IPS and controlled the IAS as a system. A portion of this software performed a compression of the full-resolution imagery data. The ISI software was completed during May 1980 as part of the IAS integration. EG&G developed a special stand-alone program that rapidly transferred the full-resolution imagery data from the input data interface to the mass storage disks. This software was delivered with the input data interface in October 1980.

NMERI developed the MOS selection software and the function key scripts for interactive damage identification. The original design and some coding of the MOS selection software and function key scripts were completed prior to May 1980, but implementation on the IAS was delayed until the system integration had been completed. NMERI received new information during May and June 1980 concerning the types of damage expected and the criteria for determining crater repair times. In light of this information, modification of the damage assessment scripts and significant redesign of the MOS selection software were required. The damage assessment scripts and MOS selection software were implemented on the IPS in July 1980 and demonstrated at North Field in August 1980.

After the North Field demonstration, NMERI developed a faster, more useful image-compression algorithm; developed the software to handle the specific data transfers between the ICS and IPS required in the damage-assessment process; and converted the North Field MOS selection software to operate on the ICS. This software was completed by November 1980 and was demonstrated in the DAS field demonstration that month. Neither the IAS software design nor the software itself could be refined or optimized during this effort because of the limited time available. The software did perform all required tasks except the automated feature extraction..

A tradeoff analysis of camera stabilization versus software image correction was conducted after the airborne testing of the Fairchild sensor during June 1980. NMERI recommended that camera stabilization and software image correction be incorporated into an operational system, but suggested that software image correction alone would be adequate for the concept verification of the DAS. The software image correction was included in the MOS selection software.

EFFECTS OF ADVERSE WEATHER ON FSP SENSOR

NMERI was required to assess the effects of adverse weather conditions such as fog, rain, snow, and high winds on the resolution capabilities of the FSP sensor. For the purposes of this study the FSP sensor was assumed to be the Fairchild CCD 1400 line-scan camera. It became apparent during the investigation that adverse weather conditions significantly affect image parameters other than resolution. These parameters were therefore included in the study.

Gusting winds, fog, smoke, dust, rain, and snow all adversely affect the performance of the FSP sensor. Gusty wind conditions cause undesirable motions of the carrier aircraft, and these cause a distortion of the gathered image and errors in the displayed damage locations. Fog, smoke, dust, rain, and snowfall reduce transmissivity and scene contrast so that a larger lighting system is required and feature recognition becomes more difficult. The minimum resolution element size, however, is not drastically affected by these conditions. Careful design of the camera and lighting systems, selection

of the proper carrier aircraft, and use of additional instrumentation and computer software will minimize the effects of adverse weather. However, extremely high winds or gusts, moderate to dense fog and smoke, or heavy rain or snowfall will render even the most carefully designed system inoperable. The various weather conditions, their effects, and the related design considerations are discussed in more detail below.

Wind and Gusts

The FSP is designed to be carried by a helicopter or a low-speed, fixed-wing aircraft. Ideally, the FSP is flown at a constant speed of 70 knots and a constant altitude of 270 feet directly over the centerline of the runway; the optical axis of the camera is vertical; and the axis of the CCD array is perpendicular to the direction of motion over the ground. Any deviation from this ideal will cause distortion of the image produced by the CCD camera. Some nonideal motion of the carrier aircraft is to be expected even in still air because of lag in the aircraft's response to control inputs and limitations in the pilot's ability to determine his exact speed, altitude, and lateral position. Wind--especially gusts--causes additional undesirable motion of the carrier aircraft. The amount and type of motion caused by a given wind condition depend on the type of aircraft being used and on the pilot's skill. Translational motion of the aircraft is transmitted directly to the camera. The extent to which rotational motion of the aircraft is transmitted to the camera depends on the sophistication of the camera stabilization system. Extremely high winds or large gust spreads will ground any of the carrier aircraft considered.

The aircraft considered as carriers for the FSP were the UH-1N helicopter, the OV-10 fixed-wing aircraft, and the Cessna models 172 and 180 light fixed-wing aircraft. NMERI was unable to find documented specifications for aircraft stability under various wind conditions at flying speeds suitable to the FSP. Therefore, experienced pilots, familiar with the stability and handling characteristics of each aircraft, were consulted, and estimates of each aircraft's performance under a variety of wind conditions were obtained.

In still air the UH-1N and Cessna models can maintain flight within ±10 feet laterally, ±10 feet vertically, and ±5 knots of the nominal flight parameters. The OV-10 has a minimum flying speed of 80 knots, which is higher than desired, and it displays significant adverse roll-yaw coupling that makes it difficult to handle at speeds below 100 knots. This adverse coupling does not disappear until the airspeed exceeds 120 knots. To fly the camera at the increased speeds compatible with the OV-10 would require significant modification of the FSP. Under calm conditions, roll, pitch, and yaw motion on all aircraft should be less than ±1 degree.

A steady wind will not significantly affect the flight envelope achievable by any of the aircraft. By adjusting his airspeed and crabbing into the wind, a pilot can achieve the desired ground speed and heading within the tolerances obtainable in calm conditions. The yaw angle would increase, but it should remain constant, ± 1 degree, during a given pass.

Gusts and turbulence will cause more serious problems. The mass of the aircraft, the amount of surface area acted on by the gust, the responsiveness of the aircraft, and the pilot's skill all influence the magnitude of the motion resulting from given gust conditions. The H-1 tolerances increase to ±40 to ±50 feet altitude (without radar altimeter), ±30 to ±40 feet laterally, and ±10 knots velocity for gust spreads of 20 knots. The Cessnas should be able to maintain ±25 to ±30 feet vertically (with radar altimeter), ±30 to ±40 feet laterally, and ±10 to ±15 knots forward velocity in the same gust spread. Gusts and turbulence will also introduce significant amounts of roll, pitch, and yaw. The H-1 and Cessna aircraft should stay within ±5 to ±8 degrees of the nominal attitude in gust spreads up to 20 knots. The pilot of a fixed-wing aircraft must increase airspeed somewhat in gust conditions to provide a margin of safety above stall speed.

The 1550th Air Crew Training and Test Wing (ATTW) at Kirtland Air Force Base, New Mexico, grounds its aircraft when wind speed exceeds 30 knots or when gust spreads exceed 20 knots. The aircraft can fly in more severe conditions, but there is a safety risk. If gust spread exceeds 20 knots, it is questionable that the FSP could produce a usable image. It should be noted

that all of the aircraft performance figures presented above are based on estimates obtained from various pilots.

The FSP was tested only in a Cessna 180. Neither still air nor high wind conditions were encountered during testing. In very light wind the lateral drift of the aircraft remained within ±10 feet, but in a 6- to 12-knot wind the lateral drift increased to ±30 feet. The roll motion of the aircraft was higher than anticipated. Aircraft roll of ±3 degrees was not uncommon. This motion was at least partially due to the pilot's use of banking to maintain lateral position above the runway.

Fog, Rain, and Snow

The atmospheric phenomena of fog, rain, and snow interfere with the desired transmission of light from ground to camera, from ground to pilot, and from lighting system to ground. The most detrimental effects appear to be a reduction of transmissivity and contrast due to scattering. Absorption is much less significant and optical distortion appears to be insignificant over the distance from the ground to the camera (less than 300 feet). Other effects such as back-scattering from the lighting system and droplets contacting the lens surfaces are not extensively documented, but are intuitively considered undesirable.

Transmittance through the atmosphere along a given path can be expressed as the product of transmittance due to absorption and transmittance due to scattering. Transmittance due to absorption is highly wavelength-dependent for the sensitivity range of the CCD sensor. Water vapor is the only significant absorber in the sensitivity bandwidth of the CCD. The amount of water vapor along a path is expressed as millimeters of precipitable water. Table 12 lists transmittances by wavelength for typical and worst-case water vapor contents over the sensitivity range of the CCD (Reference 5). Even under worst-case conditions, transmittance remains above 80 percent.

Two types of scattering affect the transmission of light. The first, Rayleigh scattering, is strongly wavelength-dependent. Rayleigh scattering occurs when the scattering particles are smaller than the wavelengths of the

TABLE 12. TRANSMITTANCE DUE TO ABSORPTION BY WATER VAPOR

Wavelength, microns	Transmittance	
	2 mm H_2O	10 mm H_2O
0.3	0.911	0.802
0.4	0.911	0.802
0.5	0.937	0.861
0.6	0.955	0.900
0.7	0.960	0.910
0.8	0.950	0.891
0.9	0.844	0.661
1.0	0.955	0.900
1.1	0.856	0.707

(Data reproduced from Reference 5 by permission of John Wiley and Sons, Inc.)

Notes: 2 mm H_2O represents 68°F; 65 percent relative humidity; 600-foot path length at sea level.

10 mm H_2O represents 100°F; 100 percent relative humidity; 800-foot path length at sea level.

incident light. Because shorter wavelengths are scattered more than longer wavelengths, selective filtering of the scattered light can be used to improve the observed contrast. The second type, Mie scattering, is independent of wavelength. It occurs when particle radii are larger than the wavelengths of the incident light. Contrast cannot be improved by selective filtering when Mie scattering occurs. The following equations (Reference 5), can be used to calculate the effect on transmissivity of scattering due to spherical particles:

$$\tau = e^{-\gamma x} \tag{7}$$

$$\gamma = \pi \, nKr^2 \tag{8}$$

where

τ = transmissivity

x = path length

n = number of particles per milliliter

r = particle radius

γ = scattering coefficient

K = scattering area ratio

K is obtained from Figure 13 (Reference 5), and λ is the wavelength of the incident light.

Scattering reduces the observed contrast between objects by reducing the intensity of the transmitted light, lowering the transmittance, and increasing the background intensity. The human eye can distinguish a 2-percent contrast. The contrast distinguishable by the CCD sensor is limited by the dynamic range of the camera. The dynamic range of the camera is 200:1. Eight-bit digitization allows for 256 intensity levels.

The CCD is sensitive to radiation with wavelengths between 0.3 and 1.1 microns. Most fog droplets, ice crystals, and smoke particles have radii greater than 5 microns. Rain droplets have radii greater than 250 microns. Consequently, scattering due to these phenomena will be Mie scattering, and the CCD sensor will offer no advantage over the human eye in penetrating fog, rain, snow, or smoke. The CCD sensor would provide an advantage in hazes and extremely fine mists or smoke, but these conditions do not present a serious scattering problem over the short distances of concern.

Fog and low-lying clouds present a very serious problem to the operation of the FSP. A very light fog, one that limits visibility to 3000 feet, has about 25 particles per milliliter with radii of about 5 microns and will reduce transmittance over the 600-foot path to less than 50 percent. A heavy fog, one with 200 particles per milliliter, will reduce transmittance over a 300-foot path to less than 6 percent and over a 600-foot path to less than 0.33 percent. The reduction of contrast is harder to quantify. However if enough light is available for the CCD sensor to use the lower half of its dynamic range, the CCD camera should be able to distinguish contrasts about as well as the human eye. In a light fog, transmittance 50 percent, the lighting requirements will be increased by 100 percent. Rain and snow should not affect the CCD sensor as drastically as does fog. Although rain and snow particles are significantly larger than fog particles, the number of particles per milliliter is much smaller. Table 13 (Reference 5) lists transmittances

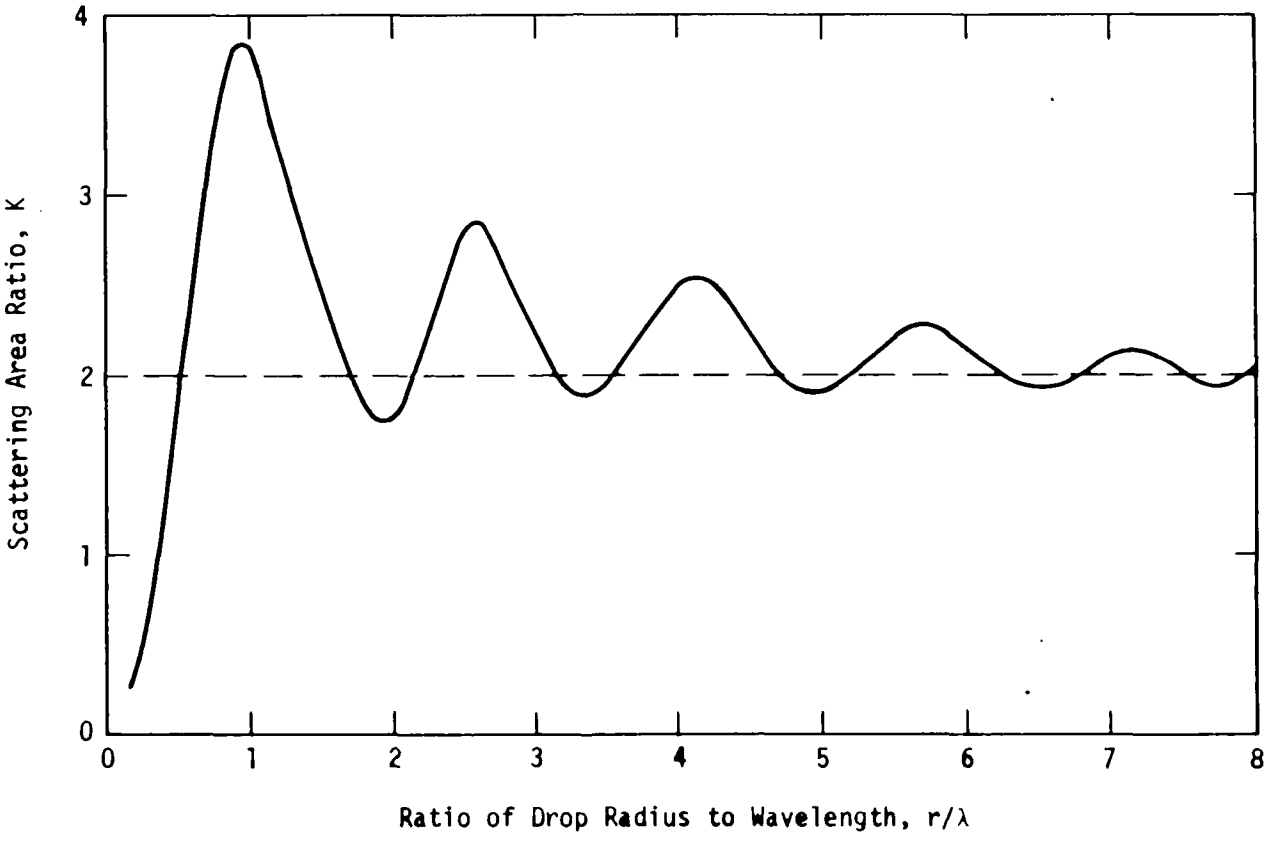

Figure 13. Scattering Area Ratio for Transmissivity Calculation (after Reference 5 by permission of John Wiley and Sons, Inc.)

along a 6000-foot path in various rain conditions. Little information is available on transmittance through falling snow. The particle size of both rain and snow produces Mie scattering in the sensitivity range of the CCD array; therefore, the loss of contrast will again be similar to that sensed by the human eye. Both rain and snow will increase the lighting requirements of the system.

TABLE 13. TRANSMITTANCE OF A 6000-FOOT PATH THROUGH RAIN

Condition	Rainfall Rate, mm/h	Transmittance (6000-ft path)
Light Rain	2.5	0.88
Medium Rain	12.5	0.74
Heavy Rain	25.0	0.65
Cloudburst	100.0	0.38

(Data reproduced from Reference 5 by permission of John Wiley and Sons, Inc.)

Fog, smoke, rain, and snow can produce back-scattering when the illumination source is close to the camera. Back-scattering will further reduce the observed contrast between objects by raising the background illumination level. Separating the light source from the camera will reduce the amount of back-scattered light sensed by the camera.

In general, the CCD camera system offers no advantage over the human eye in penetrating fog, clouds, smoke, rain, or snow. The camera system will require a significant increase in lighting capacity over that required in clear air to operate in even the lightest fogs and smokes or in moderate rain and snow storms.

Miscellaneous Effects

Several other weather conditions that could affect the CCD system should be mentioned. These conditions and their effects were not extensively investigated, but they should be considered in the design of the system and recognized as potential problems in the operation of the system.

Rain and snow accumulate on the ground, changing the reflective properties of the observed surfaces. Rain first moistens, then wets, then submerges ground surfaces. Snow either melts when it strikes the ground, producing the same effects as rain, or accumulates, covering and obscuring the surfaces. Qualitatively, wetting will reduce the diffuseness of a surface, making it more mirror-like. The spectral reflectance (dependent on wavelength) of a surface may change. Effects vary from surface to surface. Puddling could obscure small runway features and produce nonuniform reflectance from undamaged surfaces, which would complicate feature recognition. However, puddling should not have time to occur in recently disturbed areas, and the moisture could actually facilitate the recognition of damage. Similarly, snowfall should not have time to accumulate on recently damaged areas and may melt selectively around such features, facilitating recognition.

The effects of fog, rain, and snow are discussed in the preceding subsection, but the effects of only a uniform condition were considered. Conditions could vary over the length of a 10,000-foot runway, resulting in continually changing lighting requirements and reflective properties on the ground. Electrical storms could also present a problem. Lightning would drastically increase the illumination level on the ground for short periods of time.

EFFECTS OF NONIDEAL CAMERA MOTION

Nominally, each pixel in the CCD camera will instantaneously sense an area 1.9 inches wide on the ground, and that area will move 1.9 inches along the length of the runway between successive samplings. Nominal altitude is 270 feet; nominal ground speed is 70 knots; and nominal line-scan rate is 732.4 lines per second. The lateral location of features is determined by the location in the CCD of the pixels that sense the feature; the longitudinal location is determined by the number of lines between a reference scan, such as the beginning of the runway, and the scan in which the feature is detected. The lateral dimension of a feature is determined by the number of pixels that sense the feature during one line scan and the longitudinal dimension by the number of successive samplings in which the feature is sensed by a given pixel.

The most significant effects of nonideal camera motion appear to be distortion of feature dimensions and errors in recorded feature locations. By assuming that the camera is rigidly attached to the carrier aircraft; defining roll, pitch, and yaw axes and angles as shown in Figure 14; and summing the additive effects of the various types of aircraft motion, the following equations for errors in feature positions and dimensions were derived. The error in recorded lateral position for a pixel sensing a location on the ground an angle ϕ from the optical axis of the camera, where ϕ is measured in the same plane as roll angle, is given by the following equation:

$$\Delta Y_{tot} = \Delta Y_c + (h + \Delta h)\left[\frac{\tan(\phi + \alpha)}{\cos\beta}\cos\gamma - \tan\beta\sin\gamma\right] - h\tan\phi \qquad (9)$$

where

ΔY_{tot} = total lateral error (feet)

ΔY_c = lateral camera position error (feet)

h = altitude (feet)

Δh = altitude error (feet)

ϕ = angular position of pixel from camera axis (radian) measured in same plane as roll angle

α = roll angle (radians)

β = pitch angle (radians)

γ = yaw angle (radians)

This equation takes into account changes in lateral position and altitude and in roll, pitch, and yaw angles. Errors in longitudinal position for the same pixel are given by the following equation:

$$\Delta X_{tot} = t\,\Delta\bar{\dot{X}} + (h + \Delta h)\left[\tan\beta\cos\gamma + \frac{\tan(\phi + \alpha)}{\cos\beta}\sin\gamma\right] \qquad (10)$$

where

ΔX_{tot} = error in longitudinal position (feet)

$\Delta\bar{\dot{X}}$ = error in average longitudinal velocity (feet per second)

t = elapsed time from reference point (seconds)

This equation takes into account changes in altitude and deviations from the nominal ground speed and roll, pitch, and yaw angles.

Axes conversions:

$$\bar{z} = \bar{z}_1$$
$$\bar{y} = \bar{y}_1\cos\gamma + \bar{x}_1\sin\gamma$$
$$\bar{x} = \bar{x}_1\cos\gamma + \bar{y}_1\sin\gamma$$

$$\bar{z}_1 = \bar{z}_2\cos\beta + \bar{x}_2\sin\beta$$
$$\bar{y}_1 = \bar{y}_2$$
$$\bar{x}_1 = \bar{x}_2\cos\beta - \bar{z}_2\sin\beta$$

$$\bar{z}_2 = \bar{z}_3\cos\alpha + \bar{x}_3\sin\alpha$$
$$\bar{y}_2 = \bar{y}_3\cos\alpha + \bar{z}_3\sin\alpha$$
$$\bar{x}_2 = \bar{x}_3$$

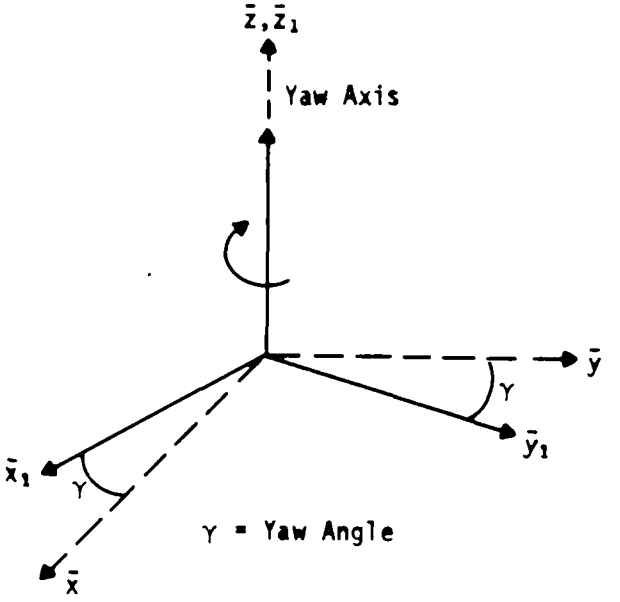

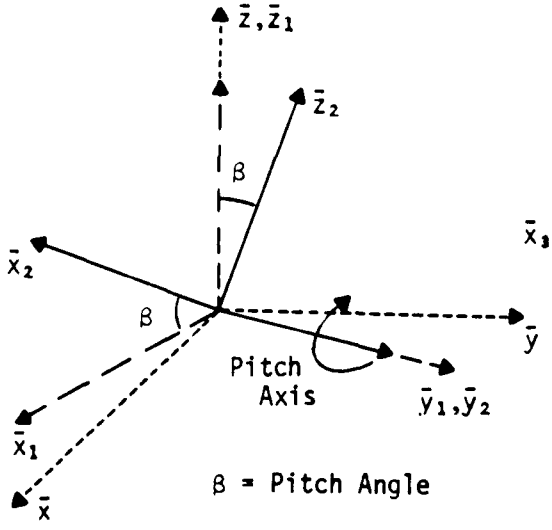

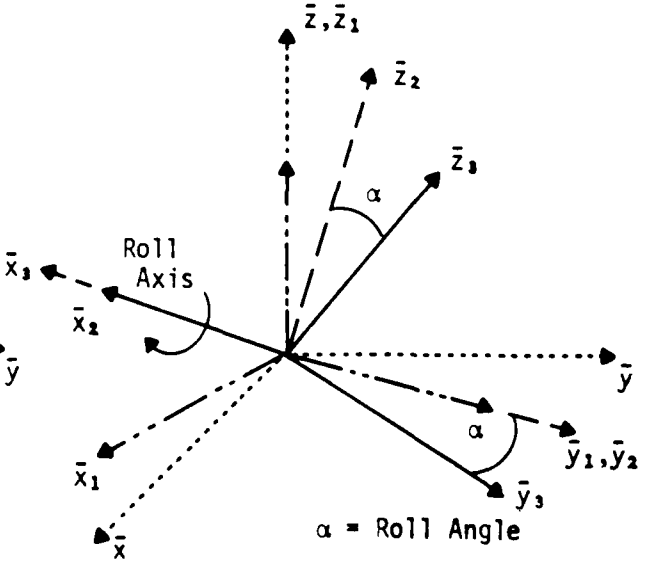

Figure 14. Axes of Rotation

The lateral dimension of a feature is determined by the number of adjacent pixels it covers. Changes in the center-to-center lateral spacing of areas sensed by adjacent pixels will alter the apparent lateral dimension of the feature. Equation (11) expresses the percent error in lateral dimension of a feature centered on a pixel an angle ϕ from the optical centerline of the camera, due to deviations from nominal altitude and roll, pitch, and yaw angles. Lateral velocities may cause blurring of feature edges and skewing of the image but will not affect the lateral spacing of areas sensed by adjacent pixels.

$$E_y = 1 - \frac{(h + \Delta h)\cos(\phi)\cos\gamma}{h\cos\beta\cos(\phi + \alpha)} \tag{11}$$

where E_y = the percent error in displayed lateral dimension.

The longitudinal dimension of a feature is determined by the number of successive times it is sensed by a given pixel (the number of lines it spans). Deviations from the nominal longitudinal distance traveled between successive samplings of the pixel will cause an error in the longitudinal dimension of the feature. The percent error in longitudinal dimension indicated by the pixel mentioned above will be

$$E_x = 1 - \frac{\dot{X}_n + \Delta\dot{X} + \Delta\dot{h}[\tan\beta\cos\gamma + \tan(\phi + \alpha)\sin\gamma/\cos\beta]}{\dot{X}_n}$$

$$- \frac{(h + \Delta h)\dot{\gamma}[\tan(\phi + \alpha)\cos\gamma/\cos\beta - \tan\beta\sin\gamma]}{\dot{X}_n}$$

$$- \frac{(h + \Delta h)\dot{\beta}[\cos\gamma(1 - \tan^2\beta) - \tan(\phi + \alpha)\sin\gamma\sin\beta/\cos^2\beta]}{\dot{X}_n}$$

$$- \frac{(h + \Delta h)\dot{\alpha}[1 - \tan^2(\phi + \alpha)]\sin\gamma}{\dot{X}_n} \tag{12}$$

where

E_x = percent error in longitudinal dimension

$\Delta\dot{X}$ = error in instantaneous longitudinal velocity (feet per second)

$\dot{X}_n$ = nominal longitudinal velocity (feet per second)

$\Delta\dot{h}$ = rate of change of altitude (feet per second)

$\dot{\gamma}$ = yaw rate (radians per second)

$\dot{\beta}$ = pitch rate (radians per second)

$\dot{\alpha}$ = roll rate (radians per second)

Changes in forward velocity; roll, pitch, and yaw angles and rates; altitude; and rate of altitude change will affect the displayed longitudinal dimension.

The following are the expected deviations from the nominal flight parameters for the UH-1N helicopter in 20-knot gust spreads:

Roll and pitch angles, α and β: 0.140 radian (8 degrees)

Yaw angle, γ: 0.175 radian (10 degrees)

Roll, pitch, and yaw rates, $\dot{\alpha}$, $\dot{\beta}$, and $\dot{\gamma}$: 0.087 radian per second (5 degrees per second)

Altitude error, Δh: 50 feet

Rate of altitude change, $\Delta\dot{h}$: 10 feet per second

Lateral position error, ΔY_c: 40 feet

Average velocity error, $\Delta\bar{\dot{X}}$: 8.4 feet per second (5 knots)

Instantaneous velocity error, $\Delta\dot{X}$: 16.8 feet per second (10 knots)

The nominal flight parameters are

Altitude, h: 245 feet

Velocity, $\dot{X}_n$: 118 feet per second

Time, t, at end of run: 80 seconds

A pixel at the edge of the camera's field of view (ϕ = 28 deg) is considered because it will be most severely affected. The following are the

positional and dimensional errors caused by motion along or about each axis separately:

Errors due to roll angle and rate only:

$\Delta Y_{tot} \approx 48$ feet

$\Delta X_{tot} \approx 0$ feet

$E_y \approx -9$ percent

$E_x \approx 0$ percent

Errors due to pitch angle and rate only:

$\Delta Y_{tot} \approx 1$ foot

$\Delta X_{tot} \approx 35$ feet

$E_y \approx -1$ percent

$E_x \approx -18$ percent

Errors due to yaw angle and rate only:

$\Delta Y_{tot} \approx -2$ feet

$\Delta X_{tot} \approx 23$ feet

$E_y = 2$ percent

$E_x = -10$ percent

Errors due to altitude error and rate of change only:

$\Delta Y_{tot} = 27$ feet

$\Delta X_{tot} = 0$ feet

$E_y = -20$ percent

$E_x = 0$ percent

Errors due to lateral displacement only:

ΔY_{tot} = 40 feet

ΔX_{tot} = 0 feet

E_y = 0 percent

E_x = 0 percent

Errors due to velocity changes only:

ΔY_{tot} = 0 feet

ΔX_{tot} = 672 feet

E_y = 0 percent

E_x = -14 percent

Combining all of the above undesirable motions, one obtains

ΔY_{tot} = 116 feet

ΔX_{tot} = 751 feet

E_y = -31 percent

E_x = -52 percent

The deviations from nominal flight parameters used in this example are the maximum values expected from the UH-1N aircraft and were selected to give the maximum additive effect. The errors attributed to rotational motion could be reduced by using a 3-axis stabilized platform. The magnitude of the remaining errors indicates that other corrective measures such as additional instrumentation or corrective software are also required.

The dynamic resolution element is defined as the area scanned by a single pixel during a single exposure period: nominally, 1.9 inches laterally and 4.4 inches longitudinally. Nominally, there will be a 2.5-inch overlap in the longitudinal direction. The size of the static component is affected only by

changes in effective altitude. The percent change in static component size is opposite to the percent error in lateral dimension as calculated in Equation (11). The dynamic component of a resolution element is determined by the effective velocity of the element and the integration time. The percent change in dynamic component size is opposite to the percent error in longitudinal dimension as calculated in Equation (12). Thus, on the basis of the parameters used in the previous example, the maximum static component size anticipated is 31 percent larger than the nominal size, or 2.5 inches by 3.25 inches. The maximum dynamic component length anticipated would be 80 percent greater than the nominal length, or 3.4 inches. Although the dynamic resolution element length is much larger than the static width, the motion of the camera during the integration period and the static length of the resolution element weigh the center portion of the dynamic element length much more heavily than the ends. The central 1.9-inch by 1.9-inch section of the nominal 1.9-inch by 4.4-inch dynamic resolution element would account for more than 70 percent of the signal produced by a uniform field.

LIGHTING REQUIREMENTS

The factors found to influence the lighting requirements can be generally described as affecting the intensity and efficiency of the light source. A wide range of factors influence the intensity of the light source. Essentially, they can be sorted into the following categories:

1. Irradiation required at the observed ground
2. Required area of lighted ground
3. Efficiency of the lamp design

The factors affecting the efficiency of the light source include the radiometric efficiency of the lamp and the efficacy of the source spectral distribution with respect to the spectral response of the sensor. All of these factors affect the electrical power requirements of the lighting system.

Irradiance Required at Observed Ground

The irradiation required on the observed ground was found to be a function of lens speed designation, maximum integration time, peak-to-peak noise

level of sensor, system input noise level, spectral reflectance of observed ground, and light transmission losses through the camera lens and through the atmosphere.

The lens speed designation, or f stop number, is one of two characteristics (the other being the focal length) that describe a camera lens. The lens speed designation is a direct measure of the amount of light that passes through the lens. The lower the f stop number, the more light passes through. The amount of light varies inversely as a square of the f stop number. Hence, in low light level applications, it is desirable to use a lens with a low f stop number. As the f stop number decreases, however, image distortion due to aberrations increases, and a point is reached at which image quality is sacrificed for increased light. A 25-mm lens with an f stop number of 1.2 was initially selected for use with the CCD camera.

The line-scan time, the dynamic component, the aperture width of the CCD array projected onto the ground (static width), the acceptable degree of image blur, and the velocity of the carrier aircraft all affect the lighting requirements by their influence on the permissible exposure or integration time (the length of time each element of the CCD array is irradiated). To minimize the intensity of light required, it is necessary to use the maximum acceptable integration time.

For a given integration time, the minimum irradiation required on the array sensor is a function of the minimum exposure. The lower bound of the exposure that may generate an adequate image is the exposure at the peak-to-peak noise level of the sensor. A minimum exposure of 0.01 nJ/mm^2 was used in these lighting calculations.

The amount of ground irradiation that will be needed to provide the irradiation required on the array sensor is dependent on the spectral reflectance of the observed ground and on light transmission losses through the atmosphere and through the camera lens. The irradiation requirement is computed by determining the extent of the light transmission losses through the

lens and atmosphere and correlating the minimum exposure that will generate an adequate image with the lowest percentage of the on-ground irradiation reflected to the sensor.

Light transmission losses are negligible over the transmission distance of the reconnaissance when the atmosphere is clear. When haze, fog, clouds, snow, rain, dust, or smoke are present, light transmission losses are significant.

Light transmission losses through the lens range from 10 percent to 35 percent. A common lens usually has a transmissivity of about 80 percent. A transmissivity of 85 percent was assumed in the lighting computations.

The range of the spectral reflectance of materials that can be encountered in the rapid runway repair (RRR) reconnaissance is broad. The spectral reflectance of some of these materials is given in Table 14 (Reference 6). Black asphalt has the lowest spectral reflectance (6 percent) throughout the spectral response region of the CCD sensor, but the lowest percentage of the on-ground irradiation reflected to the sensor will come from the cylindrical surface of a deep and narrow hole in the asphalt pavement, created by a piece of unexploded ordnance. Depending on the location of the hole relative to the aircraft, the irradiation on the sensor, reflected from the circular surface of the hole, will range from nearly zero to about one-half of the irradiation reflected from the asphalt pavement.

Because the energy reflected from the hole in the asphalt pavement represents the lowest percentage of the on-ground irradiation reflected to the array sensors, it was correlated with the exposure at the peak-to-peak noise level of the sensor. The on-ground irradiation corresponding to this energy was easily determined when the energy reflected from the hole was expressed in terms of a spectral reflectance relative to the asphalt pavement. A spectral reflectance of 3 percent was used in the lighting calculations.

Area of Lighted Ground Required

The ground area lighted with the high-intensity lamp must be large enough to ensure adequate lighting over the area scanned by the CCD array.

TABLE 14. SPECTRAL REFLECTANCE OF COMMON MATERIALS

Material	Spectral Reflectance,[a] percent
Concrete[b]	40-45
Cement Block	37-39
Blacktop Asphalt	6-7
Brick, Dull Red and Face	28-45
Dolomite (Crushed Stone)	18
Sand, Dark and Wet	8
Sand, Dark and Dry	18
Sand, White and Wet	40-45
Sand, White and Dry	68-76
Soil, Dark, Wet and Dry	27-30
Soil, Light and Wet	34-40
Soil, Light and Dry	64-69
Green Leaf, Bottom and Top Sides	48-50

(Reference 6)

a. Spectral reflectance for wavelengths between 700 nm and 1000 nm. The spectral reflectance values tabulated are for a dry surface unless otherwise indicated.

b. The spectral reflectance of concrete was not given. Because concrete is a little lighter in color than cement blocks, its spectral reflectance was estimated to be within the range of 40 to 45 percent.

The size of the area required is primarily dependent on whether or not the lighting and camera platforms are aligned and stabilized. If they are stabilized, the size of the lighted area will be dependent on the lag in tracking time between platforms and on the precision of their alignment. If the light and camera platforms are mounted on a single rigid frame that can be attached to the carrier aircraft, a fine positioning of the platforms and a well aligned on-ground projection of the light beam and CCD array can be achieved. Preliminary calculations indicate that an allowance of ±1 degree about each

axis of the area scanned by the CCD array may provide adequate coverage for the lag in tracking time and the tolerance in alignment of the platforms. This means that at a reconnaissance elevation of 270 feet, a rectangular area of 9 feet by 280 feet must be lighted to ensure coverage of the 2.5-inch by 270-foot area scanned by the CCD array. If the lighting and camera platforms were mounted directly on the carrier aircraft, accurate alignment would be difficult and uncertain, and the allowance for misalignment would have to be increased. In addition, the hardware could not be mounted on a different aircraft without realignment because it is unlikely that the hard mounting points on the two aircraft would be identical in position and orientation.

If only one of the two platforms is stabilized, the size of the lighted ground area will be determined primarily by the stability of the aircraft and by the initial alignment of the two platforms. If neither platform is stabilized, the size of the lighted area will be dependent only on the alignment of the platforms. However, the path of the on-ground projection of the light beam and CCD array will be determined by the stability of the aircraft. Generally, the stability of the aircraft increases with increased size and weight. The size of lighted ground area that will ensure adequate lighting for various degrees of yaw, roll, and pitch can be determined by using Equations (9) through (12).

Efficiency of Lamp Design

The light source consists of several high-intensity lamps and an array of mirrors designed to reflect the light from the lamps to a rectangular area on the ground. The efficiency of the lamp design is determined by the percentage of light output that is confined to the desired ground area and the variation in ground irradiation parallel to the scanning direction of the CCD array and perpendicular to that direction.

The degree to which the lamp design confines the light output to the desired area directly affects the intensity required of the light source and the electrical power requirement for the lighting system. Discussions with a lamp manufacturer indicate than an efficiency of 50 percent may be expected.*

*Communication with Paul Burke, Optical Radiation Corporation, Azuza, California, November 7, 1978.

Similarly, the electrical power requirement of the lighting system may be minimized if the ground irradiation is made as uniform as possible over the entire area. It appears that a lamp may be designed to provide nearly uniform irradiation in the direction perpendicular to the scanning direction of the CCD array, but it may not be feasible to design a lamp in such a way as to compensate for the variation in irradiation in the scanning direction. Therefore, the irradiation in this direction will be a function of the angle between the vertical axis of the stabilized platform and the line of sight from the camera to the observed surface. The maximum irradiation (E_c) will occur at the center of the lighted area and will decrease towards the end of the area in proportion to $\cos^4\theta$. For a reconnaissance elevation of 270 feet and a lighted area 280 feet in length, the irradiation at the end of the area (E_y) is given as:

$$E_y = E_c \cos^4 27.4 \text{ deg}$$

Therefore,

$$E_y = 0.62\ E_c$$

or

$$E_c = 1.61\ E_y \tag{13}$$

The efficiency of the light source is determined by the number of radiometric watts generated per electrical watt and on the efficiency of the spectral distribution of the source in relation to the spectral response of the CCD device. Ray Pfoutz of the Reticon Corporation has indicated that the CCD sensor is sensitive to from 20 to 25 percent of the input wattage of a tungsten halogen lamp.*

The xenon lamp was one of the most efficient of the lamps reviewed. The xenon spectrum is substantially continuous in the ultraviolet, visible, and near-infrared wavelengths, with some particularly strong lines in the 800-nm to 1000-nm wavelength. The lamp appears to be about 33 percent more efficient than the tungsten halogen lamp.

---

*Letter, November 9, 1978.

Electrical Requirements

The electrical power and the on-ground irradiation required to provide adequate irradiation on the 1728-element CCD array were estimated. The computations were based on the following parameters:

Aircraft velocity = 70 knots (80.5 mph)
Field of view = 270 feet
Lens speed designation = 1.2
Aperture opening = 16 μm

The ground resolution of each element was 1.9 inches using a 1728-element CCD array for a field view of 270 feet. The static width of the line scan was 1.9 inches for an aperture opening of 15 μm. A line-scan time of 1.32 ms was required for a dynamic component equal to the static width. This time was obtained when a sampling frequency of 1.31 MHz was used. The integration time was set equal to the line-scan time. Assuming that an exposure of 0.01 nJ/mm^2 will generate an adequate image, the irradiance required at the CCD device was computed as 7.6 nW/mm^2. With negligible light transmission losses through the atmosphere (clear atmosphere), a lens transmissivity of 85 percent, a lens f stop number of 1.2, and a spectral reflectance of 3 percent, the minimum irradiation required on the ground to provide the irradiation required on the CCD sensor was computed as 0.156 W/ft^2. However, this value was increased by a factor of 1.61 to compensate for the $\cos^4\theta$ variation in irradiation over the lighted area in the scanning direction. Therefore the irradiation required on the ground directly below the camera was 0.251 W/ft^2.

The electrical power required to light the 9-foot by 280-foot ground area was computed as 4217 watts for a xenon light source. This value was based on the assumption that the CCD sensor is sensitive to 30 percent of the input wattage and that the lamp design is 50 percent efficient.

The 4.2-kW electrical power requirement of the lighting system is an optimistic estimate. The actual power requirement may be substantially higher. The parameters that may raise the power requirement significantly

above the estimate are primarily the limiting value of the percent increase of the dynamic width scanned by the array over the static width and the minimum exposure based on the actual system input noise level and the CCD noise level.

CONCEPTUAL LIGHTING SYSTEM AND PLATFORM DESIGNS FOR FSP

In an investigation of the feasibility of developing a universal platform and mounting system for the FSP, NMERI obtained information on the mounting points, stability, vibrational characteristics, payload capacity, and electrical capacities of the specified carrier aircraft. The camera stability required to produce a usable image was investigated. After the camera lighting requirements had been examined, it was decided that the lighting system should be considered in the universal platform and mounting system because the camera and light source would have to be very carefully aligned in order to keep electrical power requirements within reasonable limits. It was determined that a universal mounting system was not feasible, primarily because of the bulk of the anticipated lighting system and variations in the hard mounting points on the various aircraft. When a more sensitive sensor is selected, the lighting requirements will be reduced and the feasibility of a universal mounting system should be reexamined. AFESC indicated that the UH-1N type helicopters and the OV-10 aircraft would be favored as carriers. The OV-10 proved to be an unsuitable carrier because of its high minimum flying speed and its undesirable low-speed handling characteristics. Therefore, a conceptual design was made of a lighting system and platform and a mounting system compatible with the UH-1N-type helicopter. The mounting system includes two stabilized platforms, one for the camera and one for the light source. The platforms are located in a single, rigid frame to simplify alignment, and they are stabilized about all three axes. One vertical reference unit is used to position both platforms. Accelerometers are mounted on the camera platform, and a radar altimeter is attached to the mounting frame to provide image-correction signals.

Lighting System Design

To make the CCD camera system operable at low light levels and at night, it is necessary to provide artificial lighting. A conceptual design of the

lighting system was undertaken with the purpose of developing an adequate and simple system at a minimum cost. The study of the CCD camera lighting requirements has shown that it is necessary to minimize the size of the ground area that must be lighted to ensure adequate lighting over the area scanned by the CCD sensor. To accomplish this, the lighting system was designed to consist of a single, custom-designed, high-intensity light source mounted on a three-axis gyrostabilized platform with a manual yaw adjustment. The camera platform will be in extreme compliance with the output of the lighting platform's roll, pitch, and yaw synchros.

An allowance of ±1 degree about each axis of the area scanned by the CCD array will provide adequate coverage. Therefore, at a reconnaissance elevation of 270 feet, a rectangular area of 9 feet by 280 feet must be illuminated to adequately cover the 2.5-inch by 270-foot area scanned by the CCD array. Although the aspect ratio of the lighted area is unusually large, a lamp manufacturer has indicated that a light that will cover this area can be manufactured.*

The light source consists of several high-intensity lamps and an array of mirrors designed to reflect most of the light from the lamps to a rectangular area on the ground. The array of mirrors is arranged to produce a uniform irradiance on the ground in the direction of the motion of the aircraft. The irradiance perpendicular to this direction is a cosine function. Computer techniques can be used to compensate for variations in the brightness of the image resulting from variations in irradiance. Xenon lamps with a total wattage of at least 4.2 kW are specified. In the conceptual design of the lighting system, the camera and the light source are separated as much as possible.

Universal Platform

NMERI considered the feasibility of developing a universal platform for the camera alone. A completely stabilized platform (three axes) including camera and gyros would be a relatively small package, roughly 24 inches by 18 inches by 12 inches, and would weigh less than 50 pounds. The platform

*Communication with Paul Burke, Optical Radiation Corporation, Azuza, California, November 7, 1978.

would compensate for the angular motion of any of the aircraft considered, and the package would be small enough to be safely mounted on a beam projecting from the side or rear door of the aircraft. Specialized electrical adaptors and mounting fasteners would be required for the various aircraft.

After the lighting requirements of the CCD camera were examined, it became apparent that a very large lighting system would be required. To keep the electrical requirements of the lighting system within reasonable limits, the ground area to be illuminated would have to be limited by a carefully focused beam, and the light source would have to be carefully aligned with the field of view of the CCD camera. Alignment of the camera and light source would require that the light source be stabilized about the same axis as the camera; otherwise, the ground area sensed by the camera could deviate from the area illuminated by the light source. To maintain the proper alignment, gyroscopes would be used to stabilize one platform, and the second platform would track the position of the first by following signals from the synchros on the first.

It was estimated that an unstabilized 5 kW light source, including lamp, reflectors, and power convertors, would measure approximately 36 inches by 18 inches by 18 inches and would weigh approximately 150 pounds. A stabilized light source, including platform, would have dimensions of approximately 52 inches by 24 inches by 24 inches and would weigh approximately 300 pounds. The bulk of the unstabilized light source would require the use of hard mounting points such as bomb shackles, sling attachment points, hoist attachment points, or other external mounts. Because no hard mounting points are common to all of the aircraft considered, a universal mounting system does not appear to be feasible.

Platform Design

In developing the conceptual platform design, NMERI examined both the expected motion of the UH-1N helicopter and the effects of camera motion on the displayed image. (These topics are discussed elsewhere in this report.) Stabilizing the platform about three, two, one, or no axis and using a manual

yaw adjustment were considered. In light of the large translational and rotational motions anticipated for the UH-1N in heavy gust conditions (±40 to 50 feet altitude, ±30 to 40 feet lateral motion, ±10 knots velocity, and ±5 to 8 degrees rotation in a 20-knot gust spread), it was decided that a three-axis stabilized platform would be required to keep the runway within the camera's field of view. A manual yaw adjustment would be used to orient the CCD camera on the approach to the runway.

The platform design incorporates a standard three-axis, gyrostabilized platform, similar to a USAF Type A-28, to stabilize the lighting system. An additional gyroscope is mounted on the azimuth ring, along with the lighting system, to provide yaw angle feedback.

The camera platform is custom fabricated. It has pitch and roll gimbals and an azimuth ring and is tied in to the output of the lighting system platform's roll, pitch, and yaw synchros. The azimuth ring is large enough to accommodate the CCD camera head and two accelerometers aligned parallel with and perpendicular to the CCD axis. The two platforms are mounted 8 feet apart in a single rigid frame (Figure 15).

The mounting system attaches the frame, containing the gyroplatforms, to the helicopter; isolates the frame from the vibration of the helicopter; and positions the frame so both the camera and lighting system have a clear view of the ground while the aircraft is in flight. The mounting system consists of cross-braced struts attached to four external hard mounting points, normally used for minigun or rocket pod mounts, below the side door of the helicopter and four points on the platform frame. The attachment point on the platform frame incorporates vibration-isolation devices. Additional isolation devices could be incorporated in the struts themselves. Electrical cables linking the various devices mounted on the platforms to devices in the helicopter are secured to one of the struts and enter the helicopter through the side door. The entire camera-lighting system platform is enclosed in a streamlined pod. The mounting struts could also be streamlined. Figure 16 shows the complete stabilized platform and mounting system in place on the

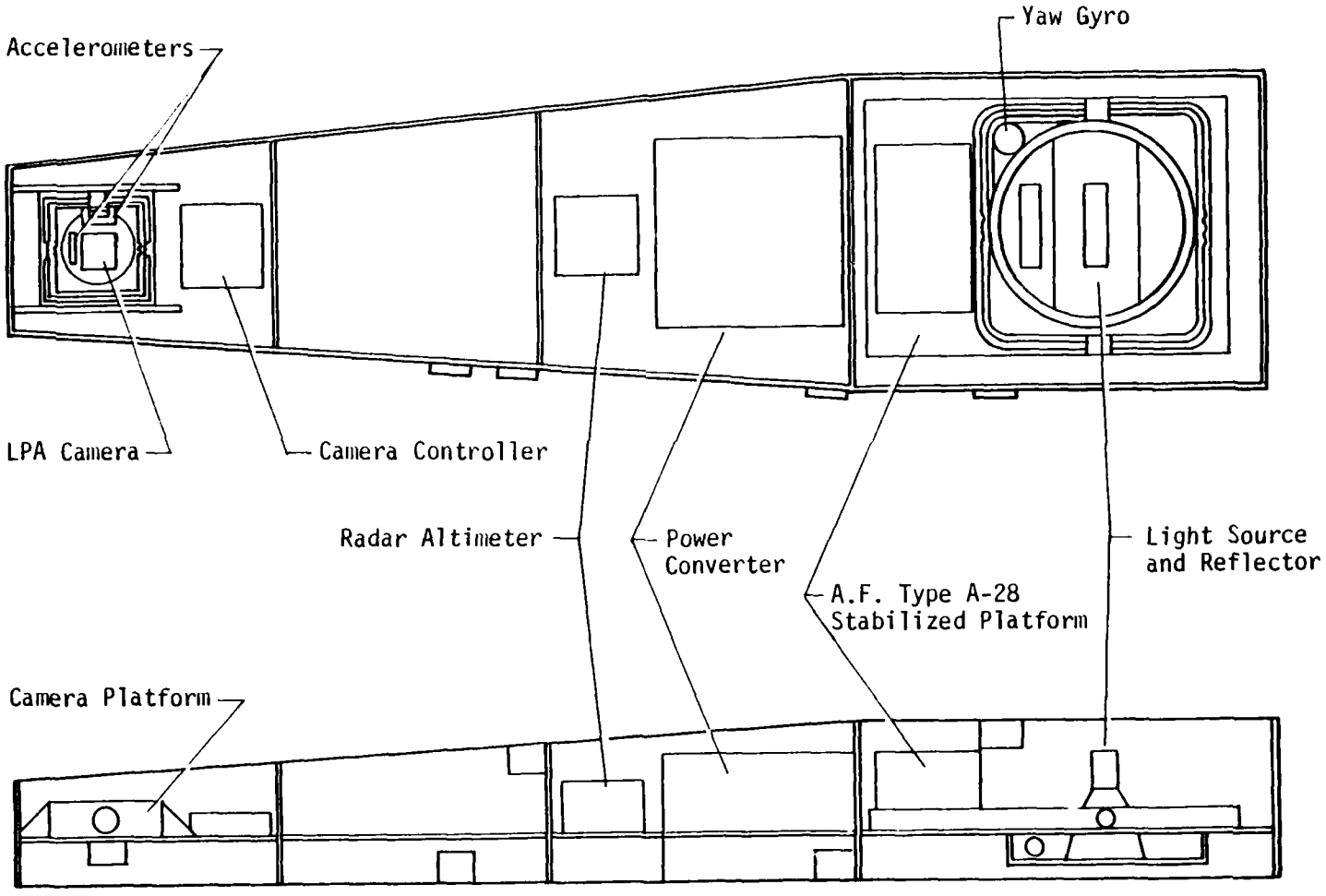

Figure 15. Design for Stabilized Platform

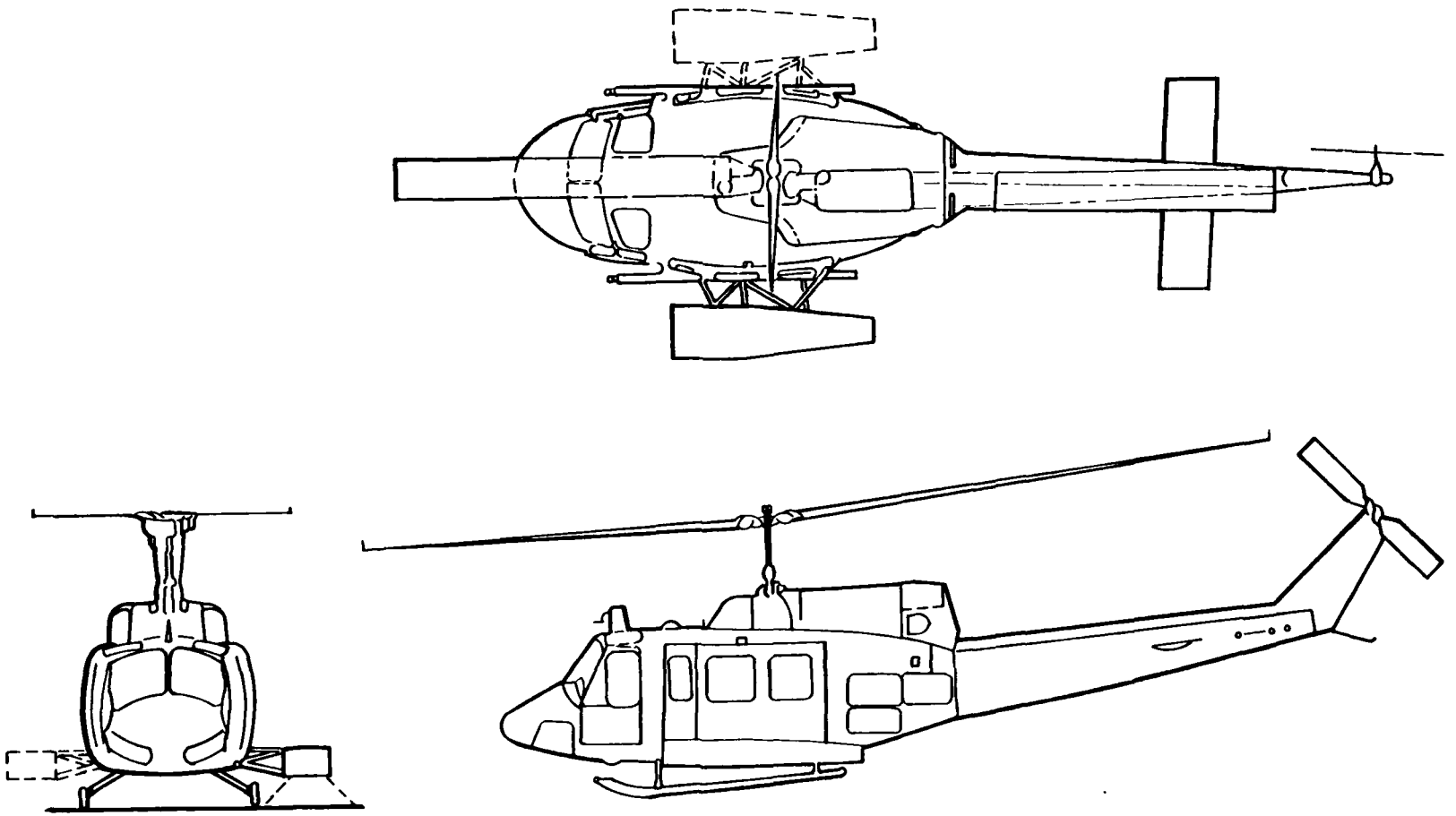

Figure 16. Stabilized Platform Mounted on H-1 Helicopter

helicopter. A dummy pod may be required on the opposite side of the helicopter to counterbalance the weight and aerodynamic drag caused by the camera pod. The dummy pod could be used to store equipment such as power supplies, battery packs, digitizer, recorder, transmitters, additional lighting, or a complete backup system.

This conceptual design is intentionally a generalized design. The lighting requirements of the CCD camera and the size and weight of the lighting system were found to be extremely high. The sensitivity of CCD devices is constantly being improved, and techniques for intensifying existing devices are being developed. A study of possible improvements to the CCD camera and alternate sensors has been conducted. The recommended sensor change would result in significant changes in the size, weight, and power requirement of the lighting system, which, in turn, would significantly alter the requirements for the platform and mounting system. For this reason, neither a lighting system nor a stabilized platform was constructed for the concept verification DAS.

DATA LINK TRADEOFF ANALYSIS

NMERI conducted a tradeoff analysis of possible data-transfer devices for linking the FSP and the IAS. The purpose of the data-transfer device is to transfer the imagery data gathered by the line-scan camera of the FSP to the mass storage disks of the IAS. NMERI investigated the following data-transfer device options:

1. Digital radio frequency (RF) transmission system
2. Analog RF transmission system
3. Digital airborne magnetic tape recorder system
4. Analog airborne magnetic tape recorder system

Several variations of each were considered. The following factors were assessed in the tradeoff analysis:

1. Data rate capability
2. Data transfer time
3. Data survivability

4. Data quality
5. Denial of data to enemy
6. Flexibility
7. Reliability
8. Maintainability
9. Cost

In the selection of a data-transfer device for the concept verification system, the following criteria were applied:

1. The transfer device should not limit the data precision (gray scale) the camera is capable of generating.
2. The transfer device should be capable of reducing the data rate generated by the camera (1.5 Mbytes/s) to a rate acceptable to the Unibus used in the IAS (approximately 500 kbytes/s).

NMERI recommended that an airborne digital magnetic tape recorder with ground playback capability be selected for the demonstration system.

Data-Transfer Device Options

In considering the four data-transfer device options, NMERI assumed that the rate of data output by the camera would be 1.5 Mpixels/s, which converts to 1.5 Mbytes/s for 8-bit/pixel precision. It was also assumed that the carrier aircraft would remain within three miles of the ground station while gathering data, that the flying altitude would be between 200 and 500 feet, that the flying speed would be approximately 70 knots, and that line-of-sight could be maintained between the aircraft and a ground antenna.

The digital RF link consisted of a digitizer, an encoder, a transmitter, and an antenna mounted in or on the aircraft as well as an antenna, a receiver, a decoder, a bit synchronizer, and an interface on the ground. A digital tape recorder and an additional interface on the ground were required. The analog RF link consisted of an encoder, a transmitter, and an antenna in the aircraft and an antenna, a receiver, a decoder, a digitizer, and an interface on the ground. Either a digital or an analog recorder and appropriate

interfaces were also required on the ground. In both systems, transmitter power, antenna design, and receiver-preamplifier gain were balanced against bandwidth and range to obtain the desired signal-to-noise ratio (SNR) and fade margin. Enciphering equipment could be added to either system for data protection or denial.

The digital and analog airborne recorder systems were very similar. The same transport and head mechanism could be used for either option. Only the electronics differed. In the digital system, the digitizer was located in the aircraft; in the analog system, the digitizer was located on the ground. An interface to the PDP-11 Unibus was required. Both fixed- and rotary-head recorders were examined. The concept of moving the entire tape transport and head mechanism from the aircraft to the ground station and transporting only the tape, which would require two transport and head mechanisms, was considered.

Tradeoff Analysis

Data Rate

Only the fixed-head analog tape recorder and the rotary-head digital recorder could not handle the anticipated data rate. The fixed-head analog recorder, in which wide band II-type electronics are used, is limited to approximately 1 Mpixels/s; the rotary-head digital recorder is limited to about 1.25 Mbytes/s.

Data Transfer Time

In the concept verification system, where a 4:1 reduction in the data rate is required to load the mass storage disks, the RF links would require about 10 minutes to complete the transfer of data from a single runway. The airborne recorders would require about 15 minutes.

Data Survivability

The tape recording systems appear to be less susceptible to data loss than the RF links. The RF links would be susceptible to jamming, spurious RF signals, and multipath interference. Equipment malfunctions could

affect any system. Data survivability in the RF link can be enhanced by increasing the SNR and fade margins and by careful antenna design, all of which increase the cost of the system.

Data Quality

The digital RF link and the airborne digital recorder system both digitize the imagery data at the output of the camera. The camera clock is used to synchronize the digitizer. This method of digitization represents the camera signal more accurately than would the digitizing of a recorded or transmitted analog signal. Both the digital RF link and the recorder are capable of handling 8 bits/pixel of data at the required rates. The bit error rate (BER) of the RF link is dependent on the SNR and can be better than 1 in 10^{11}. This BER is comparable to that anticipated for the mass storage disk system. The BER for a fixed-head digital recorder is better than 1 in 10^{7} bits. The analog RF link requires 3 dB of SNR for each bit of pixel precision. The RF link SNR can be designed to carry an 8-bit precision analog signal. An analog recorder requires 6 dB of SNR for each bit of pixel precision desired. The rotary-head video recorder had the highest SNR, at 40 dB, of any of the analog recorders investigated. This SNR is good for a precision of less than 7 bits/pixel.

Data Denial

Data being transmitted by RF link is susceptible to interception by an enemy. Enciphering and deciphering equipment can be added to the RF link to make the data more difficult for an enemy to use. Careful design of the transmitting antenna will limit the locations at which an enemy receiver could pick up the data. The airborne recorders would be much less susceptible than the RF links to data interception.

Flexibility

All of the options considered are capable of handling a variety of data rates. Only the recorder systems are capable of reducing the input data rate at the output of the device.

Reliability

All of the options considered can be assembled from components that meet military specifications for airborne or other harsh environments. The major components of each option have been in service for a number of years and have proven themselves reliable. The reliability of a particular option will depend more on the manufacturer and model of the equipment used and on the maintainence of that equipment than on the type of option selected.

Maintainability

The maintainability of the data-transfer device depends more on the manufacturer and model of the equipment used than on the option selected. The mechanical components, such as tape transports and tracking antenna, require more maintenance and adjustment than the electrical components, but the degree of maintainability depends a great deal on the specific equipment selected.

Cost

The analog airborne recorder appears to be the least expensive option considered; however, this system is not capable of the 8-bit/pixel precision desired. The cost of a good, rugged, airborne analog recorder and playback system with digitizer and interfaces would be in the $90,000 range. The cost of a similar digital recorder system would be about $110,000. The price of the RF options can vary greatly depending on data rate, SNR, fade margin, enciphering equipment, antenna design, and other factors. An RF system capable of 8-bit precision and 1.5-Mpixel/s sampling rates, including a tracking ground antenna without enciphering equipment or ground tape system, would run approximately $130,000 for an analog system and $150,000 for a digital system.

Recommendation

As a result of the data-link tradeoff analysis, NMERI recommended that a digital airborne recorder system be selected as the data transfer device to be used in the concept verification system.

STABILIZED PLATFORM VERSUS IMAGE CORRECTION

NMERI conducted a tradeoff analysis of FSP sensor stabilization and image-correction techniques. The purpose of the analysis was to determine the best means of minimizing loss of resolution and errors in measured damage sizes and locations caused by nonideal aircraft motion. The results of the analysis were used in platform and software development for the concept verification system and in making design recommendations for future DAS development.

Four degrees of FSP sensor stabilization were investigated:

1. No stabilization
2. Stabilization about the roll axis
3. Stabilization about the roll and pitch axes
4. Stabilization about the roll, pitch, and yaw axes

Three types of image correction were investigated:

1. Use of operator interaction
2. Use of correction signals produced in the FSP and aircraft
3. Use of automated feature recognition in the IAS

Stabilization and image correction were considered both separately and in combination. The following parameters were evaluated for each option:

1. Size, weight, and ease of mounting
2. Data quality
3. Data processing time required
4. Cost
5. Maintainability and reliability.

The anticipated aircraft motion, effects of camera motion or the gathered image, and results of preliminary FSP testing discussed elsewhere in this report were used to evaluate the various options.

Stabilized Platforms

For the stabilized platforms considered in this study, a feedback control [illegible] and synchros was used to stabilize each axis.

The tolerance to which an axis is stabilized depends on the system design and components used. Tolerances of 0.5 degree and 0.5 degree per second were assumed in this study. These tolerances allow a position error on the ground of 2.4 feet about the roll and pitch axes and a maximum of 1.2 feet about the yaw axis when these axes are stabilized. Stabilized platforms compensate for angular motion of the aircraft but will not correct for linear motion such as changes in altitude or lateral drift, or for changes in forward velocity or linear vibration.

A roll-stabilized platform for the Fairchild CCD camera would measure approximately 1.5 feet long by 1 foot wide by 1 foot deep and would weigh approximately 30 pounds (including camera). A roll- and pitch-stabilized platform, with or without yaw stabilization, would measure approximately 1.5 feet by 1.5 feet by 1 foot and would weigh 50 to 60 pounds. Mounted in a streamlined pod, either of these platforms could easily be attached to the UH-1N or the T-41 aircraft. A specialized pod would be required for each type of aircraft. An unstabilized platform would be just large enough to accept the camera and would be mounted in a streamlined pod; the platform would be approximately 8 inches long by 6 inches wide by 10 inches deep (including camera). The total weight could be less than 10 pounds. An unstabilized platform would be extremely easy to mount on either a UH-1N or a T-41 aircraft.

By using Equation (9) it was determined that roll, pitch, and yaw increase the static component size of the ground resolution element of an unstabilized camera by 22.5 percent for the worst anticipated aircraft motion and by 3.0 percent for the aircraft motion encountered during the preliminary FSP testing. Roll stabilization would reduce these values to 1.4 percent and 0.5 percent, respectively. Roll and pitch stabilization, with or without yaw stabilization, would reduce the effect on the size of the static component to 0.5 percent for both conditions. The static component error due to change in altitude is 20.4 percent for the worst anticipated aircraft motion and was 3.7 percent during testing.

From Equation (10) it was determined that roll, pitch, and yaw increase the dynamic component of an unstabilized camera by 39.8 percent for the worst anticipated aircraft motion. A roll-stabilized platform reduces the error to 34.2 percent. Roll and pitch stabilization reduce the error to 14.9 percent. Roll, pitch, and yaw stabilization limit the error in dynamic component due to roll, pitch, and yaw of the aircraft to 3.4 percent. The increase in the length of the dynamic component due to the worst anticipated error in forward speed is 14.2 percent.

Equations (7) and (8) were used to calculate the maximum positional errors in the gathered image due to the worst anticipated angular motion of the carrier aircraft and the maximum anticipated altitude error. The lateral error was 86 feet; the longitudinal error was 78 feet. No yaw angle was considered in the lateral error because yaw angle reduces the error. The greatest errors occur at the edge of the camera's field of view. Roll stabilization would reduce the error values to 31 feet laterally and 68 feet longitudinally. Roll and pitch stabilization would further reduce the errors to 30 feet laterally and 30 feet longitudinally. Stabilization about the roll, pitch, and yaw axes would reduce the maximum errors to 30 feet laterally and 4 feet longitudinally. Of the remaining 30-foot lateral error, 27 feet are due to altitude error exclusively. An additional lateral error of 40 feet, due to the maximum lateral drift expected, is not affected by stabilization. Another 672-foot longitudinal error, due to the maximum error in average velocity, is expected at the end of the run.

It was noted during the preliminary FSP airborne tests that the carrier aircraft was much less susceptible to disturbances about the pitch and yaw axes than had originally been estimated. Pitch and yaw could be kept within ±1 degree under the conditions encountered during testing.

The time required to correct image distortion by using a given algorithm depends on the complexity and amount of distortion present in the image and the degree and accuracy to which the image is corrected. Generally, the less

distorted the image is, the less time is required for processing. This indicates that the more effectively stabilized the camera is, the less image-correction processing time will be required. However, significant image distortion is expected, even with perfect camera stabilization.

The cost of a stabilized platform depends on a number of factors including the number of axes stabilized, the precision and accuracy required, and the size of the sensor to be stabilized. Estimates on the cost of developing a platform for the Fairchild CCD camera range from $15,000 for a simple unit with a single stabilized axis to $60,000 for a device having three stabilized axes.

The Air Force currently uses and maintains a variety of gyrostabilized platforms for airborne camera systems. The amount of maintenance that would be required for a stabilized platform for the FSP would depend on the design and construction of the platform. With proper maintenance, gyrostabilized platforms are reliable; without proper maintenance, reliability drops rapidly.

Image Correction

Computer processing of the image gathered by the FSP sensor can correct geometric distortion caused by both angular and linear motion of the carrier aircraft. However, the size of the resolution element cannot be reduced, nor can imagery data from outside the field of view of the sensor be added, by post-processing. Features within the distorted image can be measured accurately either by restructuring the image to the correct geometry before taking measurements or by taking measurements from the distorted image and then correcting them. The first approach usually results in the loss of high-resolution data in the corrected image and requires much more processing time than does the second approach. The second approach is good enough to enable humans to recognize features with the amounts of distortion anticipated, but it complicates the automated recognition of damages.

NMERI considered three image-correction techniques in this analysis. By means of the first technique, the interactive capabilities of the IPS are used to enable the operator to mark features of known location, such as runway

edges and ends, taxiway intersections, and runway markings, on the distorted image. The ICS then uses these locations to interpolate the locations and sizes of other features marked on the distorted image. By means of the second method, aircraft motion error signals recorded with the imagery data and equations similar to Equations (7) through (10) are used to correct measurements of the distorted image. Three reference points are interactively marked on the IPS to enable the operator to correlate the runway and image coordinate systems. By means of the third technique, automated feature recognition is used to identify the same features that the operator would identify if the first technique were used. This information is then used for interpolation of the locations and sizes of other features.

The only image-correction technique that would affect the size, weight, and ease of mounting the FSP is the error signal method. Sensors used to measure angular motion can be very small: 3 inches by 1 inch by 1 inch per axis. A radar altimeter measures approximately 1 foot by 1 foot by 6 inches. Sensors that could be used to accurately measure lateral drift and forward ground speed could not be located during this investigation. Linear accelerometers were considered, but they proved inadequate.

The size of the ground resolution element cannot be improved by image correction. If the image is corrected before damaged areas are identified, the size of the resolution element will effectively increase. The precision with which the image-correction techniques correct for dimension and location errors depends on the coarseness of the interpretation grid, the accuracy of the aircraft motion error signals, the sophistication of the correction algorithm, and the accuracy with which reference points are measured. It was assumed that locations within ±10 feet laterally and ±50 feet longitudinally of the actual locations and dimensions within 10 percent of the actual dimensions would be adequate.

The interactive correction method would require a grid of reference points on both sides of the runway, separated by 25 feet longitudinally, to correct an image produced by an unstabilized sensor experiencing the worst

anticipated aircraft motion. The points would have to be marked only in regions where severe distortion occurred. It is expected that a portion of the runway surface would leave the sensor's field of view during these conditions, and images of that portion of the runway would be lost. If the sensor were stabilized, reference points would be required only every 200 feet along the edges of the runway, and the longitudinal location would have to be measured only every 1000 feet. The reference points would have to be measured to within ±1 foot in the distorted image. A two-dimensional interpolation between four reference points would be required for the unstabilized case. A one-dimensional interpolation at each reference point, to compensate for lateral drift, and lateral and longitudinal scale factors calculated less frequently could be used if the sensor were stabilized. By the interactive method, existing runway features could be used as reference points. This method is the simplest and most certain of the image-correction techniques considered.

For the aircraft motion error signal-correction technique, gyroscopes for each unstabilized axis, an altitude sensor, a ground velocity sensor, and accelerometers would be required. The accuracy of these sensors will determine the best correction possible. Adequate gyroscopes and altimeters are available, but sensors for measuring lateral and longitudinal ground speed could not be located during this investigation. Without these sensors, image correction will be incomplete. Equations (7) through (10), implemented in the software, would correct for location and dimension errors from an unstabilized camera. Significant portions of these equations would be eliminated if the sensor were stabilized.

The automated feature recognition technique would require the same number of reference points as the interactive approach and would perform the same correction algorithms. Automated recognition would require the use of distinctive and easily detectable markings as reference points. It is uncertain how well this method would actually work.

Using the interactive correction technique, the operator would need approximately ten minutes to identify reference points and two minutes to correct all the measured damage locations and dimensions if the sensor were unstabilized; the operator would need six minutes to identify reference points and one minute to correct damages if the sensor were completely stabilized. By the error signal method, one minute would be required for correcting all damage locations and dimensions for an unstabilized sensor and less than one minute for a stabilized sensor. The time required for the identification of reference points by the automated feature recognition technique is uncertain but is expected to be more than two minutes. The correction time for this technique would be the same as that for the interactive technique.

The cost of developing the interactive technique was estimated to be $2000 for software development on the existing IAS. The interactive capabilities of the IPS are required. The cost of the error signal method was estimated to be $2000 for software development, $6000 for data-link modification, and $6000 for altimeters and gyroscopes. The cost of the sensors that would measure ground velocity is not known. The cost of developing the automatic feature recognition software was estimated at $10,000. An additional $2000 would be required for the development of the correction software. How effective the automatic feature recognition software would be if it were developed is questionable.

Maintenance requirements for any of the techniques discussed would be no higher than the normal requirements of the IAS. The gyros and altimeters required for the error signal correction technique are low-maintainance, high-reliability components. The maintainability and reliability of the ground velocity sensors are not known.

Recommendations

An unstabilized platform and interactive image correction were implemented in the concept verification system. By means of this approach, image correction for all types of aircraft motion could be provided within the

schedule and budget limits of the effort documented in this report. NMERI recommended that roll-stabilization of the sensor and interactive image correction be incorporated in the future development of the DAS. It was also recommended that the investigation of sensors for measuring ground velocity and lateral drift, as well as automated image correction software, be continued because these devices show promise for improving the speed with which image distortion may be corrected.

SENSOR TRADEOFF ANALYSIS

Examination of Options

The Fairchild CCD line-scan camera used for concept verification of the DAS requires an extremely large artificial lighting system for low light level and night-time operation. NMERI conducted a tradeoff analysis of options for reducing the artificial lighting requirements of the FSP sensor by using either a different sensor or an image intensifier. Six options were examined in detail: two improved CCD line-scan sensors, two types of image intensifiers, and two laser line-scan sensors. Each option was assessed for cost, weight, size, data quality, maintainability, reliability, effect on lighting requirements, and other factors related to its use in the FSP portion of the DAS. None of the options investigated currently exists as a complete camera suitable for use in the FSP.

Before the current CCD line-scan sensor was selected for use in the concept verification, all possible sensors, including low light level video, thermal IR, microwave, and magnetic sensors, were investigated. The CCD line-scan sensor was selected because of its high resolution and efficient data format. At the time of this investigation, AFWAL/AARF was evaluating the various sensors for use in a study of runway damage assessment. NMERI's sensor tradeoff study was limited to near-visible, reflectance-measuring, line-scan sensors. The one exception to this rule was the relief-measuring laser line scanner, which had not been investigated before and which promises to offer significant advantages in automatic feature-recognition processing. The following is a detailed description of the six options examined by NMERI.

Fairchild CCD 122

The Fairchild CCD 122 is an improved second generation of the CCD 121 chip used in the current Fairchild CCD 1400 camera. Sensitivity has been improved by a factor of approximately 2.5, and the spectral response has been smoothed. Use of this sensor would require the development of a rugged airborne camera.

Cost: Sensor, $950.
Camera development, ≈ $30,000.
Lighting system development, ≈ $30,000.
Camera quantities > 50, $3,000 to $5,000.
Lighting system quantities > 50, ≈ $10,000.

Weight: Camera and control unit, ≈ 5 lb.
Lighting system, ≈ 350 lb.

Size: Camera and control, ≈ 0.5 ft^3.
Lighting system, ≈ 20 ft^3.

Data Quality: Ground resolution elements 1.9 by 1.9 inches; dynamic range 200:1; data quality essentially the same as current sensor.

Maintainability: Would depend on camera design.

Reliability: Depends on camera design; sensor very good.

Lighting Requirements: 0.4 of the current sensor; extremely large (10 kW) stabilized lighting system still required.

Development Time: 1 year.

Fairchild Time Delay and Integration (TDI) Sensor

The Fairchild TDI Sensor is a 1024- by 64-element CCD array. The elements are arranged in 64 lines of 1024 elements each. Rather than transferring the charge accumulated at each photograph site to the output of the sensor at the end of the exposure period, the sensor transfers the charge on

each element of the first line to the corresponding element of the next line, where it continues to accumulate charge. This line-to-line transfer continues through the entire array, and the total charge accumulated in the elements of the last line produces the output of the device. The shift of charge packets is coordinated from line to line with the motion of the camera; thus, the photograph sites on successive lines will scan the same area on the ground, and the exposure time for each line of output is effectively increased by a factor of 64. The name (time delay and integration) is descriptive of the process. The Fairchild TDI Sensor is currently being used in the Air Force Long-Range Electro-Optical Reconnaissance Sensor (LOREORS) Program. The LOREORS camera is extremely sophisticated and would not be directly applicable to the DAS. Because the TDI sensor contains only 1024 elements per line, multiple sensors would have to be used to obtain the resolution required by the DAS. The resolution of the sensor is sensitive to velocity errors between the line shift rate and the object being viewed, to lateral motions of the camera, and to nonuniformity of photograph site response.

Cost: Sensor, < $10,000.
Camera development, $80,000 to $100,000.
Lighting system development, $15,000 to $20,000.
Camera quantities ≈ 50, $30,000 to $50,000.
Lighting system quantities ≈ 50, ≈ $5,000.

Weight: Camera and control unit, ≈ 20 lb.
Lighting system, ≈ 150 lb.

Size: Camera and control unit, ≈ 1.5 ft^3.
Lighting system, 10 ft^3.

Data Quality: Theoretically, two sensors (2048 elements) would provide better resolution than the current sensor, and dynamic range could be nearly 1000:1; velocity errors and camera motion would degrade the resolution much more quickly than in the current sensor.

Maintainability: Depends on camera design.

Reliability: Depends on camera design; sensor is very good.

Lighting Requirements: Reduced by a factor of 64; significant nonstabilized lighting system (≃ 5 kW) still required.

Development Time: 2 to 2-1/2 years.

ITT Proximity Focused Channel Intensifier Tubes (PFCIT)

The PFCIT is a miniaturized, high-gain image intensifier tube. It consists of a photocathode, a channel electron multipler/matrix, and a phosphor screen. The gain of the tube can be varied up to 1000:1. The PFCIT is very compact: approximately 2 inches in diameter by 1 inch long. ITT has optically coupled PFCITs with a number of CCD arrays and has indicated that the technique can be used on almost any CCD array. For evaluation purposes, NMERI assumed that the PFCIT would be coupled to a Fairchild CCD 122 array. The resolution of the PFCIT is limited to 25 line pairs per millimeter (a 20-micron spot size compared to a 13-micron photosite dimension in the CCD 122 array). The limited resolution of the PFCIT plus the effects of the optical coupling would reduce the resolution of the CCD sensor by 50 to 100 percent. The PFCIT has not been coupled to a high-resolution CCD array, although the technique should be directly transferable from ITT's experience with low-resolution arrays. In order to meet the resolution requirement of the DAS, NMERI assumed that the camera developed to house the intensified array would use two intensified 1728-element sensors and lens systems arranged so that each would scan one-half the width of the runway.

Cost: Intensified array development (each), $10,000 to $15,000.
Camera development, $50,000 to $70,000.
Lighting system development, $8,000 to $10,000.
Camera quantities > 50, $15,000 to $20,000.
Lighting system quantities > 50, $1,000 to $3,000.

Weight: Camera and control unit, ≃ 10 lb.
Lighting system, ≃ 50 lb.

Size: Camera and control unit, ≈ 1 ft^3.
Lighting system, ≈ 2 ft^3.

Data Quality: Resolution of two 1728-element arrays approximately 1.5 to 2 inches ground resolution element (800 to 1100 samples/line/array); dynamic range approximately 200:1 at given gain; intensity gain adjustable up to 1000:1.

Maintainability: Essentially same as unintensified CCD: good.

Reliability: Good; solid-state electronics.

Lighting Requirements: With a gain of 1000:1 and the sensitivity improvement of 2.5 times provided by the CCD 122, a low-power (≈500-W), unstabilized, broadly focused lighting system would suffice.

Development Time: 1.5 years.

ITT Proximity Focused Diode (PFD)

The PFD is a relatively low-gain image-intensifier tube. It consists of the photocathode and a phosphor screen without a channel electron multiplier matrix. The lack of a channel plate limits the gain of the device to less than 50:1, but resolution improves to nearly 50 line pairs per millimeter. The coupling technique described for the PFCIT could be used to couple the PFD to a CCD array. NMERI assumed that the Fairchild CCD 142, a 2048-element version of the CCD 122, would be used. The resolution of the CCD array would be reduced by only 20 to 30 percent. The development costs and problems associated with the PFCIT sensor would also apply to the PFD. A significant lighting system would still be required with a PFD.

Cost: Intensified array development, $10,000 to $15,000.
Camera development, $40,000 to $50,000.
Lighting system development, $15,000 to $20,000.
Camera quantities > 50, $10,000 to $15,000.
Lighting system quantities > 50, $5,000 to $8,000.

Weight: Camera and control unit, ≈ 7 lb.
Lighting system, ≈ 150 lb.

Size: Camera and control unit, ≈ 0.7 ft^3.
Lighting system, ≈ 10 ft^3.

Data Quality: Ground resolution element size for 2048-element array approximately 1.98 inches to 2.25 inches (1434 to 1638 samples per line); dynamic range approximately 200:1; gain adjustable to approximately 50:1.

Maintainability: Same as CCD camera: good.

Reliability: Good; solid-state electronics.

Lighting Requirements: With a gain of 50:1 and the sensitivity improvement of 2.5 times provided by the CCD, this unit will still require either a large (2-kW), unstabilized lighting system or a smaller, carefully aligned and stabilized lighting system.

Development Time: 1.5 years.

Perkin Elmer System B Day/Night Reconnaissance System

The System B is a compact version of the KA-98 Day/Night Sensor currently in the Air Force inventory. A prototype has been built and tested with excellent results. The sensor uses a solid-state GaAs laser to provide its own illumination. A rotating mirror sweeps the laser beam across the field of view. A second mirror, mounted on the same shaft, transfers the reflected light to the photodetector. The system is currently configured for medium-altitude, medium-resolution reconnaissance and would provide a resolution spot size of 3.6 inches at an altitude of 300 feet. Perkin Elmer has indicated that the sensor could be tuned for the DAS requirements, through several straightforward modifications, to produce a resolution spot size of 2.0 inches. The sensor can provide internal roll compensation. No other

lighting system is required. The low power requirement (less than 200 watts) attests to the efficiency of the system. The entire package is small and lightweight and thus could be mounted easily on a variety of aircraft.

Cost: First unit, $50,000 to $100,000.
Quantities 50 to 100, $25,000 to $50,000.
Lighting system, $0.

Weight: Complete sensor system, roll-stabilized, < 21 lb.

Size: Complete sensor system, < 0.3 ft^3.

Data Quality: Resolution currently 3.6 inches; element size could be improved to < 2.0 inches.

Maintainability: Mechanical mechanism may cause difficulties for field adjustment; otherwise generally good.

Reliability: Components of system have proven reliable individually; complete system should be good.

Lighting Requirements: No additional lighting required.

Development Time: 1 year.

Perkin Elmer System B Relief Measuring Sensor

The System B Relief Sensor is a modified System B Day/Night Sensor. The laser has been modified, and an electronics package has been added to allow the intensity of the laser beam to be modulated and the phase shift of the returning signal to be determined. The phase shift measured produces a signal proportional to the relief of an object being sensed. The sensor also produces a normal monochrome reflectance image. The System B Relief Sensor is still under development; however, the capabilities of the sensor--both the field demonstration version and one tuned to meet the DAS requirements--should be examined closely when a sensor is selected for the DAS. The relief data produced by this sensor would help distinguish ports of entry, spalls, and debris. The algorithms for automated feature recognition would be dramatically simplified if relief data could be used, and automated damage sizing, location, and classification in the DAS would then be practical.

AD-A107 712 NEW MEXICO ENGINEERING RESEARCH INST ALBUQUERQUE F/G 1/5
RAPID DAMAGE ASSESSMENT. VOLUME II. DEVELOPMENT AND TESTING OF --ETC(U)
FEB 81 C W WILSON F29601-76-C-0015
UNCLASSIFIED NMERI-5.08-AP-39 AFESC/ESL-TR-80-47-VOL-2 NL

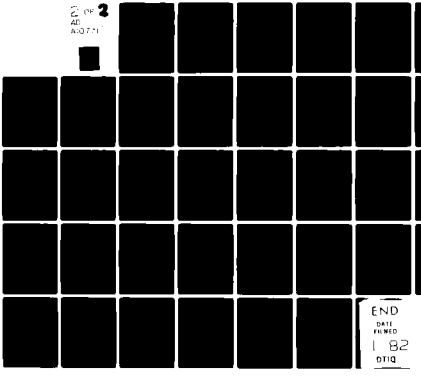

Cost:	First camera, $100,000 to $150,000. Quantities 50 to 100, $40,000 to $80,000. Lighting system, $0.
Weight:	Complete sensor and electronics, ≈ 30 lb.
Size:	Complete sensor and electronics, ≈ 0.8 ft^3.
Data Quality:	Classified.
Maintainability:	Same as System B Day/Night: good.
Reliability:	Same as System B Day/Night: good.
Lighting Requirements:	No additional lighting system required.
Development Time:	2 years.

Tradeoff Analysis

The power requirements and the bulk of the lighting systems required for the Fairchild CCD 122 and TDI sensors effectively eliminate them from consideration for use in the FSP as it is currently conceived. The PTD intensified array is borderline in this respect.

Development costs for all the intensified array sensors with lighting systems and the System B Day/Night Sensor fall within the $50,000 to $100,000 range. Development cost for the System B Relief Sensor should be under $150,000. In quantities of 50 to 100, the intensified array systems hold a cost advantage over the System B Day/Night Sensor: $15,000 to $25,000 versus $25,000 to $50,000. In quantities of 1000, however, the cost of all the systems falls to a point between $2,000 and $3,000. The System B Relief Sensor would cost between $40,000 and $80,000 in quantities of 50 to 100.

The System B sensors are far more compact than the other devices and consume much less power. They could also be more easily adapted than the others to a variety of carrier aircraft. The PFCIT intensified array system could be packaged in a reasonably adaptable form. The PDT intensified array would require a very bulky package specifically designed for each aircraft. The T-41 would probably be eliminated as a sensor carrier.

The maintainability and reliability of each of the sensor systems will depend on the final system design. The time requirements for the development of a prototype system are similar for all six options. In no case would more than two and one-half years be required. The System B Day/Night Sensor already exists in a prototype form and would have only to be modified to meet DAS needs. The System B Sensor could therefore be implemented very quickly. More uncertainty is associated with the development of the other systems.

Conclusions

In light of the information gathered for this tradeoff analysis, it appears that the System B Day/Night Sensor would best solve the lighting requirement problems associated with the current FSP sensor. It is the most compact system considered and is in the most advanced stage of development. Its development costs are nearly identical to those for the intensified arrays, although the quantity cost estimate is somewhat higher. The System B Day/Night Sensor also has the advantage of sharing many components with the System B Relief Sensor. The Relief Sensor could significantly reduce the damage assessment time through its fast automatic feature-recognition algorithms. Development of the Relief Sensor would take significantly more time than would development of either the Day/Night Sensor or the intensified arrays.

The PFCIT intensified array offers a good alternative to the System B sensors. The PFCIT system could be very compact, and the lighting system could be very simple. The PFCIT system shares no components with the System B Relief Sensor.

The current development status and costs of the various sensors must be reevaluated before a sensor is selected for the prototype DAS.

TESTING OF FSP SENSOR

The Fairchild CCD 1400 line-scan camera obtained by NMERI was tested at the factory for responsivity to tungsten and xenon light sources. Two types of light sources were used in the responsivity tests: a tungsten incandescent

lamp and a xenon arc lamp. The tungsten source, with a color temperature of 2854 K, is an industry standard. The xenon arc lamp produces a spectral distribution that matches the spectral sensitivity of the sensor much more closely. Responsivity to each light source was measured with and without a Corning Type 1-75 infrared (IR) filter on the camera. The purpose of the IR filter is to reduce cross talk between adjacent pixels in the sensor by means of the deep penetration of IR photons. Responsivity of the sensor to the tungsten light source was measured at 2.56 $V/nJ/mm^2$ with the IR filter in place and 7.71 $V/nJ/mm^2$ without the filter. Responsivity of the sensor to the xenon source was 8.04 $V/nJ/mm^2$ with the IR filter and 24.6 $V/nJ/mm^2$ without the filter.

The vibration tests were conducted by NMERI. These subjected the camera and control unit to linear accelerations ranging from 0.5 g to 2 g at frequencies ranging from 5 Hz to 2000 Hz. These accelerations were applied to the camera along the axis of the CCD array and along an axis in the focal plane of the camera normal to the array axis. The control unit was also tested along two axes. The range of frequencies and accelerations is that specified in MIL-STD-810C, Method 514.2, for equipment carried in propeller-driven aircraft and helicopters. Displacement double amplitudes were less than 0.2 inch throughout the testing. The frequency of vibration was increased logarithmically from 5 Hz to 200 Hz over a period of 5 minutes. The sweep was then reversed. The acceleration was increased from 0.5 g to 2 g between 5 Hz and 20 Hz. During each test, the camera output was monitored and mechanical resonances were noted. The tests indicated that the camera and control unit will operate in this type of vibrational environment. The magnitude of the displacements involved, combined with the 1.36-ms exposure time, indicates that translational vibrations will not degrade the dynamic, on-the-ground resolution of the CCD camera.

Field testing of the FSP sensor consisted of determining an effective ASA number (film speed) for the Fairchild camera, using the hardcopy recorder to measure airborne dynamic resolution and effects of undesirable camera motion, and using the IAS to determine airborne dynamic resolution.

The effective ASA number of the Fairchild sensor was determined by taking light meter readings of surfaces typical of those encountered on a damaged runway surface, adjusting the lens aperture to obtain the best contrast on the hardcopy output, and reading the ASA number associated with the sensor exposure time and the lens aperture setting from the light meter. Results indicated that the effective ASA of the sensor was approximately 90. This ASA number was used successfully in setting the lens aperture during the remaining FSP tests and demonstrations.

The hardcopy recorder was used for a preliminary measurement of sensor airborne dynamic resolution and the effects of undesirable camera motion. This test could determine only a lower limit to the camera's resolution because the resolution of the hardcopy recorder is smaller than the resolution of the sensor, and the bandwidth of the airborne tape recorder used was smaller than the camera bandwidth. Airborne testing was conducted at the Mid-Valley Air Park near Los Lunas, New Mexico. Eight of the Type 1 resolution test patterns shown in Figure 17 were arranged in a grid at the end of the Mid-Valley runway. The 6-inch bars in the resolution test patterns could be distinguished in the hardcopy reproduction of the recorded imagery data taken from an altitude of 270 feet at a ground speed of 70 knots. The hardcopy reproduction of the imagery also indicated that the roll motion and lateral drift of the aircraft were the most significant factors contributing to distortion of the image geometry. On the relatively calm days (winds less than 10 knots) during which the tests were conducted, the roll motion of the aircraft was less than ±3 degrees, and lateral drift was less than ±30 feet. Three degrees of roll produced an apparent 20-foot error in the lateral position in the image. Both types of motion introduced a waviness in the image. The roll motion amplitude was less than 40 feet in the ground image with a wavelength of approximately 100 to 200 feet, indicating a maximum roll rate of less than 7 degrees per second. The distortion due to lateral drift had an amplitude of less than 60 feet and a wavelength of between 500 and 1000 feet, indicating a maximum drift rate of less than 14 feet per second. Neither type of motion significantly affected the ground resolution of the camera. Errors in altitude, speed, and yaw angle also distorted the image, but these errors

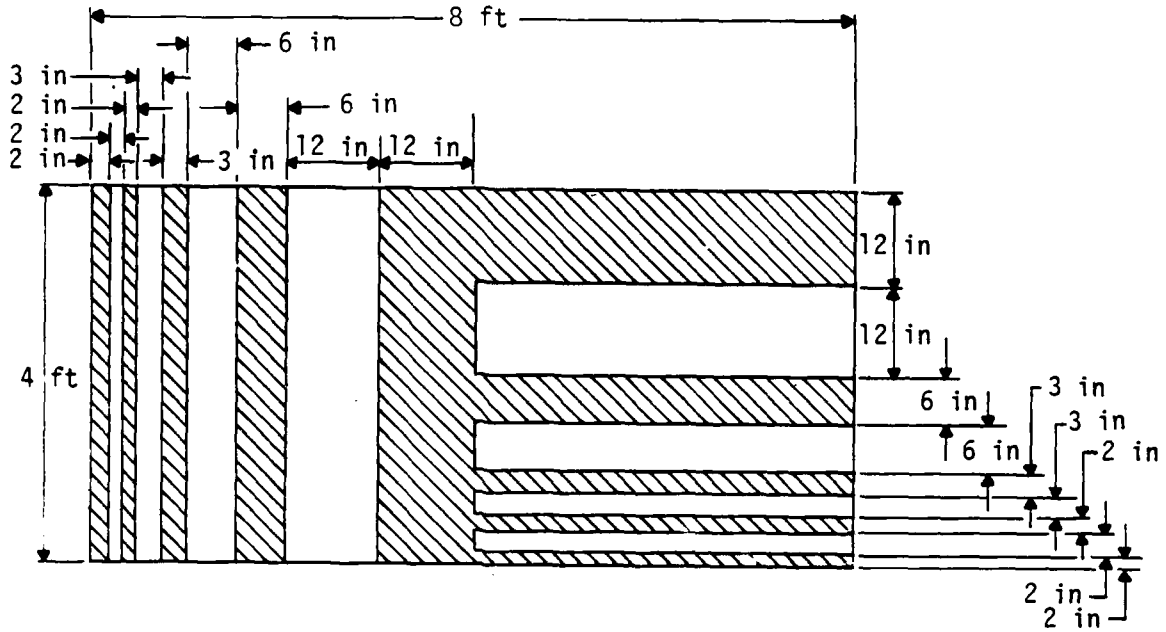

(a) Type 1

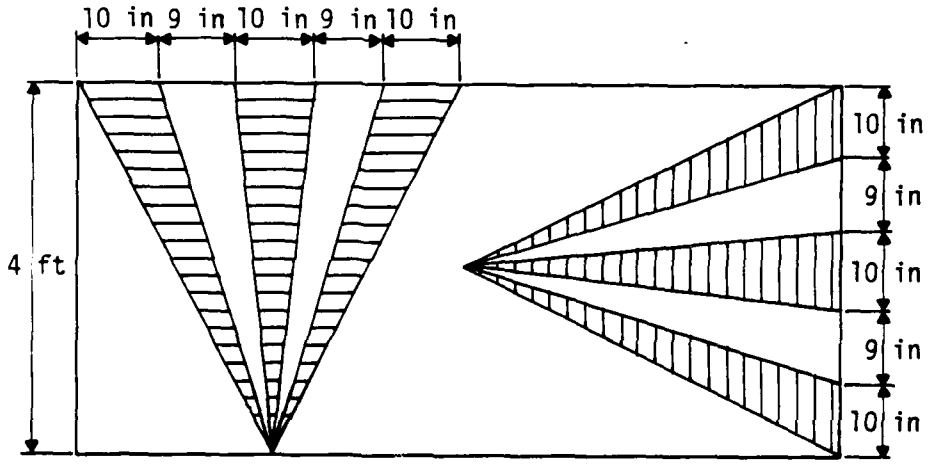

(b) Type 2

Figure 17. Resolution Test Targets for DAS Field Demonstration

were nearly constant over a given pass. Appropriate scaling factors could be used to compensate for their effects. An altitude within 10 feet and a speed within 5 knots of nominal were achieved. The yaw angle for a 6-knot cross-wind component was less than 5 degrees.

The IPS was used to measure the resolution element size produced by the airborne sensor during the field demonstration. The physical dimensions and separation of the resolution targets were carefully measured. The IPS was used to measure the number of pixels separating features in the image of the resolution targets. The measured resolution element sizes ranged from 1.24 to 1.78 inches laterally and from 1.78 to 2.18 inches longitudinally. Altitude during the image-gathering passes ranged from 210 to 250 feet and ground speed from 65 to 73 knots.

TESTING OF IAS

IAS testing consisted of verifying that specific tasks had been accomplished and measuring the time required to perform each task. The tasks tested were the transfer of imagery data from data link to mass storage, the transfer of imagery from the ICS to the IPS, the creation of a low-resolution image from high-resolution data, interactive damage identification on the IPS, damage identification and input to ICS using the hardcopy recorder and an ICS terminal, and selection of the MOS.

The transfer of a high-resolution image of a 10,000-foot by 270-foot runway from tape to disk was accomplished in 5 minutes 58 seconds. The transfer of imagery data from the ICS to the IPS required 10 or 20 seconds depending on whether 256 or 512 kbytes of refresh memory were loaded. The 64:1 compression of the full-resolution image to create a low-resolution image required 6 minutes 3 seconds using the averaging algorithm. It was shown that 125 damages could be interactively identified, located, sized, and classified on the IPS in 32 minutes 14 seconds by an operator with limited training. This time includes the transferring of images between the ICS and the IPS. It required 46 minutes 53 seconds to locate, size, and classify the same 125 damages using a hardcopy recording and loading the information to the ICS by means of a keyboard terminal. Both these damage-assessment times were obtained when only

one operator was identifying damages. In the hardcopy recording test, a second person fed data to the terminal as the operator identified the damages on the hardcopy image. Once the data input was completed, the MOS selection program required 16 minutes 50 seconds to select the three best MOSs in each category using a lateral step size of 25 feet, a longitudinal step size of 100 feet, and five angled positions for each MOS. The runway length and width were 10,000 feet and 150 feet, respectively. The MOS was 5000 by 50 feet.

Tests to determine the accuracy and error rates obtained when the IPS and the hardcopy recorder were used in locating, sizing, and classifying damaged areas were not performed because of a lack of realistic damage imagery data and limited time available. No accuracy or error-rate criteria had been specified.

SECTION V
FIELD DEMONSTRATION

A complete field demonstration of the DAS was conducted at Kirtland AFB and Mid-Valley Air Park, New Mexico, between 10 November 1980 and 21 November 1980. The purpose of the demonstration was to verify the concept of the DAS. A test plan was submitted to and approved by AFESC. A summary of the test results as of 18 November 1980 was presented on that day to representatives from AFESC and from Aeronautical Systems Division (ASD), the Tactical Air Command (TAC), and the Air Force Wright Aeronautical Laboratories (AFWAL). Requirements for the system, except the use of automatic detection and feature extraction and completion of the damage assessment and MOS selection within 30 minutes, were successfully met. The AFESC task officer was present during the test to verify the results.

GATHERING IMAGERY DATA USING FLIGHT SENSOR PACKAGE

The FSP was rigidly mounted in a Cessna 180 aircraft for the field demonstration (Figure 5). The resolution targets shown in Figure 17 were arranged in a grid at the end of runway 17/35 at Mid-Valley Air Park (Figure 18). The aircraft made five passes over the resolution grid. The first four passes were made at altitudes of 210 to 250 feet and at speeds of 65 to 73 knots. During the first of these passes, aircraft motion over the target area was minimized. During the following passes, the pilot induced moderate roll, heavy roll, and heavy yaw while over the target area. The fifth pass over the resolution grid was made at an altitude of 150 feet and a speed of 61 knots. The data gathered at Mid-Valley Air Park were used to demonstrate the effects of aircraft motion on the size of the resolution element.

A single pass was made over runway 8/26 at Kirtland AFB. The altitude during the pass was 300 feet and the speed was 70 knots. Aircraft motion was minimized. Data from this pass were used to verify the field of view and data quantity requirements of the FSP and the IAS.

Weather conditions during FSP testing were clear. The temperature ranged from 60°F to 70°F. Winds were light and variable, less than 5 knots. The

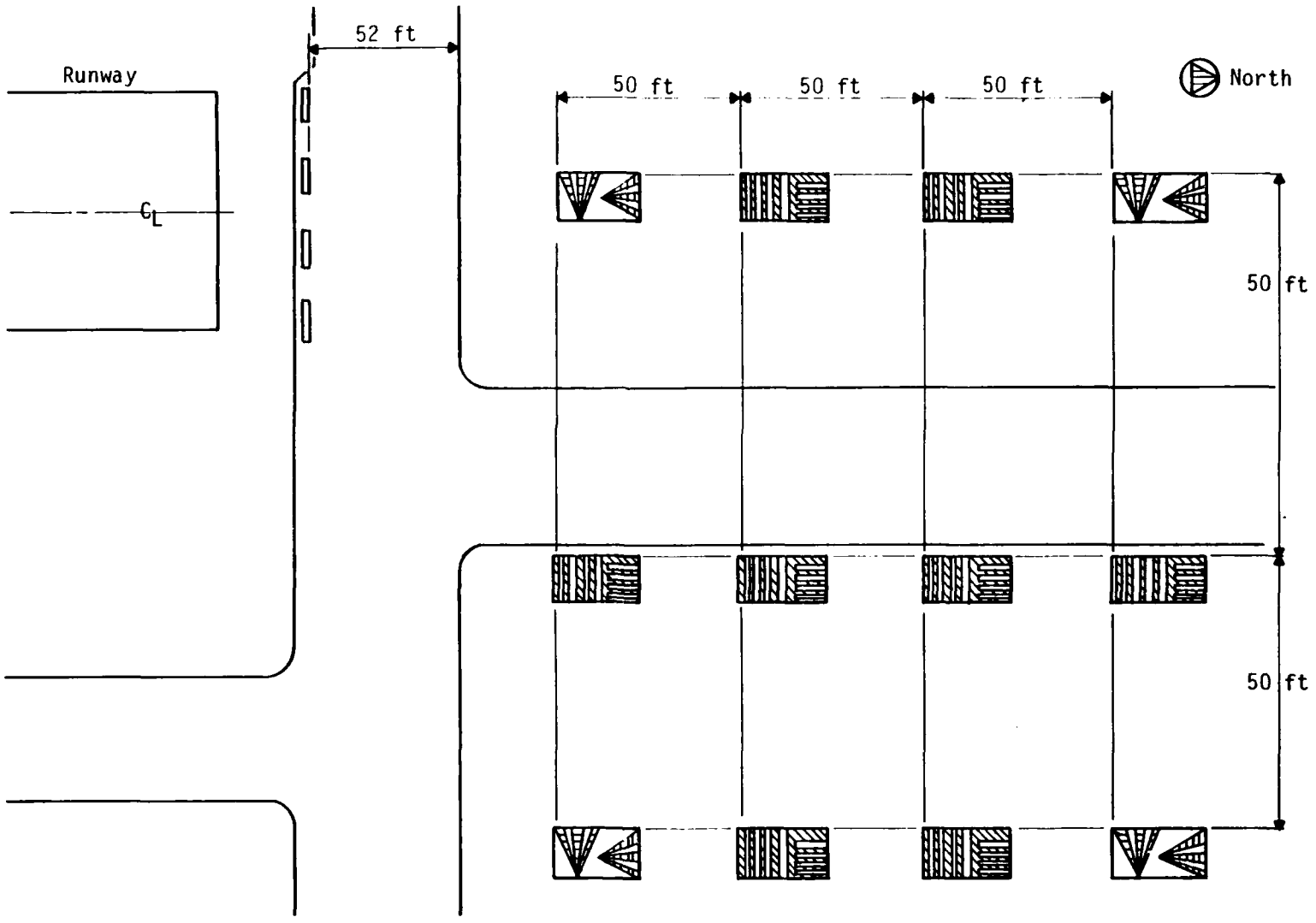

Figure 18. Resolution Target Arrangement

tests were conducted between 11:00 a.m. and 2:00 p.m. A pilot and an equipment operator were aboard the Cessna 180 during testing.

DATA QUANTITY AND RATES

The imagery data of the Kirtland AFB runway gathered by the FSP were transferred to the IAS mass storage disks through the input data interface. This operation was timed. Features at both ends of the stored image were examined and compared with a map of the runway to determine the length and width of the stored image. The number of pixels in the width of the runway was counted using the IPS, and the number of lines in the stored image was obtained from the line count recorded with the imagery data. The average resolution element dimensions were determined using the number of lines and pixels and the known dimensions of the recorded image.

The full-resolution image was compressed by a factor of 64:1 to produce a low-resolution runway image that could be scanned rapidly. The time required to scan the entire low-resolution image of the runway was measured. The imagery data for the Kirtland runway were also transferred from the airborne recorder to the hardcopy recorder. This operation was timed.

Table 15 lists the significant quantities, the specified values, and the values obtained from the Kirtland AFB runway imagery data.

TABLE 15. DATA QUANTITIES AND RATES FROM IMAGERY DATA OF KIRTLAND AFB RUNWAY

Data Quantities and Rates	Specified Value	Measured Value
Stored Image Dimensions		
Length	10,000 feet	10,938 feet
Width	250 feet	267 feet
Resolution Element Dimensions		
Length	1.7 to 2.1 inches	2.00 inches
Width	1.7 to 2.1 inches	1.85 inches
IAS Runway Image Storage Time	300 seconds	
Mass Storage Disks	---	358 seconds
Hardcopy Recorder	---	125 seconds
IAS Runway Image Display Time	300 seconds	
IPS Display	---	363 seconds
Hardcopy Recorder	---	125 seconds

DETERMINATION OF RESOLUTION ELEMENT SIZE

The ground resolution element size of the stored imagery data from Mid-Valley Air Park was determined by counting the number of pixels and lines within features of known dimensions or between features of known separation and dividing the known dimension or separation by the number of lines or pixels. Resolution element size was calculated using the 4-foot and 8-foot dimensions of the resolution target and the 50-foot target separation for the no-roll, moderate-roll, and heavy-roll passes. The roll rates were also determined from the imagery. Table 16 lists the minimum and maximum lateral and longitudinal resolution element dimensions measured for each pass along with altitude, speed, and calculated roll rate.

TABLE 16. MEASURED RESOLUTION ELEMENT DIMENSIONS

Pass	Lateral Dimension, inches		Longitudinal Dimension, inches		Altitude, feet	Speed, knots	Roll Rate, degrees/second
	Minimum	Maximum	Minimum	Maximum			
No Roll	1.24	1.27	1.80	2.00	210	65	1.3
Moderate Roll	1.50	1.71	2.02	2.18	250	73	13.3
Heavy Roll	1.55	1.78	1.78	2.04	250	67	20.7

The dimensions measured demonstrated that roll motion of the aircraft does not significantly alter the resolution element size and that altitude and aircraft velocity are the most significant factors.

DATA ENTRY TO IMAGE ANALYSIS SYSTEM

The IAS accepts data from three sources. Imagery data from the FSP can be input through the input data interface. Imagery data from photographic transparencies can be input through the IPS using the vidicon/light table. Damage data such as type, size, and location can be input manually at the ICS terminals. Manual entry of damage data was demonstrated by loading a complete list of the damage types, sizes, and locations used at the North Field Interim Crater Repair Test. The input data were accepted by PART.01 of the MOS selection software, which created damage files in the appropriate format for use in

PART.02 of the MOS selection software. The damage files were displayed when the data input was completed, and it was demonstrated that the operator could delete, change, or add data values to the damage files from the keyboard terminal.

Imagery input from the vidicon/light table was accomplished by placing a photographic transparency on the light table, aligning and focusing the vidicon using the video display monitor, transferring the displayed image to refresh memory, capping the vidicon lens, and recalling the stored image from refresh memory to the video display.

The transfer of imagery data from the FSP was demonstrated during the verification of data quantities and rates. Data were transferred to both the mass storage disks and the hardcopy recorder.

IMAGE ANALYSIS USING IMAGE ANALYSIS SYSTEM

Imagery data gathered during the North Field Test were used to demonstrate the image-analysis capabilities of the IAS. The runway imagery was compressed using both the straight averaging mode and the differencing routine. The results of both compressions were displayed on the IPS. The quality of these low-resolution images was compared to that of the high-resolution image.

The capability for magnifying both the high- and low-resolution displays using the trackball and using function keys was demonstrated. The capability for translating within the magnified image using the trackball and using function keys was also demonstrated. The motion within the image was controlled by the operator. The translation could be stopped when desired.

The function keys and trackball were used to mark the location and size of damages in both high- and low-resolution images. The color and size of the markings used indicated the type of damage and difficulty of repair. Storage of the damage data from the IPS on the ICS was verified by displaying the damage files on the ICS terminal. The capability for marking noisy data on the IPS and examining the lost-data flags stored with the image data were demonstrated.

The following image-enhancement functions were demonstrated on the IPS:

1. Intensity gain and slope adjustment from the keyboard and with the trackball
2. Contouring of the image data values
3. False color generation
4. Magnification and translation
5. Image marking

Scaling of the image using separate lateral and longitudinal scale factors derived from reference points marked on the IPS and correction of lateral damage locations using the runway edge marks produced on the IPS were demonstrated on the ICS using the PART.00 program.

REPAIR AREA SELECTION

The repair area selection capabilities of the IAS were demonstrated in the following manner. A small number of damages, carefully located so that only one undamaged 5000- by 50-foot MOS was left on the runway, were input using program PART.01. The MOS selection program, PART.02, was then run. The program selected the undamaged MOS as the best repair area for the up-runway, down-runway, and bidirectional MOS. A complete list of type, size, and location damage data used during the second day of field testing at the North Field Test were input using PART.01. Program PART.02 was run using the following step sizes: (1) 500 feet longitudinally and 50 feet laterally with three angular positions per MOS start location; (2) 100 feet longitudinally and 25 feet laterally with five angular positions per MOS start location; and (3) 50 feet longitudinally and 10 feet laterally with 11 angular positions per MOS start location. The best MOS selected when the largest step size was used was a completely different location from those selected when the smaller step sizes were used; also, the repair time was much higher. The MOS locations and the associated repair times selected when the smaller step sizes were used were very close. These were qualitative observations made during the demonstration. They support the use of a step size of 100 feet longitudinally and 25 feet laterally, with five angular positions for each MOS start location.

The system's ability to consider all buried UXO either as duds (short repair time) or as detonation craters (standard crater repair techniques) was demonstrated. The system's ability to accept various density ratios was also displayed.

Appendix A contains a listing of the North Field damage data and the MOS selections that resulted when a step size of 100 feet longitudinally and 25 feet laterally with five angular positions for each MOS start location were used.

DEMONSTRATION OF TOTAL SYSTEM FUNCTION

Essentially two different DASs were demonstrated. Both used the FSP to gather imagery data and the ICS to select the best MOSs. One system used the IPS to locate, size, and classify damages; the other used hardcopy image recording, manual measurement of damage location and size, and manual entry of the damage data at an ICS keyboard terminal. The demonstration consisted of performing the complete damage assessment and MOS selection, timing each of the basic functions, and verifying that the function had been performed. The times required to perform these basic functions were added together to determine the total time requirement for each system. The same times for imagery data collection, using the FSP, and MOS selection, using the ICS, were used for both systems. The time required for each system to size, locate, and classify 125 damages was calculated from the time required to classify a smaller number of damages from the imagery gathered at the North Field Test. The average time required to classify a single damage was assumed to be a constant for each system, and the time required to classify 125 damages was extrapolated from the time required to process the damages actually classified. Table 17 lists the functions and the measured or calculated times.

TABLE 17. DAS FUNCTIONS AND TIME REQUIREMENTS

Function	Time Required	
	Using IPS	Using Hardcopy Recorder
Gather Imagery Data with FSP (from time aircraft is started to time recorder is removed on the ground; imagery gathered from one 10,000-foot runway.)	14 minutes 32 seconds	14 minutes 32 seconds
Transport tape to IAS Hook-up	2 minutes	2 minutes
Transfer Imagery Data to Mass Storage Disks	5 minutes 58 seconds	[a]---
Compress Full-Resolution Image (average only)	6 minutes 3 seconds	[a]---
Transfer Imagery Data to Hardcopy Recording	[a]---	1 minute 25 seconds
Measured Damage Classification and Input Time	16 minutes 30 seconds (64 damages)	21 minutes 0 seconds (56 damages)
Calculated Time for Classifing 125 Damages	32 minutes 14 seconds	46 minutes 53 seconds
Run MOS Selection Program (PART.02)	16 minutes 50 seconds	16 minutes 50 seconds
List Results	1 minute 15 seconds	1 minute 15 seconds
Total Damage Assessment and MOS Selection Time	78 minutes 52 seconds	82 minutes 55 seconds

a. Not applicable.

SECTION VI
CONCLUSIONS AND RECOMMENDATIONS

The concept that the Air Force can assess runway damage by using an airborne sensor and computerized image processing equipment was verified in this effort. Although the system developed by NMERI does not meet the 30-minute goal for damage assessment and MOS selection established by the Air Force, a similar system employing a real-time RF data link, a mass storage system capable of accepting real-time imagery data, a faster minicomputer, and multiple (four) interactive video display stations could meet the 30-minute time limit for 125 damages on a single 10,000- by 250-foot runway. If it were necessary to process more damages or more pavement surfaces, the size of the IAS could be increased proportionately; the only increase in assessment time would be the additional reconnaissance time. This DAS provides a faster, safer, less labor-intensive method of reconnaissance and assessment.

A sensor with day/night capability should be used in the DAS of the future. A thermal IR, a more sensitive vidicon with a lighting system, or an active sensor should be provided. NMERI recommends the use of the Perkin-Elmer KA-98 System B day/night camera modified for lower altitude, higher resolution operation. This device is an active laser line-scan sensor requiring no additional lighting system. The unit is compact and is internally roll-compensated.

It should not be necessary to develop a completely new telemetry link because RF and microwave telemetry links are available both commercially and within the military. Data integrity and protection in a hostile electronic environment must be considered. An airborne recorder should be included in the system for backup. AMPEX manufactures a 300-Mbyte disk storage system capable of accepting data at a rate of approximately 10 Mbytes per second. This system, which costs about $300,000, would be adequate for accepting imagery data in real time.

Selection of a minicomputer should await the further development of MOS selection software. Alternative MOS selection algorithms should be investigated. Factors other than repair time should be considered. An optimum hardware-software combination should be selected.

Numerous interactive video display and image processing systems are on the market today. A system much less sophisticated than the ISI system could be used, but multiple display stations would be essential. Each display station must be capable of indicating the location, size, and type of damage and the location and type of other features interactively on the video screen.

An alternative to the fast mass storage system and multiple video display stations would be to use a hard-copy image, manual measurement of feature location and size, and manual loading of damage data to the minicomputer through multiple keyboard terminals. A greater number of damage assessors and keyboard terminals with operators would be required in this system than the number of video display stations required for the previously described system because feature measurement is a slower process when it is done manually than when an interactive display is used. It should be possible to implement the hardcopy image system more rapidly and at a lower cost than the system requiring interactive display terminals. The hardcopy image system could be used as an interim system while the more sophisticated video display system is developed.

NMERI recommends that the investigation of a real-time damage assessment system be initiated. The Perkin Elmer System B relief sensor appears to offer significant advantages over reflectance sensors for automated feature recognition. It may be possible to process the relief data in real time on board the aircraft, using hardware being developed at Perkin Elmer, and to transmit only damage type, size, and location to the ground for MOS selection. This system would require a relatively simple data link, storage device, and minicomputer system and should be able to select an MOS within 5 to 10 minutes after aerial reconnaissance had been completed, regardless of the number of damages and pavement surfaces examined. Figures 19, 20, and 21 present the three damage assessment systems recommended by NMERI.

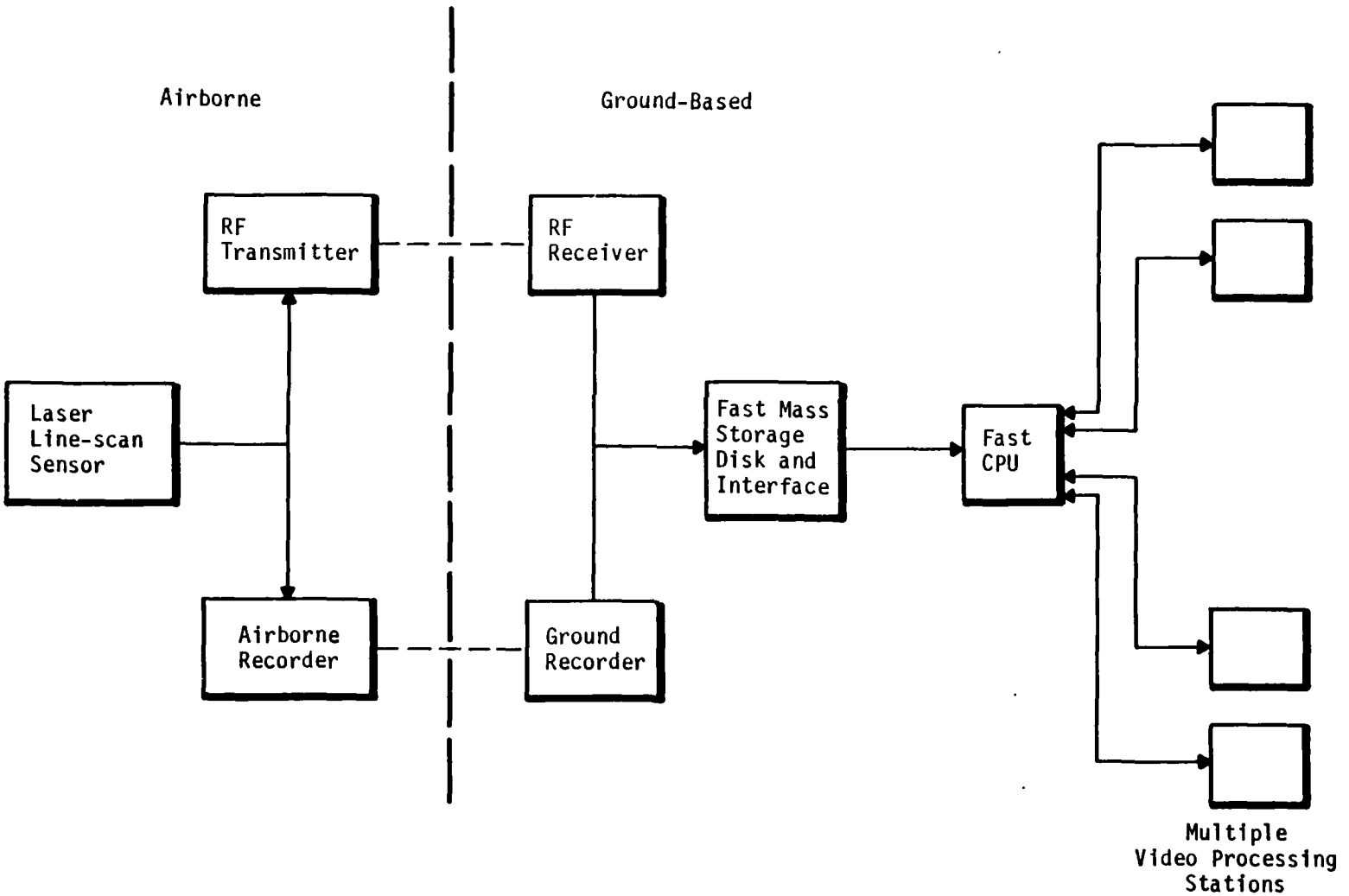

Figure 19. Multiple Video Processing Station DAS

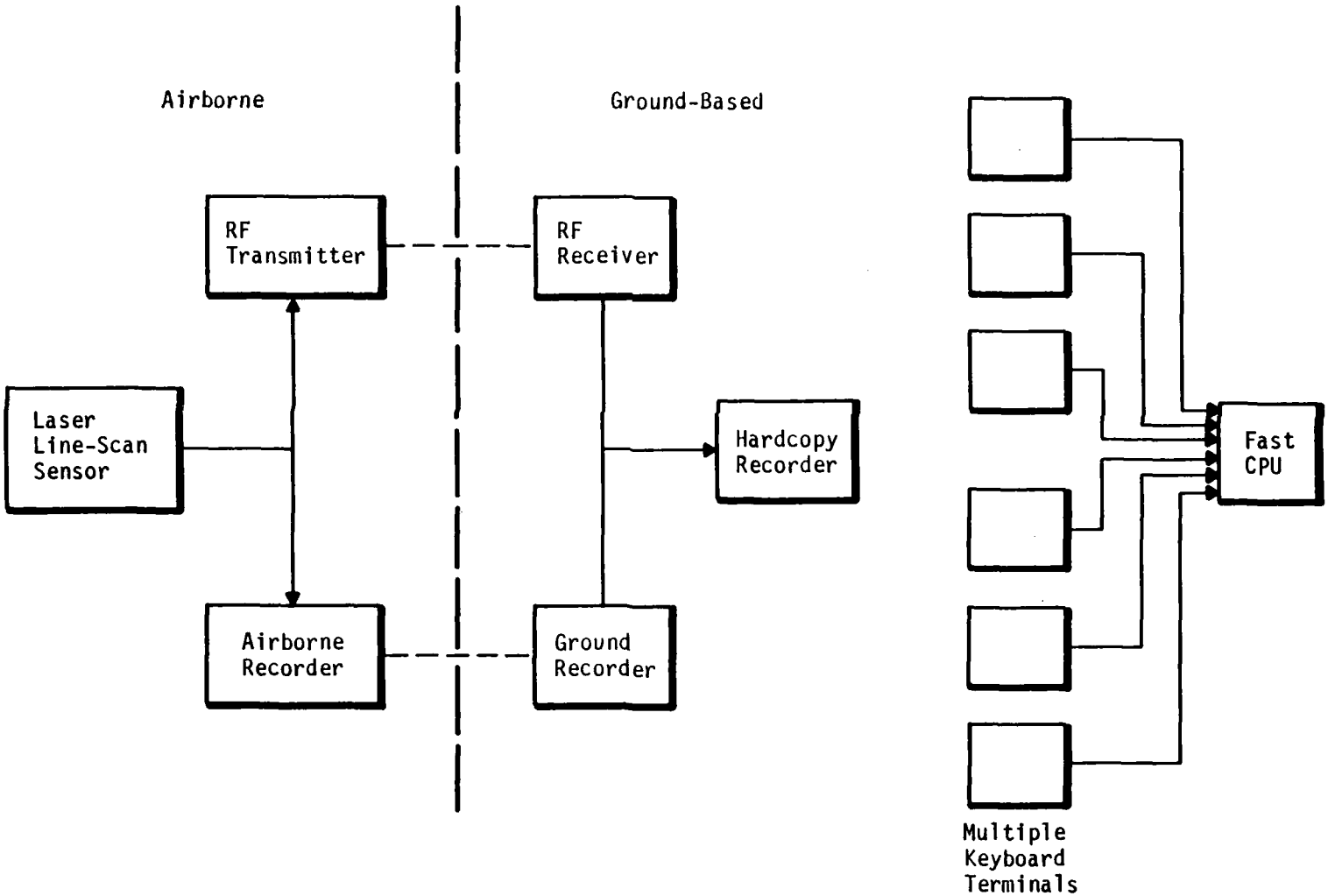

Figure 20. Hardcopy DAS

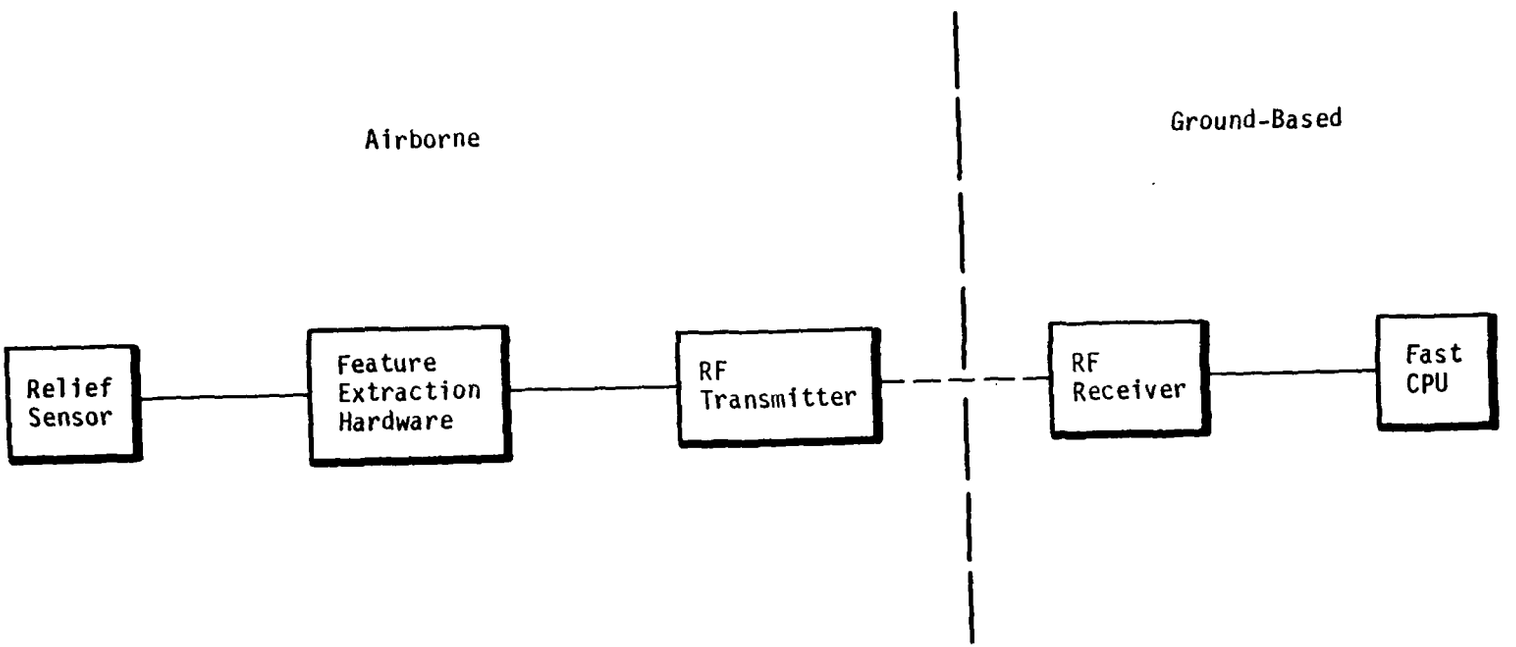

Figure 21. Real Time DAS

REFERENCES

1. Hokanson, L. D., and Rollings, R. S., *Field Test of Standard Bomb Damage Repair Techniques for Pavements*, AFWL-TR-75-148, Air Force Weapons Laboratory, Kirtland Air Force Base, New Mexico, October 1975.
2. Hokanson, L. D., *Tyndall Air Force Base Bomb Damage Repair Field Test Documentation and Analysis*, AFWL-TR-74-226, Air Force Weapons Laboratory, Kirtland Air Force Base, New Mexico, October 1975.
3. Brooks, G. W., Cunningham, J. E., and Mayer, P. W., *Bomb Damage Repair (BDR) Damage Prediction*, Volumes I and II, TRW-75-24, Air Force Weapons Laboratory, Kirtland Air Force Base, New Mexico.
4. Caldwell, L. R., and Jacobsen, F. J., *Interim Guidance for Surface Roughness Criteria*, ESL-TR-79-37, Air Force Engineering and Service Center, Tyndall Air Force Base, Florida, October 1979.
5. Hudson, Richard D., Jr., *Infrared System Engineering*, John Wiley & Sons, New York, 1969.
6. Woodlief, Thomas, Jr., *SPSE Handbook of Photographic Science and Engineering*, John Wiley & Sons, New York, 1972.

(The reverse of this page is blank)

APPENDIX A
SAMPLE MOS SELECTION SOFTWARE INPUT AND OUTPUT

Title	Page
North Field Damage Data and Command Input Sequence	112
MOS Selection Output	134

```
>RUN PART01


  CHOOSE: 1 - ENTER TAXI DAMAGES FOR A NEW PATH
          2 - MAKE CORRECTIONS TO TAXI DATA
          3 - STORE TAXI DATA ON DISC
          4 - GO ON TO RUNWAY DAMAGES.....1


    BURIED UXOS CAN BE CONSIDERED TWO WAYS:
           1 - REPAIRED BEFORE EXPLODING, OR
           2 - REPAIRED AS POST-EXPLOSION CRATER....1


  SCALING FACTOR IN THE X DIRECTION FOR TW1
  100 FT (REAL) = XX.XXX INCHES (ON FILM STRIP).
   ENTER X.....100


  SCALING FACTOR IN THE Y DIRECTION FOR TW1
  100 FT (REAL) = YY.YYY INCHES (ON FILM STRIP).
   ENTER Y.....100




 ENTER: THE DAMAGES ON A PATH THROUGH   TW1
   THAT WOULD MAKE IT USABLE AS A TAXIWAY.
 ENTER: T, XXX.XXX, YYY.YYY; WHERE:
  XXX.XXX = DISTANCE DOWN  TW1
  YYY.YYY = DISTANCE FROM CENTERLINE (+RT, -LT)
       T = TYPE OF DAMAGE   1 - CRATER
                            2 - CAMO-HEAVE
                            3 - SPALL FIELD
                            4 - BOMBLET FIELD
                            5 - SURFACE UXO
                            6 - BURIED UXO


 NOTES: 1) TO END DATA INPUT... ENTER <CR>.
        2) FOR RNWY THE PATH SHOULD BEGIN AT THE TW1
           ENTRANCE TO THE RUNWAY AND END AT THE 5000
           FT. MARK.
        3) RMP1 = PATH FROM AIRCRAFT DISPERSAL AREA
           TO TW1. RMP2 = PATH FROM A.D.A. TO TW2.
```

```
 ?5,190,25
ENTER: DIAMETER OF SURFACE UXO (FT) [DDD.DDD]: .75

 ?

 DATA INPUT CONCLUDED FOR   TW1  A TOTAL OF      1 DAMAGES



 SCALING FACTOR IN THE X DIRECTION FOR TW2
 100 FT (REAL) = XX.XXX INCHES (ON FILM STRIP).
  ENTER X.....100


 SCALING FACTOR IN THE Y DIRECTION FOR TW2
 100 FT (REAL) = YY.YYY INCHES (ON FILM STRIP).
  ENTER Y.....100



ENTER: THE DAMAGES ON A PATH THROUGH   TW2
  THAT WOULD MAKE IT USABLE AS A TAXIWAY.
ENTER: T, XXX.XXX, YYY.YYY; WHERE:
 XXX.XXX = DISTANCE DOWN  TW2
 YYY.YYY = DISTANCE FROM CENTERLINE (+RT, -LT)
      T = TYPE OF DAMAGE    1 - CRATER
                            2 - CAMO-HEAVE
                            3 - SPALL FIELD
                            4 - BOMBLET FIELD
                            5 - SURFACE UXO
                            6 - BURIED UXO


NOTES: 1) TO END DATA INPUT... ENTER <CR>.
       2) FOR RNWY THE PATH SHOULD BEGIN AT THE TW1
          ENTRANCE TO THE RUNWAY AND END AT THE 5000
          FT. MARK.
       3) RMP1 = PATH FROM AIRCRAFT DISPERSAL AREA
          TO TW1. RMP2 = PATH FROM A.D.A. TO TW2.

 ?1,150,-30
ENTER: APPARENT CRATER DIAMETER (FT) [DDDD.DD]: 30
```

```
 ?1,200,-30
ENTER: APPARENT CRATER DIAMETER (FT) [DDDD.DD]: 30

 ?1,880,-30
ENTER: APPARENT CRATER DIAMETER (FT) [DDDD.DD]: 40

 ?1,1000,-30
ENTER: APPARENT CRATER DIAMETER (FT) [DDDD.DD]: 40

 ?6,770,20
ENTER: DIAMETER OF BURIED UXO ENTRANCE (FT) [DDD.DDD]: .75

 ?6,1050,10
ENTER: DIAMETER OF BURIED UXO ENTRANCE (FT) [DDD.DDD]: .75

 ?6,1100,0
ENTER: DIAMETER OF BURIED UXO ENTRANCE (FT) [DDD.DDD]: .75

 ?5,700,2
ENTER: DIAMETER OF SURFACE UXO (FT) [DDD.DDD]: .75

 ?

 DATA INPUT CONCLUDED FOR   TW2  A TOTAL OF      8 DAMAGES



 SCALING FACTOR IN THE X DIRECTION FOR RMP1
 100 FT (REAL) = XX.XXX INCHES (ON FILM STRIP).
  ENTER X.....100


 SCALING FACTOR IN THE Y DIRECTION FOR RMP1
 100 FT (REAL) = YY.YYY INCHES (ON FILM STRIP).
  ENTER Y.....100
```

```
ENTER: THE DAMAGES ON A PATH THROUGH   RMP1
  THAT WOULD MAKE IT USABLE AS A TAXIWAY.
ENTER: T, XXX.XXX, YYY.YYY; WHERE:
 XXX.XXX = DISTANCE DOWN  RMP1
 YYY.YYY = DISTANCE FROM CENTERLINE (+RT, -LT)
      T = TYPE OF DAMAGE    1 - CRATER
                            2 - CAMO-HEAVE
                            3 - SPALL FIELD
                            4 - BOMBLET FIELD
                            5 - SURFACE UXO
                            6 - BURIED UXO


NOTES: 1) TO END DATA INPUT... ENTER <CR>.
       2) FOR RNWY THE PATH SHOULD BEGIN AT THE TW1
          ENTRANCE TO THE RUNWAY AND END AT THE 5000
          FT. MARK.
       3) RMP1 = PATH FROM AIRCRAFT DISPERSAL AREA
          TO TW1. RMP2 = PATH FROM A.D.A. TO TW2.

 ?1,260,-300
ENTER: APPARENT CRATER DIAMETER (FT) [DDDD.DD]: 20

 ?1,290,-280
ENTER: APPARENT CRATER DIAMETER (FT) [DDDD.DD]: 20

 ?

 DATA INPUT CONCLUDED FOR   RMP1 A TOTAL OF      2 DAMAGES



 SCALING FACTOR IN THE X DIRECTION FOR RMP2
 100 FT (REAL) = XX.XXX INCHES (ON FILM STRIP).
  ENTER X.....100


 SCALING FACTOR IN THE Y DIRECTION FOR RMP2
 100 FT (REAL) = YY.YYY INCHES (ON FILM STRIP).
  ENTER Y.....100
```

```
ENTER: THE DAMAGES ON A PATH THROUGH   RMP2
  THAT WOULD MAKE IT USABLE AS A TAXIWAY.
ENTER: T, XXX.XXX, YYY.YYY; WHERE:
 XXX.XXX = DISTANCE DOWN  RMP2
 YYY.YYY = DISTANCE FROM CENTERLINE (+RT, -LT)
      T = TYPE OF DAMAGE    1 - CRATER
                            2 - CAMO-HEAVE
                            3 - SPALL FIELD
                            4 - BOMBLET FIELD
                            5 - SURFACE UXO
                            6 - BURIED UXO


NOTES: 1) TO END DATA INPUT... ENTER <CR>.
       2) FOR RNWY THE PATH SHOULD BEGIN AT THE TW1
          ENTRANCE TO THE RUNWAY AND END AT THE 5000
          FT. MARK.
       3) RMP1 = PATH FROM AIRCRAFT DISPERSAL AREA
          TO TW1. RMP2 = PATH FROM A.D.A. TO TW2.

 ?4,2400,0
ENTER: DIAMETER OF BOMBLET FIELD (FT) [DDDD.DD]: 600
ENTER: NUMBER OF BOMBLETS IN FIELD [NNNNNN]: 75

 ?

 DATA INPUT CONCLUDED FOR   RMP2 A TOTAL OF      1 DAMAGES




 SCALING FACTOR IN THE X DIRECTION FOR RNWY
 100 FT (REAL) = XX.XXX INCHES (ON FILM STRIP).
  ENTER X.....100


 SCALING FACTOR IN THE Y DIRECTION FOR RNWY
 100 FT (REAL) = YY.YYY INCHES (ON FILM STRIP).
  ENTER Y.....100
```

```
ENTER: THE DAMAGES ON A PATH THROUGH   RNWY
  THAT WOULD MAKE IT USABLE AS A TAXIWAY.
ENTER: T, XXX.XXX, YYY.YYY; WHERE:
 XXX.XXX = DISTANCE DOWN  RNWY
 YYY.YYY = DISTANCE FROM CENTERLINE (+RT, -LT)
      T = TYPE OF DAMAGE    1 - CRATER
                            2 - CAMO-HEAVE
                            3 - SPALL FIELD
                            4 - BOMBLET FIELD
                            5 - SURFACE UXO
                            6 - BURIED UXO


NOTES: 1) TO END DATA INPUT... ENTER <CR>.
       2) FOR RNWY THE PATH SHOULD BEGIN AT THE TW1
          ENTRANCE TO THE RUNWAY AND END AT THE 5000
          FT. MARK.
       3) RMP1 = PATH FROM AIRCRAFT DISPERSAL AREA
          TO TW1. RMP2 = PATH FROM A.D.A. TO TW2.

 ?1,430,-30
ENTER: APPARENT CRATER DIAMETER (FT) [DDDD.DD]: 30

 ?4,345,0
ENTER: DIAMETER OF BOMBLET FIELD (FT) [DDDD.DD]: 690
ENTER: NUMBER OF BOMBLETS IN FIELD [NNNNNN]: 750

 ?3,330,-4-\-\0
ENTER: DIAMETER OF SPALL FIELD (FT) [DDDD.DD]: 660
ENTER: NUMBER OF SPALLS IN FIELD [NNNNNN]: 90

 ?3,1590,0
ENTER: DIAMETER OF SPALL FIELD (FT) [DDDD.DD]: 840
ENTER: NUMBER OF SPALLS IN FIELD [NNNNNN]: 100

 ?3,2565,0
ENTER: DIAMETER OF SPALL FIELD (FT) [DDDD.DD]: 750
ENTER: NUMBER OF SPALLS IN FIELD [NNNNNN]: 72

 ?4,3510,0
ENTER: DIAMETER OF BOMBLET FIELD (FT) [DDDD.DD]: 1680
ENTER: NUMBER OF BOMBLETS IN FIELD [NNNNNN]: 750

 ?

 DATA INPUT CONCLUDED FOR   RNWY A TOTAL OF      6 DAMAGES
```

```
END - TAXIWAY DATA INPUT

 THE REPAIR TIME IS:        60.0 FOR THE TOTAL      TW1

 THE REPAIR TIME IS:       790.0 FOR THE TOTAL      TW2

 THE REPAIR TIME IS:       200.0 FOR THE TOTAL      RMP1

 THE REPAIR TIME IS:         0.0 FOR THE TOTAL      RMP2

 THE REPAIR TIME IS:       412.0 FOR THE TOTAL      RNWY


CHOOSE: 1 - ENTER TAXI DAMAGES FOR A NEW PATH
        2 - MAKE CORRECTIONS TO TAXI DATA
        3 - STORE TAXI DATA ON DISC
        4 - GO ON TO RUNWAY DAMAGES.....2


TAXIWAY DATA CORRECTION ROUTINE
CHOOSE: 1 - READ A TAXI FILE FROM DISC
        2 - DUMP TAXI ARRAYS TO TERMINAL
        3 - CORRECT A KNOWN BAD POINT
        4 - EXIT.....2
```

TW1 = 1

J = 1	2	3	4	5	I	K
5	190	25	9	2	1	1
0	0	0	0	0	2	1
0	0	0	0	0	3	1
0	0	0	0	0	4	1
0	0	0	0	0	5	1
0	0	0	0	0	6	1
0	0	0	0	0	7	1
0	0	0	0	0	8	1
0	0	0	0	0	9	1
0	0	0	0	0	10	1
0	0	0	0	0	11	1
0	0	0	0	0	12	1
0	0	0	0	0	13	1
0	0	0	0	0	14	1
0	0	0	0	0	15	1
0	0	0	0	0	16	1
0	0	0	0	0	17	1
0	0	0	0	0	18	1
0	0	0	0	0	19	1
0	0	0	0	0	20	1

TW2 = 2

J = 1	2	3	4	5	I	K
1	150	-30	30	3	1	2
1	200	-30	30	3	2	2
1	880	-30	40	4	3	2
1	1000	-30	40	4	4	2
6	770	20	9	2	5	2
6	1050	10	9	2	6	2
6	1100	0	9	2	7	2
5	700	2	9	2	8	2
0	0	0	0	0	9	2
0	0	0	0	0	10	2
0	0	0	0	0	11	2
0	0	0	0	0	12	2
0	0	0	0	0	13	2
0	0	0	0	0	14	2
0	0	0	0	0	15	2
0	0	0	0	0	16	2
0	0	0	0	0	17	2
0	0	0	0	0	18	2
0	0	0	0	0	19	2
0	0	0	0	0	20	2

RMP1 = 3

J =	1	2	3	4	5	I	K
	1	260	-300	20	2	1	3
	1	290	-280	20	2	2	3
	0	0	0	0	0	3	3
	0	0	0	0	0	4	3
	0	0	0	0	0	5	3
	0	0	0	0	0	6	3
	0	0	0	0	0	7	3
	0	0	0	0	0	8	3
	0	0	0	0	0	9	3
	0	0	0	0	0	10	3
	0	0	0	0	0	11	3
	0	0	0	0	0	12	3
	0	0	0	0	0	13	3
	0	0	0	0	0	14	3
	0	0	0	0	0	15	3
	0	0	0	0	0	16	3
	0	0	0	0	0	17	3
	0	0	0	0	0	18	3
	0	0	0	0	0	19	3
	0	0	0	0	0	20	3

RMP2 = 4

J =	1	2	3	4	5	I	K
	4	2400	0	600	75	1	4
	0	0	0	0	0	2	4
	0	0	0	0	0	3	4
	0	0	0	0	0	4	4
	0	0	0	0	0	5	4
	0	0	0	0	0	6	4
	0	0	0	0	0	7	4
	0	0	0	0	0	8	4
	0	0	0	0	0	9	4
	0	0	0	0	0	10	4
	0	0	0	0	0	11	4
	0	0	0	0	0	12	4
	0	0	0	0	0	13	4
	0	0	0	0	0	14	4
	0	0	0	0	0	15	4
	0	0	0	0	0	16	4
	0	0	0	0	0	17	4
	0	0	0	0	0	18	4
	0	0	0	0	0	19	4
	0	0	0	0	0	20	4

```
RNWY  =     5

          J =     1       2       3       4       5          I   K
-------------------------------------------------------------------
                  1     430     -30      30       3          1   5
                  4     345       0     690     750          2   5
                  3     330     -40     660      90          3   5
                  3    1590       0     840     100          4   5
                  3    2565       0     750      72          5   5
                  4    3510       0    1680     750          6   5
                  0       0       0       0       0          7   5
                  0       0       0       0       0          8   5
                  0       0       0       0       0          9   5
                  0       0       0       0       0         10   5
                  0       0       0       0       0         11   5
                  0       0       0       0       0         12   5
                  0       0       0       0       0         13   5
                  0       0       0       0       0         14   5
                  0       0       0       0       0         15   5
                  0       0       0       0       0         16   5
                  0       0       0       0       0         17   5
                  0       0       0       0       0         18   5
                  0       0       0       0       0         19   5
                  0       0       0       0       0         20   5


TAXIWAY DATA CORRECTION ROUTINE
CHOOSE: 1 - READ A TAXI FILE FROM DISC
        2 - DUMP TAXI ARRAYS TO TERMINAL
        3 - CORRECT A KNOWN BAD POINT
        4 - EXIT.....3


ENTER: I,J,K FOR NEW VALUE
       <CR> TO END


?2,5,5
ENTER NEW VALUE FOR: ITAXID(  2,  5,  5).....62
?


TAXIWAY DATA CORRECTION ROUTINE
CHOOSE: 1 - READ A TAXI FILE FROM DISC
        2 - DUMP TAXI ARRAYS TO TERMINAL
        3 - CORRECT A KNOWN BAD POINT
        4 - EXIT.....4
CORRECTION ROUTINE CONCLUDED
```

```
 THE REPAIR TIME IS:        60.0 FOR THE TOTAL      TW1

 THE REPAIR TIME IS:       790.0 FOR THE TOTAL      TW2

 THE REPAIR TIME IS:       200.0 FOR THE TOTAL      RMP1

 THE REPAIR TIME IS:         0.0 FOR THE TOTAL      RMP2

 THE REPAIR TIME IS:       412.0 FOR THE TOTAL      RNWY


CHOOSE: 1 - ENTER TAXI DAMAGES FOR A NEW PATH
        2 - MAKE CORRECTIONS TO TAXI DATA
        3 - STORE TAXI DATA ON DISC
        4 - GO ON TO RUNWAY DAMAGES.....3


CHOOSE: 1 - ENTER TAXI DAMAGES FOR A NEW PATH
        2 - MAKE CORRECTIONS TO TAXI DATA
        3 - STORE TAXI DATA ON DISC
        4 - GO ON TO RUNWAY DAMAGES.....4


CHOOSE: 1 - ENTER RUNWAY DAMAGES
        2 - MAKE CORRECTIONS TO RUNWAY DATA
        3 - STORE RUNWAY DATA ON DISC
        4 - GO BACK TO TAXI SECTION
        5 - GO ON TO VIEWS DAMAGES......1


RUNWAY SCALING FACTOR IN THE X DIRECTION
 100 FT (REAL) = XX.XXXX INCHES (ON FILM STRIP).
  ENTER X.....100


 RUNWAY SCALING FACTOR IN THE Y DIRECTION
 100 FT (REAL) = YY.YYYY INCHES (ON FILM STRIP).
  ENTER Y.....100
```

```
THE DATA INPUT NECESSARY TO FILL THE DAMAGE ARRAY IS:

T,    XXX.XXX,    YYY.YYY;        WHERE:

   XXX.XXX IS THE DISTANCE FROM THE END OF THE RUNWAY
       TO THE DAMAGE.
   YYY.YYY IS THE DISTANCE FROM THE CENTERLINE OF THE RUNWAY
       (POSITIVE=RIGHT, NEGATIVE=LEFT) TO THE DAMAGE.
   T IS THE TYPE OF DAMAGE:
       1 - CRATER
       2 - CAMOHEAVE
       3 - SPALL FIELD
       4 - BOMBLET FIELD
       5 - SURFACE UXO
       6 - BURIED UXO


TO END DATA INPUT ROUTINE... ENTER <CR>.
 ?1,160,-90
ENTER: APPARENT CRATER DIAMETER (FT) [DDDD.DD]: 40
 ?1,320,15
ENTER: APPARENT CRATER DIAMETER (FT) [DDDD.DD]: 30
 ?1,370,20
ENTER: APPARENT CRATER DIAMETER (FT) [DDDD.DD]: 30
 ?1,370,90
ENTER: APPARENT CRATER DIAMETER (FT) [DDDD.DD]: 40
 ?1,430,-30
ENTER: APPARENT CRATER DIAMETER (FT) [DDDD.DD]: 30
 ?1,2830,-100
ENTER: APPARENT CRATER DIAMETER (FT) [DDDD.DD]: 40
 ?1,2850,-43.7
ENTER: APPARENT CRATER DIAMETER (FT) [DDDD.DD]: 20
 ?1,3075,20
ENTER: APPARENT CRATER DIAMETER (FT) [DDDD.DD]: 20
 ?1,3110,-50
ENTER: APPARENT CRATER DIAMETER (FT) [DDDD.DD]: 20
 ?1,3150,-90
ENTER: APPARENT CRATER DIAMETER (FT) [DDDD.DD]: 30
 ?1,3360,-30
ENTER: APPARENT CRATER DIAMETER (FT) [DDDD.DD]: 30
 ?1,3970,50
ENTER: APPARENT CRATER DIAMETER (FT) [DDDD.DD]: 40
 ?1,1200,-100
ENTER: APPARENT CRATER DIAMETER (FT) [DDDD.DD]: 40
 ?1,4360,-20
ENTER: APPARENT CRATER DIAMETER (FT) [DDDD.DD]: 20
 ?1,4525,20
ENTER: APPARENT CRATER DIAMETER (FT) [DDDD.DD]: 20
 ?1,4685,-90
ENTER: APPARENT CRATER DIAMETER (FT) [DDDD.DD]: 20
 ?1,5450,45
ENTER: APPARENT CRATER DIAMETER (FT) [DDDD.DD]: 40
 ?1,5450,65
```

```
ENTER: APPARENT CRATER DIAMETER (FT) [DDDD.DD]: 40
 ?1,5610,80
ENTER: APPARENT CRATER DIAMETER (FT) [DDDD.DD]: 20
 ?1,5640,75
ENTER: APPARENT CRATER DIAMETER (FT) [DDDD.DD]: 20
 ?1,5740,50
ENTER: APPARENT CRATER DIAMETER (FT) [DDDD.DD]: 20
 ?1,5750,-70
ENTER: APPARENT CRATER DIAMETER (FT) [DDDD.DD]: 40
 ?1,6710,0
ENTER: APPARENT CRATER DIAMETER (FT) [DDDD.DD]: 30
 ?1,6780,-70
ENTER: APPARENT CRATER DIAMETER (FT) [DDDD.DD]: 30
 ?1,6830,100
ENTER: APPARENT CRATER DIAMETER (FT) [DDDD.DD]: 30
 ?1,8100,-60
ENTER: APPARENT CRATER DIAMETER (FT) [DDDD.DD]: 40
 ?1,8390,100
ENTER: APPARENT CRATER DIAMETER (FT) [DDDD.DD]: 30
 ?1,8470,0
ENTER: APPARENT CRATER DIAMETER (FT) [DDDD.DD]: 30
 ?1,8700,35
ENTER: APPARENT CRATER DIAMETER (FT) [DDDD.DD]: 40
 ?1,9650,-10
ENTER: APPARENT CRATER DIAMETER (FT) [DDDD.DD]: 30
 ?1,9808,15
ENTER: APPARENT CRATER DIAMETER (FT) [DDDD.DD]: 30
 ?1,9838,50
ENTER: APPARENT CRATER DIAMETER (FT) [DDDD.DD]: 30
 ?6,1030,-30
ENTER: DIAMETER OF BURIED UXO ENTRANCE (FT) [DDD.DDD]: .75
 ?6,2680,-30
ENTER: DIAMETER OF BURIED UXO ENTRANCE (FT) [DDD.DDD]: .75
 ?6,2840,140
ENTER: DIAMETER OF BURIED UXO ENTRANCE (FT) [DDD.DDD]: .75
 ?1,2980,-10
ENTER: APPARENT CRATER DIAMETER (FT) [DDDD.DD]: .75
 ?1,3340,-30
ENTER: APPARENT CRATER DIAMETER (FT) [DDDD.DD]: .75
 ?1,3340,-100
ENTER: APPARENT CRATER DIAMETER (FT) [DDDD.DD]: .75
 ?6,3350,60
ENTER: DIAMETER OF BURIED UXO ENTRANCE (FT) [DDD.DDD]: .75
 ?6,3370,180\081\-180
ENTER: DIAMETER OF BURIED UXO ENTRANCE (FT) [DDD.DDD]: .75
 ?6,3650,-80
ENTER: DIAMETER OF BURIED UXO ENTRANCE (FT) [DDD.DDD]: .75
 ?6,3660,-90
ENTER: DIAMETER OF BURIED UXO ENTRANCE (FT) [DDD.DDD]: .75
 ?6,3780,-140
ENTER: DIAMETER OF BURIED UXO ENTRANCE (FT) [DDD.DDD]: .75
 ?6,3810,-90
ENTER: DIAMETER OF BURIED UXO ENTRANCE (FT) [DDD.DDD]: .75
```

```
 ?6,3900,80
ENTER: DIAMETER OF BURIED UXO ENTRANCE (FT) [DDD.DDD]: .75
 ?6,4100,80
ENTER: DIAMETER OF BURIED UXO ENTRANCE (FT) [DDD.DDD]: .75
 ?6,4190,90
ENTER: DIAMETER OF BURIED UXO ENTRANCE (FT) [DDD.DDD]: .75
 ?6,4230,50
ENTER: DIAMETER OF BURIED UXO ENTRANCE (FT) [DDD.DDD]: .75
 ?6,4350,-150
ENTER: DIAMETER OF BURIED UXO ENTRANCE (FT) [DDD.DDD]: .75
 ?6,4385,-60
ENTER: DIAMETER OF BURIED UXO ENTRANCE (FT) [DDD.DDD]: .75
 ?6,4440,-120
ENTER: DIAMETER OF BURIED UXO ENTRANCE (FT) [DDD.DDD]: .75
 ?6,4470,50
ENTER: DIAMETER OF BURIED UXO ENTRANCE (FT) [DDD.DDD]: .75
 ?6,4470,-40
ENTER: DIAMETER OF BURIED UXO ENTRANCE (FT) [DDD.DDD]: .75
 ?6,4510,100
ENTER: DIAMETER OF BURIED UXO ENTRANCE (FT) [DDD.DDD]: .75
 ?6,4520,110
ENTER: DIAMETER OF BURIED UXO ENTRANCE (FT) [DDD.DDD]: .75
 ?6,4570,13\31\-130
ENTER: DIAMETER OF BURIED UXO ENTRANCE (FT) [DDD.DDD]: .75
 ?6,4605,30
ENTER: DIAMETER OF BURIED UXO ENTRANCE (FT) [DDD.DDD]: .75
 ?6,4610,50
ENTER: DIAMETER OF BURIED UXO ENTRANCE (FT) [DDD.DDD]: .75
 ?6,4610,-30
ENTER: DIAMETER OF BURIED UXO ENTRANCE (FT) [DDD.DDD]: .75
 ?6,4680,-70
ENTER: DIAMETER OF BURIED UXO ENTRANCE (FT) [DDD.DDD]: .75
 ?6,4700,75
ENTER: DIAMETER OF BURIED UXO ENTRANCE (FT) [DDD.DDD]: .75
 ?6,4745,-150
ENTER: DIAMETER OF BURIED UXO ENTRANCE (FT) [DDD.DDD]: .75
 ?6,4785,115
ENTER: DIAMETER OF BURIED UXO ENTRANCE (FT) [DDD.DDD]: .75
 ?6,4965,-55
ENTER: DIAMETER OF BURIED UXO ENTRANCE (FT) [DDD.DDD]: .75
 ?6,4990,0
ENTER: DIAMETER OF BURIED UXO ENTRANCE (FT) [DDD.DDD]: .75
 ?6,5070,-140
ENTER: DIAMETER OF BURIED UXO ENTRANCE (FT) [DDD.DDD]: .75
 ?6,5110,65
ENTER: DIAMETER OF BURIED UXO ENTRANCE (FT) [DDD.DDD]: .75
 ?6,5155,-80
ENTER: DIAMETER OF BURIED UXO ENTRANCE (FT) [DDD.DDD]: .75
 ?6,5180,-10
ENTER: DIAMETER OF BURIED UXO ENTRANCE (FT) [DDD.DDD]: .75
 ?6,5200,-60
ENTER: DIAMETER OF BURIED UXO ENTRANCE (FT) [DDD.DDD]: .75
```

```
 ?6,5200,100
ENTER: DIAMETER OF BURIED UXO ENTRANCE (FT) [DDD.DDD]: .75
 ?6,5250,-20
ENTER: DIAMETER OF BURIED UXO ENTRANCE (FT) [DDD.DDD]: .75
 ?6,5300,-105
ENTER: DIAMETER OF BURIED UXO ENTRANCE (FT) [DDD.DDD]: .75
 ?6,5390,45
ENTER: DIAMETER OF BURIED UXO ENTRANCE (FT) [DDD.DDD]: .75
 ?6,5415,15
ENTER: DIAMETER OF BURIED UXO ENTRANCE (FT) [DDD.DDD]: .75
 ?6,5515,105
ENTER: DIAMETER OF BURIED UXO ENTRANCE (FT) [DDD.DDD]: .75
 ?6,5910,-45
ENTER: DIAMETER OF BURIED UXO ENTRANCE (FT) [DDD.DDD]: .75
 ?6,6070,-150
ENTER: DIAMETER OF BURIED UXO ENTRANCE (FT) [DDD.DDD]: .75
 ?6,6115,-90
ENTER: DIAMETER OF BURIED UXO ENTRANCE (FT) [DDD.DDD]: .75
 ?6,6120,-25
ENTER: DIAMETER OF BURIED UXO ENTRANCE (FT) [DDD.DDD]: .75
 ?6,7860,-135
ENTER: DIAMETER OF BURIED UXO ENTRANCE (FT) [DDD.DDD]: .75
 ?6,7930,-100
ENTER: DIAMETER OF BURIED UXO ENTRANCE (FT) [DDD.DDD]: .75
 ?6,8065,-190
ENTER: DIAMETER OF BURIED UXO ENTRANCE (FT) [DDD.DDD]: .75
 ?6,3480,30
ENTER: DIAMETER OF BURIED UXO ENTRANCE (FT) [DDD.DDD]: .75
 ?5,2975,-150
ENTER: DIAMETER OF SURFACE UXO (FT) [DDD.DDD]: .75
 ?5,3425,-150
ENTER: DIAMETER OF SURFACE UXO (FT) [DDD.DDD]: .75
 ?5,4850,-20
ENTER: DIAMETER OF SURFACE UXO (FT) [DDD.DDD]: .75
 ?5,4850,170
ENTER: DIAMETER OF SURFACE UXO (FT) [DDD.DDD]: .75
 ?5,5300,25
ENTER: DIAMETER OF SURFACE UXO (FT) [DDD.DDD]: .75
 ?5,5200,-75
ENTER: DIAMETER OF SURFACE UXO (FT) [DDD.DDD]: .75
 ?5,5590,90
ENTER: DIAMETER OF SURFACE UXO (FT) [DDD.DDD]: .75
 ?5,5025,-200
ENTER: DIAMETER OF SURFACE UXO (FT) [DDD.DDD]: .75
 ?4,345,0
ENTER: DIAMETER OF BOMBLET FIELD (FT) [DDDD.DD]: 690
ENTER: NUMBER OF BOMBLETS IN FIELD [NNNNNN]: 62
 ?4,2670,4350\0534,0762,4\4,4\4\3510,0
ENTER: DIAMETER OF BOMBLET FIELD (FT) [DDDD.DD]: 1680
ENTER: NUMBER OF BOMBLETS IN FIELD [NNNNNN]: 750
 ?4,5490,0
ENTER: DIAMETER OF BOMBLET FIELD (FT) [DDDD.DD]: 2190
ENTER: NUMBER OF BOMBLETS IN FIELD [NNNNNN]: 412
```

```
 ?4,7485,0
ENTER: DIAMETER OF BOMBLET FIELD (FT) [DDDD.DD]:.660
ENTER: NUMBER OF BOMBLETS IN FIELD [NNNNNN]: 100
 ?3,330,-40
ENTER: DIAMETER OF SPALL FIELD (FT) [DDDD.DD]: 660
ENTER: NUMBER OF SPALLS IN FIELD [NNNNNN]: 90
 ?3,1590,0
ENTER: DIAMETER OF SPALL FIELD (FT) [DDDD.DD]: 840
ENTER: NUMBER OF SPALLS IN FIELD [NNNNNN]: 100
 ?3,2565,0
ENTER: DIAMETER OF SPALL FIELD (FT) [DDDD.DD]: 750
ENTER: NUMBER OF SPALLS IN FIELD [NNNNNN]: 72
 ?3,4440,0
ENTER: DIAMETER OF SPALL FIELD (FT) [DDDD.DD]: 780
ENTER: NUMBER OF SPALLS IN FIELD [NNNNNN]: 135
 ?3,5025,0
ENTER: DIAMETER OF SPALL FIELD (FT) [DDDD.DD]: 150
ENTER: NUMBER OF SPALLS IN FIELD [NNNNNN]: 13
 ?3,5835,0
ENTER: DIAMETER OF SPALL FIELD (FT) [DDDD.DD]: 450
ENTER: NUMBER OF SPALLS IN FIELD [NNNNNN]: 55
 ?3,6270,0
ENTER: DIAMETER OF SPALL FIELD (FT) [DDDD.DD]: 60
ENTER: NUMBER OF SPALLS IN FIELD [NNNNNN]: 4
 ?3,7200,0
ENTER: DIAMETER OF SPALL FIELD (FT) [DDDD.DD]: 1320
ENTER: NUMBER OF SPALLS IN FIELD [NNNNNN]: 200
 ?


 DATA INPUT CONCLUDED...       104 DAMAGES


 CHOOSE: 1 - ENTER RUNWAY DAMAGES
         2 - MAKE CORRECTIONS TO RUNWAY DATA
         3 - STORE RUNWAY DATA ON DISC
         4 - GO BACK TO TAXI SECTION
         5 - GO ON TO VIEWS DAMAGES......2


 RUNWAY DAMAGE CORRECTION ROUTINE

 CHOOSE: 1 - READ RUNWAY FILE FROM DISC
         2 - DUMP CONTENTS OF TABLE TO TERMINAL
         3 - CORRECT A KNOWN BAD POINT
         4 - EXIT.....
```

3\3\2

J = 1	2	3	4	5	I
1	160	-90	40	4	1
1	320	15	30	3	2
1	370	20	30	3	3
1	370	90	40	4	4
1	430	-30	30	3	5
1	2830	-100	40	4	6
1	2850	-43	20	2	7
1	3075	20	20	2	8
1	3110	-50	20	2	9
1	3150	-90	30	3	10
1	3360	-30	30	3	11
1	3970	50	40	4	12
1	1200	-100	40	4	13
1	4360	-20	20	2	14
1	4525	20	20	2	15
1	4685	-90	20	2	16
1	5450	45	40	4	17
1	5450	65	40	4	18
1	5610	80	20	2	19
1	5640	75	20	2	20
1	5740	50	20	2	21
1	5750	-70	40	4	22
1	6710	0	30	3	23
1	6780	-70	30	3	24
1	6830	100	30	3	25
1	8100	-60	40	4	26
1	8390	100	30	3	27
1	8470	0	30	3	28
1	8700	35	40	4	29
1	9650	-10	30	3	30
1	9808	15	30	3	31
1	9838	50	30	3	32
6	1030	-30	9	2	33
6	2680	-30	9	2	34
6	2840	140	9	2	35
1	2980	-10	0	0	36
1	3340	-30	0	0	37
1	3340	-100	0	0	38
6	3350	60	9	2	39
6	3370	-180	9	2	40
6	3650	-80	9	2	41
6	3660	-90	9	2	42
6	3780	-140	9	2	43
6	3810	-90	9	2	44
6	3900	80	9	2	45
6	4100	80	9	2	46
6	4190	90	9	2	47
6	4230	50	9	2	48

6	4350	-150	9	2	49
6	4385	-60	9	2	50
6	4440	-120	9	2	51
6	4470	50	9	2	52
6	4470	-40	9	2	53
6	4510	100	9	2	54
6	4520	110	9	2	55
6	4570	-130	9	2	56
6	4605	30	9	2	57
6	4610	50	9	2	58
6	4610	-30	9	2	59
6	4680	-70	9	2	60
6	4700	75	9	2	61
6	4745	-150	9	2	62
6	4785	115	9	2	63
6	4965	-55	9	2	64
6	4990	0	9	2	65
6	5070	-140	9	2	66
6	5110	65	9	2	67
6	5155	-80	9	2	68
6	5180	-10	9	2	69
6	5200	-60	9	2	70
6	5200	100	9	2	71
6	5250	-20	9	2	72
6	5300	-105	9	2	73
6	5390	45	9	2	74
6	5415	15	9	2	75
6	5515	105	9	2	76
6	5910	-45	9	2	77
6	6070	-150	9	2	78
6	6115	-90	9	2	79
6	6120	-25	9	2	80
6	7860	-135	9	2	81
6	7930	-100	9	2	82
6	8065	-190	9	2	83
6	3480	30	9	2	84
5	2975	-150	9	2	85
5	3425	-150	9	2	86
5	4850	-20	9	2	87
5	4850	170	9	2	88
5	5300	25	9	2	89
5	5200	-75	9	2	90
5	5590	90	9	2	91
5	5025	-200	9	2	92
4	345	0	690	62	93
4	3510	0	1680	750	94
4	5490	0	2190	412	95
4	7485	0	660	100	96
3	330	-40	660	90	97
3	1590	0	840	100	98
3	2565	0	750	72	99
3	4440	0	780	135	100
3	5025	0	150	13	101
3	5835	0	450	55	102

3	6270	0	60	4	103
3	7200	0	1320	200	104
0	0	0	0	0	105
0	0	0	0	0	106
0	0	0	0	0	107
0	0	0	0	0	108
0	0	0	0	0	109
0	0	0	0	0	110
0	0	0	0	0	111
0	0	0	0	0	112
0	0	0	0	0	113
0	0	0	0	0	114
0	0	0	0	0	115
0	0	0	0	0	116
0	0	0	0	0	117
0	0	0	0	0	118
0	0	0	0	0	119
0	0	0	0	0	120
0	0	0	0	0	121
0	0	0	0	0	122
0	0	0	0	0	123
0	0	0	0	0	124
0	0	0	0	0	125
0	0	0	0	0	126
0	0	0	0	0	127
0	0	0	0	0	128
0	0	0	0	0	129
0	0	0	0	0	130
0	0	0	0	0	131
0	0	0	0	0	132
0	0	0	0	0	133
0	0	0	0	0	134
0	0	0	0	0	135
0	0	0	0	0	136
0	0	0	0	0	137
0	0	0	0	0	138
0	0	0	0	0	139
0	0	0	0	0	140
0	0	0	0	0	141
0	0	0	0	0	142
0	0	0	0	0	143
0	0	0	0	0	144
0	0	0	0	0	145
0	0	0	0	0	146
0	0	0	0	0	147
0	0	0	0	0	148
0	0	0	0	0	149
0	0	0	0	0	150

```
  RUNWAY DAMAGE CORRECTION ROUTINE

  CHOOSE: 1 - READ RUNWAY FILE FROM DISC
          2 - DUMP CONTENTS OF TABLE TO TERMINAL
          3 - CORRECT A KNOWN BAD POINT
          4 - EXIT.....


3
  ENTER: I,J TO CORRECT POINT
         <CR> TO END
  ?13,2
  ENTER NEW VALUE FOR IDAMGE( 13,  2)....4200
  ?36,1
  ENTER NEW VALUE FOR IDAMGE( 36,  1)....6
  ?37,1
  ENTER NEW VALUE FOR IDAMGE( 37,  1)....6
  ?38,1
  ENTER NEW VALUE FOR IDAMGE( 38,  1)....6
  ?


  RUNWAY DAMAGE CORRECTION ROUTINE

  CHOOSE: 1 - READ RUNWAY FILE FROM DISC
          2 - DUMP CONTENTS OF TABLE TO TERMINAL
          3 - CORRECT A KNOWN BAD POINT
          4 - EXIT.....


4


  END CORRECTION ROUTINE


  CHOOSE: 1 - ENTER RUNWAY DAMAGES
          2 - MAKE CORRECTIONS TO RUNWAY DATA
          3 - STORE RUNWAY DATA ON DISC
          4 - GO BACK TO TAXI SECTION
          5 - GO ON TO VIEWS DAMAGES......3


  CHOOSE: 1 - ENTER RUNWAY DAMAGES
          2 - MAKE CORRECTIONS TO RUNWAY DATA
          3 - STORE RUNWAY DATA ON DISC
          4 - GO BACK TO TAXI SECTION
          5 - GO ON TO VIEWS DAMAGES......5
```

```
  CHOOSE: 1 - GO BACK TO RUNWAY SECTION
          2 - MAKE CORRECTIONS TO VIEWS DATA
          3 - STORE VIEWS DATA ON DISC
          4 - GO BACK TO TAXI SECTION
          5 - EXIT PROGRAM PART01......5  .
TTO  --  STOP NORMAL END
>RUN PART02




THIS PROGRAM IDENTIFIES THE EASIEST
REPAIRED RUNWAY SEGMENTS BY SELECTING
RUNWAY SEGMENTS WITH MINIMIZED REPAIR TIMES.


 THE TAXI-WAY REPAIR INFORMATION AND RUNWAY REPAIR INFORMATION
  SHOULD HAVE BEEN PREVIOUSLY STORED ON DISK FILES.
  IF THIS HAS NOT BEEN DONE, RUN PROGRAM SEGMENT PART01.



  ENTER TAXIWAY DAMAGE FILE


  ENTER RUNWAY DAMAGE FILE


  ENTER PART00 DAMAGE FILE?

NO



  BURIED UXOS CAN BE CONSIDERED TWO WAYS:
      1 - REPAIRED BEFORE EXPLODING, OR
      2 - REPAIRED BY FIXING POST-EXPLOSION CRATER: 1  .

  ENTER THE DENSITY RATIO: (0.9 < D < 1.1)....1  .
```

```
  PREPARE TO STORE RESULTS ON A DISC FILE.


TTO  --  STOP NORMAL END
>RUN PART03

  THIS PROGRAM WILL NOT FUNCTION UNLESS PART01 AND PART02
  HAVE BEEN RUN PREVIOUSLY.

  ENTER TAXIWAY DAMAGE FILE


  ENTER RUNWAY DAMAGE FILE


  ENTER RUNWAY REPAIR FILE

TTO  --  STOP NORMAL END
```

****

RESULTS OF RUNWAY SEGMENT (MOS) SELECTION

****

THE FIVE BEST SEGMENTS IN THE
INCREASING RANGE DIRECTION:

THE NUMBER 1 SEGMENT:

STARTS AT: X = 600.0 FEET DOWN THE RUNWAY
Y = 50.0 FEET FROM CENTERLINE
ALPHA = -1.146 DEGREES FROM CENTERLINE

THE FOUR CORNERS ARE (X,Y):

599.5	25.0
600.5	75.0
5599.5	-25.0
5590.5	-75.0

THERE ARE A TOTAL OF 27. DAMAGES IN THIS SEGMENT

THE TOTAL REPAIR TIME IS ESTIMATED TO BE 1690. MINUTES.

TAXIWAY (TW1)...	60.0 MINUTES
RAMP (RMP1).....	300.0 MINUTES
RUNWAY ACCESS....	240.0 MINUTES
M.O.S.....	1190.0 MINUTES

TAXIWAY DAMAGES

LOCATION	X-COOR	Y-COOR	TYPE	TIME
TW1	190	25	SUXO	60.0
[illegible]	260	-300	CRTR	100.0
[illegible]	290	-280	CRTR	100.0
[illegible]	430	-30	CRTR	150.0
[illegible]	545	0	DMLT	0.0
[illegible]	630	-40	SPAL	90.0

RUNWAY (MOS) REPAIRS:

DAMAGE NUMBER	X-COORD. (FT.)	Y-COORD. (FT.)	TYPE	DIAMETER (FT/IN)	QUALITY (NUMBER)	TIME TO REPAIR
8	3075	20	CRTR	20	A	200.
11	3350	-30	CRTR	30	A	215.
14	4360	-20	CRTR	20	D	125.
34	2620	-30	BUXO	9		10.
36	2980	-10	BUXO	0		0.
37	3340	-30	BUXO	0		0.
50	4385	-60	BUXO	9		10.
55	4470	-40	BUXO	9		10.
59	4610	-30	BUXO	9		10.
60	4680	-70	BUXO	9		10.
64	4965	-55	BUXO	9		10.
65	4990	0	BUXO	9		10.
68	5155	-80	BUXO	9		10.
69	5170	-10	BUXO	9		10.
70	5200	-60	BUXO	9		10.
72	5250	-20	BUXO	9		10.
84	3480	30	BUXO	9		10.
87	4850	-20	SUXO	9		60.
90	5200	-75	SUXO	9		60.
93	345	0	BMLT	690	62	0.
94	3510	0	BMLT	1680	750	0.
96	5400	0	BMLT	2190	412	0.
97	330	-40	SPAL	660	90	90.
98	1590	0	SPAL	940	100	100.
99	2565	0	SPAL	750	72	72.
100	4440	0	SPAL	780	135	135.
101	3615	0	SPAL	150	13	13.

THE NUMBER 2 SEGMENT:

STARTS AT: X = 400.0 FEET DOWN THE RUNWAY
Y = 25.0 FEET FROM CENTERLINE
ALPHA = 0.000 DEGREES FROM CENTERLINE

THE FOUR CORNERS ARE (X,Y):

400.0	0.0
400.0	50.0
5400.0	50.0
5400.0	0.0

THERE ARE A TOTAL OF 28. DAMAGES IN THIS SEGMENT

THE TOTAL REPAIR TIME IS ESTIMATED TO BE 1785. MINUTES.

TAXIWAY (TW1)...	60.0 MINUTES
RAMP (RMP1).....	200.0 MINUTES
RUNWAY ACCESS....	240.0 MINUTES
M.O.S.....	1285.0 MINUTES

TAXIWAY DAMAGES

LOCATION	X-COOR	Y-COOR	TYPE	TIME
TW1	190	25	SUXO	60.0
RMP1	260	-300	CRTR	100.0
RMP1	290	-290	CRTR	100.0
TWY	430	-30	CRTR	150.0
TWY	345	0	BMLT	0.0
TWY	330	-40	SPAL	90.0

RUNWAY (MOS) REPAIRS:

DAMAGE NUMBER	X-COORD. (FT.)	Y-COORD. (FT.)	TYPE	DIAMETER (FT/IN)	QUALITY (NUMBER)	TIME TO REPAIR
8	3075	20	CRTR	20	A	200.
12	3970	50	CRTR	40	A	250.
14	4360	-20	CRTR	20	A	200.
15	4525	20	CRTR	20	D	125.
36	2900	-10	BUXO	0		0.
39	3350	60	BUXO	9		10.
48	4230	50	BUXO	9		10.
52	4470	50	BUXO	9		10.
57	4605	30	BUXO	9		10.
58	4610	50	BUXO	9		10.
61	4700	75	BUXO	9		10.
65	4990	0	BUXO	9		10.
67	5110	65	BUXO	9		10.
69	5100	-10	BUXO	9		10.
[illegible]	5250	-20	BUXO	9		10.

74	5390	45	BUXO	9		10.
75	5415	15	BUXO	9		10.
34	3480	30	BUXO	9		10.
87	4850	-20	SUXO	9		60.
89	5300	25	SUXO	9		60.
93	345	0	BMLT	690	62	0.
94	3510	0	BMLT	1680	750	0.
95	5490	0	BMLT	2190	412	0.
97	330	-40	SPAL	660	90	90.
98	1590	0	SPAL	840	100	100.
99	2565	0	SPAL	750	72	72.
100	4440	0	SPAL	780	135	135.
101	5025	0	SPAL	150	13	13.

THE NUMBER 3 SEGMENT:

STARTS AT: X = 200.0 FEET DOWN THE RUNWAY
Y = -50.0 FEET FROM CENTERLINE
ALPHA = 0.286 DEGREES FROM CENTERLINE

THE FOUR CORNERS ARE (X,Y):

200.1	-75.0
199.9	-25.0
5199.8	-0.0
5200.1	-50.0

THERE ARE A TOTAL OF 28. DAMAGES IN THIS SEGMENT

THE TOTAL REPAIR TIME IS ESTIMATED TO BE 1845. MINUTES.

TAXIWAY (TW1)...	60.0 MINUTES
RAMP (RMP1).....	200.0 MINUTES
RUNWAY ACCESS....	240.0 MINUTES
M.O.S.....	1345.0 MINUTES

TAXIWAY DAMAGES

LOCATION	X-COOR	Y-COOR	TYPE	TIME
TW1	190	25	SUXO	60.0
RMP1	260	-300	CRTR	100.0
RMP1	290	-280	CRTR	100.0

RNWY	430	-30	CRTR	150.0
RNWY	345	0	BMLT	0.0
RNWY	330	-40	SPAL	90.0

RUNWAY (MOS) REPAIRS:

DAMAGE NUMBER	X-COORD. (FT.)	Y-COORD. (FT.)	TYPE	DIAMETER (FT/IN)	QUALITY (NUMBER)	TIME TO REPAIR
5	430	-30	CRTR	30	B	205.
7	2850	-43	CRTR	20	A	200.
9	3110	-50	CRTR	20	A	200.
11	3360	-30	CRTR	30	A	215.
14	4360	-20	CRTR	20	D	125.
33	1030	-30	BUXO	9		10.
34	2630	-30	BUXO	9		10.
36	2990	-10	BUXO	0		0.
37	3340	-30	BUXO	0		0.
41	3650	-80	BUXO	9		10.
50	4385	-60	BUXO	9		10.
53	4470	-40	BUXO	9		10.
59	4610	-30	BUXO	9		10.
60	4680	-70	BUXO	9		10.
64	4965	-55	BUXO	9		10.
65	4950	0	BUXO	9		10.
69	5180	-10	BUXO	9		10.
70	5200	-60	BUXO	9		10.
87	4850	-20	SUXO	9		60.
90	5200	-75	SUXO	9		60.
93	345	0	BMLT	690	62	0.
94	3510	0	BMLT	1680	730	0.
95	5490	0	BMLT	2190	412	0.
97	330	-40	SPAL	660	90	90.
98	1590	0	SPAL	840	100	100.
99	2565	0	SPAL	750	72	72.
100	4440	0	SPAL	780	135	135.
101	5025	0	SPAL	150	13	13.

THE THREE BEST SEGMENTS IN THE DECREASING RANGE DIRECTION:

THE NUMBER 1 SEGMENT:

STARTS AT: X = 600.0 FEET DOWN THE RUNWAY
Y = 50.0 FEET FROM CENTERLINE
ALPHA = -1.146 DEGREES FROM CENTERLINE

THE FOUR CORNERS ARE (X,Y):

599.5	25.0
600.5	75.0
5599.5	-25.0
5598.5	-75.0

THERE ARE A TOTAL OF 27. DAMAGES IN THIS SEGMENT

THE TOTAL REPAIR TIME IS ESTIMATED TO BE 1660. MINUTES.

TAXIWAY (TW1)...	60.0 MINUTES
RAMP (RMP1).....	200.0 MINUTES
RUNWAY ACCESS....	240.0 MINUTES
M.O.S.....	1160.0 MINUTES

TAXIWAY DAMAGES

LOCATION	X-COOR	Y-COOR	TYPE	TIME
TW1	190	25	SUXO	60.0
RMP1	260	-300	CRTR	100.0
RMP1	290	-280	CRTR	100.0
RNWY	430	-30	CRTR	150.0
RNWY	345	0	BMLT	0.0
RNWY	330	-40	SPAL	90.0

RUNWAY (MOS) REPAIRS:

DAMAGE NUMBER	X-COORD. (FT.)	Y-COORD. (FT.)	TYPE	DIAMETER (FT/IN)	QUALITY (NUMBER)	TIME TO REPAIR
8	3075	20	CRTR	20	D	125.
11	3360	-30	CRTR	30	A	215.
14	4360	-20	CRTR	20	B	170.
34	2680	-30	BUXO	9		10.
36	2980	-10	BUXO	0		0.
37	3340	-30	BUXO	0		0.
50	4385	-60	BUXO	9		10.
53	4470	-40	BUXO	9		10.

59	4610	-30	BUXO	9		10.
60	4680	-70	BUXO	9		10.
64	4965	-55	BUXO	9		10.
65	4990	0	BUXO	9		10.
68	5155	-80	BUXO	9		10.
69	5180	-10	BUXO	9		10.
70	5200	-60	BUXO	9		10.
72	5250	-20	BUXO	9		10.
84	3480	30	BUXO	9		10.
87	4850	-20	SUXO	9		60.
90	5200	-75	SUXO	9		60.
93	345	0	BMLT	690	62	0.
94	3510	0	BMLT	1680	750	0.
95	5490	0	BMLT	2190	412	0.
97	330	-40	SPAL	660	90	90.
98	1590	0	SPAL	840	100	100.
99	2565	0	SPAL	750	72	72.
100	4440	0	SPAL	780	135	135.
101	5025	0	SPAL	150	13	13.

THE NUMBER 2 SEGMENT:

STARTS AT: X = 200.0 FEET DOWN THE RUNWAY
Y = -50.0 FEET FROM CENTERLINE
ALPHA = 0.286 DEGREES FROM CENTERLINE

THE FOUR CORNERS ARE (X,Y):

200.1	-75.0
199.9	-25.0
5199.8	-0.0
5200.1	-50.0

THERE ARE A TOTAL OF 28. DAMAGES IN THIS SEGMENT

THE TOTAL REPAIR TIME IS ESTIMATED TO BE 1785. MINUTES.

TAXIWAY (TW1)...	60.0 MINUTES
RAMP (RMP1).....	200.0 MINUTES
RUNWAY ACCESS....	240.0 MINUTES
M.O.S.....	1285.0 MINUTES

TAXIWAY DAMAGES

LOCATION	X-COOR	Y-COOR	TYPE	TIME
TW1	190	25	SUXO	60.0
RMP1	260	-300	CRTR	100.0
RMP1	290	-280	CRTR	100.0
RNWY	430	-30	CRTR	150.0
RNWY	345	0	BMLT	0.0
RNWY	330	-40	SPAL	90.0

RUNWAY (MOS) REPAIRS:

DAMAGE NUMBER	X-COORD. (FT.)	Y-COORD. (FT.)	TYPE	DIAMETER (FT/IN)	QUALITY (NUMBER)	TIME TO REPAIR
5	430	-30	CRTR	30	D	175.
7	2850	-43	CRTR	20	D	125.
9	3110	-50	CRTR	20	A	200.
11	3360	-30	CRTR	30	A	215.
14	4360	-20	CRTR	20	B	170.
33	1030	-30	BUXO	9		10.
34	2680	-30	BUXO	9		10.
36	2900	-10	BUXO	0		0.
37	3340	-30	BUXO	0		0.
41	3650	-80	BUXO	9		10.
50	4385	-60	BUXO	9		10.
53	4470	-40	BUXO	9		10.
59	4610	-30	BUXO	9		10.
60	4680	-70	BUXO	9		10.
64	4965	-55	BUXO	9		10.
65	4990	0	BUXO	9		10.
69	5180	-10	BUXO	9		10.
70	5200	-60	BUXO	9		10.
87	4850	-20	SUXO	9		60.
90	5200	-75	SUXO	9		60.
93	345	0	BMLT	690	62	0.
94	3510	0	BMLT	1680	750	0.
95	5490	0	BMLT	2190	412	0.
97	330	-40	SPAL	660	90	90.
98	1590	0	SPAL	840	100	100.
99	2565	0	SPAL	750	72	72.
100	4440	0	SPAL	780	135	135.
101	5025	0	SPAL	150	13	13.

THE NUMBER 3 SEGMENT:

STARTS AT: X = 400.0 FEET DOWN THE RUNWAY

Y = 25.0 FEET FROM CENTERLINE
ALPHA = 0.000 DEGREES FROM CENTERLINE

THE FOUR CORNERS ARE (X,Y):

400.0	0.0
400.0	50.0
5400.0	50.0
5400.0	0.0

THERE ARE A TOTAL OF 28. DAMAGES IN THIS SEGMENT

THE TOTAL REPAIR TIME IS ESTIMATED TO BE 1785. MINUTES.

TAXIWAY (TW1)...	60.0 MINUTES
RAMP (RMP1).....	200.0 MINUTES
RUNWAY ACCESS....	240.0 MINUTES
M.O.S.....	1285.0 MINUTES

TAXIWAY DAMAGES

LOCATION	X-COOR	Y-COOR	TYPE	TIME
TW1	190	25	SUXO	60.0
RMP1	260	-300	CRTR	100.0
RMP1	290	-280	CRTR	100.0
RNWY	430	-30	CRTR	150.0
RNWY	345	0	BMLT	0.0
RNWY	330	-40	SPAL	90.0

RUNWAY (MOS) REPAIRS:

DAMAGE NUMBER	X-COORD. (FT.)	Y-COORD. (FT.)	TYPE	DIAMETER (FT/IN)	QUALITY (NUMBER)	TIME TO REPAIR
9	3075	20	CRTR	20	D	125.
12	3970	50	CRTR	40	A	250.
14	4360	-20	CRTR	20	A	200.
15	4525	20	CRTR	20	A	200.
26	2980	-10	BUXO	0		0.

39	3350	60	BUXO	9		10.
48	4230	50	BUXO	9		10.
52	4470	50	BUXO	9		10.
57	4605	30	BUXO	9		10.
58	4610	50	BUXO	9		10.
61	4700	75	BUXO	9		10.
65	4990	0	BUXO	9		10.
67	5110	65	BUXO	9		10.
69	5180	-10	BUXO	9		10.
72	5250	-20	BUXO	9		10.
74	5390	45	BUXO	9		10.
75	5415	15	BUXO	9		10.
84	3480	30	BUXO	9		10.
87	4850	-20	SUXO	9		60.
89	5300	25	SUXO	9		60.
93	345	0	BMLT	690	62	0.
94	3510	0	BMLT	1680	750	0.
95	5420	0	BMLT	2190	412	0.
97	330	-40	SPAL	660	90	90.
98	1590	0	SPAL	840	100	100.
99	2565	0	SPAL	750	72	72.
100	4440	0	SPAL	780	135	135.
101	5025	0	SPAL	150	13	13.

THE THREE BEST BI-DIRECTIONAL SEGMENTS:

THE NUMBER 1 SEGMENT:

STARTS AT: X = 600.0 FEET DOWN THE RUNWAY
Y = 50.0 FEET FROM CENTERLINE
ALPHA = -1.146 DEGREES FROM CENTERLINE

THE FOUR CORNERS ARE (X,Y):

599.5	25.0
600.5	75.0
5599.5	-25.0
5598.5	-75.0

THERE ARE A TOTAL OF 27. DAMAGES IN THIS SEGMENT

THE TOTAL REPAIR TIME IS ESTIMATED TO BE 1735. MINUTES.

TAXIWAY (TW1)...	60.0 MINUTES
RAMP (RMP1).....	200.0 MINUTES
RUNWAY ACCESS....	240.0 MINUTES
M.O.S.....	1235.0 MINUTES

TAXIWAY DAMAGES

LOCATION	X-COOR	Y-COOR	TYPE	TIME
TW1	190	25	SUXO	60.0
RNP1	260	-300	CRTR	100.0
RNP1	290	-280	CRTR	100.0
RNWY	430	-30	CRTR	150.0
RNWY	345	0	BMLT	0.0
RNWY	330	-40	SPAL	90.0

RUNWAY (MOS) REPAIRS:

DAMAGE NUMBER	X-COORD. (FT.)	Y-COORD. (FT.)	TYPE	DIAMETER (FT/IN)	QUALITY (NUMBER)	TIME TO REPAIR
8	3075	20	CRTR	20	A	200.
11	3360	-30	CRTR	30	A	215.
14	4360	-20	CRTR	20	B	170.
34	2690	-30	BUXO	9		10.
36	2980	-10	BUXO	0		0.
37	3340	-30	BUXO	0		0.
50	4385	-60	BUXO	9		10.
53	4470	-40	BUXO	9		10.
59	4610	-30	BUXO	9		10.
60	4680	-70	BUXO	9		10.
64	4965	-55	BUXO	9		10.
65	4990	0	BUXO	9		10.
68	5155	-80	BUXO	9		10.
69	5180	-10	BUXO	9		10.
70	5200	-60	BUXO	9		10.
72	5250	-20	BUXO	9		10.
84	3480	30	BUXO	9		10.
87	4850	-20	SUXO	9		60.
90	5200	-75	SUXO	9		60.
93	345	0	BMLT	690	62	0.
94	3510	0	BMLT	1680	750	0.
95	5490	0	BMLT	2190	412	0.
97	330	-40	SPAL	660	90	90.
98	1590	0	SPAL	840	100	100.
99	2565	0	SPAL	750	72	72.
100	4440	0	SPAL	780	135	135.
101	5025	0	SPAL	150	13	13.

THE NUMBER 2 SEGMENT:

STARTS AT: X = 400.0 FEET DOWN THE RUNWAY
Y = 25.0 FEET FROM CENTERLINE
ALPHA = 0.000 DEGREES FROM CENTERLINE

THE FOUR CORNERS ARE (X,Y):
400.0 0.0
400.0 50.0
5400.0 50.0
5400.0 0.0

THERE ARE A TOTAL OF 28. DAMAGES IN THIS SEGMENT

THE TOTAL REPAIR TIME IS ESTIMATED TO BE 1860. MINUTES.
TAXIWAY (TW1)... 60.0 MINUTES
RAMP (RMP1)..... 200.0 MINUTES
RUNWAY ACCESS.... 240.0 MINUTES
M.O.S..... 1360.0 MINUTES

TAXIWAY DAMAGES

LOCATION	X-COOR	Y-COOR	TYPE	TIME
TW1	190	25	SUXO	60.0
RMP1	260	-300	CRTR	100.0
RMP1	290	-280	CRTR	100.0
RNWY	430	-30	CRTR	150.0
RNWY	345	0	BMLT	0.0
RNWY	330	-40	SPAL	90.0

RUNWAY (MOS) REPAIRS:

DAMAGE NUMBER	X-COORD. (FT.)	Y-COORD. (FT.)	TYPE	DIAMETER (FT/IN)	QUALITY (NUMBER)	TIME TO REPAIR

8	3075	20	CRTR	20	A	200.
12	3970	50	CRTR	40	A	250.
14	4360	-20	CRTR	20	A	200.
15	4525	20	CRTR	20	A	200.
36	2980	-10	BUXO	0		0.
39	3350	60	BUXO	9		10.
48	4230	50	BUXO	9		10.
52	4470	50	BUXO	9		10.
57	4605	30	BUXO	9		10.
58	4610	50	BUXO	9		10.
61	4700	75	BUXO	9		10.
65	4990	0	BUXO	9		10.
67	5110	65	BUXO	9		10.
69	5180	-10	BUXO	9		10.
72	5250	-20	BUXO	9		10.
74	5390	45	BUXO	9		10.
75	5415	15	BUXO	9		10.
84	3480	30	BUXO	9		10.
87	4850	-20	SUXO	9		60.
89	5300	25	SUXO	9		60.
93	345	0	BMLT	690	62	0.
94	3510	0	BMLT	1680	750	0.
95	5490	0	BMLT	2190	412	0.
97	330	-40	SPAL	660	90	90.
98	1590	0	SPAL	840	100	100.
99	2565	0	SPAL	750	72	72.
100	4440	0	SPAL	780	135	135.
101	5025	0	SPAL	150	13	13.

THE NUMBER 3 SEGMENT:

STARTS AT: X = 700.0 FEET DOWN THE RUNWAY
Y = -50.0 FEET FROM CENTERLINE
ALPHA = 0.286 DEGREES FROM CENTERLINE

THE FOUR CORNERS ARE (X,Y):
700.1 -75.0
699.9 -25.0
5699.8 -0.0
5700.1 -50.0

THERE ARE A TOTAL OF 28. DAMAGES IN THIS SEGMENT

THE TOTAL REPAIR TIME IS ESTIMATED TO BE 1875. MINUTES.
TAXIWAY (TW1)... 60.0 MINUTES
RAMP (RMP1)..... 200.0 MINUTES
RUNWAY ACCESS.... 240.0 MINUTES

M.O.S..... 1375.0 MINUTES

TAXIWAY DAMAGES

LOCATION	X-COOR	Y-COOR	TYPE	TIME
TW1	190	25	SUXO	60.0
RNP1	260	-300	CRTR	100.0
RNP1	290	-280	CRTR	100.0
RNWY	430	-30	CRTR	150.0
RNWY	345	0	BMLT	0.0
RNWY	330	-40	SPAL	90.0

RUNWAY (MOS) REPAIRS:

DAMAGE NUMBER	X-COORD. (FT.)	Y-COORD. (FT.)	TYPE	DIAMETER (FT/IN)	QUALITY (NUMBER)	TIME TO REPAIR
7	2950	-43	CRTR	20	A	200.
9	3110	-50	CRTR	20	A	200.
11	3360	-30	CRTR	30	A	215.
14	4360	-20	CRTR	20	C	135.
33	1030	-30	BUXO	9		10.
34	2680	-30	BUXO	9		10.
36	2980	-10	BUXO	0		0.
37	3340	-30	BUXO	0		0.
41	3650	-80	BUXO	9		10.
50	4385	-60	BUXO	9		10.
53	4470	-40	BUXO	9		10.
59	4610	-30	BUXO	9		10.
60	4680	-70	BUXO	9		10.
64	4965	-55	BUXO	9		10.
65	4990	0	BUXO	9		10.
69	5100	-10	BUXO	9		10.
70	5200	-60	BUXO	9		10.
72	5250	-20	BUXO	9		10.
75	5415	15	BUXO	9		10.
87	4850	-20	SUXO	9		60.
90	5200	-75	SUXO	9		60.
94	3510	0	BMLT	1680	750	0.
95	5490	0	BMLT	2190	412	0.
98	1590	0	SPAL	840	100	100.
99	2565	0	SPAL	750	72	72.

100	4440	0	SPAL	780	135	135.
101	5025	0	SPAL	150	13	13.
102	5835	0	SPAL	450	55	55.

INITIAL DISTRIBUTION

DTIC-DDA-2	12
HQ AFSC/DLWM	1
HQ AFSC/SDNE	1
HQ USAFE/EUROPS (DEXD)	1
HQ USAFE/DEX	1
AFATL/DLJK	1
AD/IN	1
USAFTAWC/THL	1
USAFTAWC/THLA	1
AFATL/DLODL (Tech Library)	1
EOARD/LNS	1
SHAPE TECHNICAL CENTER	1
HQ PACAF/DEM	1
HQ PACAF/DEPR	1
AUL/LSE 71-249	1
HQ SAC/DEM	1
US Navy Civil Engineering Lab	1
HQ ATC/DED	1
HQ MAC/DEM	1
HQ AFESC/DEMP	1
HQ AFESC/DEO	1
HQ AFESC/TST	1
HQ AFESC/RDCR	10
USAE WESGF	1
USAE WES	1
HQ USAF/LEEX	1
HQ USAF/LEYW	1
HQ USAF/RDPX	1
AFWAL/FIEM	1
AFIT/DET	1
HQ AFLC/DEMG	1
AFIT/LDE	1
ASD/RWRS	15

(The reverse of this page is blank)